NASA TN D-89

TECHNICAL NOTE
D-89

WIND-TUNNEL AND PILOTED FLIGHT SIMULATOR INVESTIGATION OF A DEFLECTED-SLIPSTREAM VTOL AIRPLANE, THE RYAN VZ-3RY

By Harry A. James, Rodney C. Wingrove, Curt A. Holzhauser, and Fred J. Drinkwater III

Ames Research Center
Moffett Field, Calif.

NATIONAL AERONAUTICS AND SPACE ADMINISTRATION

WASHINGTON November 1959

NATIONAL AERONAUTICS AND SPACE ADMINISTRATION

TECHNICAL NOTE D-89

WIND-TUNNEL AND PILOTED FLIGHT SIMULATOR INVESTIGATION OF A DEFLECTED-SLIPSTREAM VTOL AIRPLANE, THE RYAN VZ-3RY

By Harry A. James, Rodney C. Wingrove, Curt A. Holzhauser, and Fred J. Drinkwater III

SUMMARY

A wind-tunnel investigation of a deflected-slipstream VTOL airplane was undertaken to determine if this type of machine were capable of performing a transition from hovering to normal flight. Sufficient additional information was obtained to enable a flight simulation of this VTOL machine. The ground simulation was made to obtain an early indication of the handling qualities and to give the pilots experience in "flying" this new type of vehicle; the simulator cockpit was free to pitch and roll.

The wind-tunnel tests indicated that the airplane could hover and perform a transition out of ground effect. The vehicle required increasing thrust with decreasing airspeed below 60 knots, and it had stick-fixed angle-of-attack instability below about 30 knots. An increasing forward stick position was required with decreasing airspeed. The primary effect of approaching the ground during hovering was a pitch-down moment beyond the trimming capabilities of the longitudinal control. This moment was brought under control by the addition of a leading-edge slat.

The piloted simulation was performed with the data pertaining to the airplane out of the ground effect and without a leading-edge slat. Under these conditions, the pilots could control the vehicle throughout the speed range and within certain boundary conditions governed by the previously mentioned pitch-up characteristics and by structural limitations defined by the manufacturer. When the pitch-up boundary was approached, the pilots found it necessary to keep low pitch rates. Longitudinal control could be regained after moderate pitch-ups by throttle control with a loss in altitude of from 100 to 300 feet, or by increasing the flap deflection with a much smaller loss in altitude.

INTRODUCTION

Small-scale studies have indicated both statically (refs. 1, 2, and 3) and in free flight (refs. 4 and 5) that VTOL operation can be achieved through the deflected slipstream principle. To determine if these indications would be borne out in practice, a testbed VTOL machine

using this principle was constructed. The airplane was built by Ryan Aeronautical Company under the auspices of the Office of Naval Research and the Army Transportation Research and Engineering Command (TRECOM). Prior to flight tests of the machine, its static characteristics were investigated in the Ames 40- by 80-foot wind tunnel, and a piloted motion simulation was made in the Ames pitch-roll cockpit. This report presents the results of the studies.

The major objectives of the wind-tunnel study were to determine if the machine could achieve steady-state VTOL operation; to determine under what conditions operation would become impossible or unsafe from either an aerodynamic or structural limit; and to obtain the information necessary for the piloted motion simulation of the aircraft. This ground simulation was conducted to obtain an early indication of the handling qualities of the airplane in the speed range of 0 to 55 knots and to give the pilots the general "feel" and orientation of flying this new type of vehicle. The simulation also served to document those control problems that might bother the pilot or make the vehicle unflyable, and to indicate ways for the pilot to control the vehicle in both the normal and extreme circumstances. The material in this report covers all of these objectives, with the exception of the structural aspect. In addition, some of the aerodynamic characteristics are related to previously reported small-scale work, and existing and proposed handling quality requirements are examined with respect to the pilot's comments of this simulation.

NOTATION

b wing span, ft

$\bar{c}$ mean aerodynamic chord, ft

C_l rolling-moment coefficient, $\frac{\text{rolling moment}}{q_\infty Sb}$

$C_{L,S}$ lift coefficient based on slipstream velocity, $\frac{\text{lift}}{q_S S}$

C_{L_α} horizontal-tail lift-curve slope

C_n yawing-moment coefficient, $\frac{\text{yawing moment}}{q_\infty Sb}$

C_P propeller power coefficient, $\frac{\text{engine torque}}{2\rho n^3 D_p^5}$

C_T propeller thrust coefficient, $\frac{\text{total thrust}}{2\rho n^2 D_p^4}$

$C_{T,S}$ propeller thrust coefficient, based on slipstream velocity, $\frac{\text{total thrust}}{q_S S_p}$

$C_{X,S}$ longitudinal-force coefficient, based on slipstream velocity, $\frac{\text{longitudinal force}}{q_S S}$, positive in the drag direction

D drag including thrust component

D_p propeller diameter, ft

F resultant force, $\sqrt{(\text{lift})^2 + (\text{drag})^2}$, lb

g acceleration of gravity, 32.2 ft/sec^2

h height of flap trailing edge above ground or wind tunnel floor, ft

h_p pressure altitude, ft

HP required horsepower

I_X, I_Y, I_Z, I_{X_Z} moments of inertia about the x, y, and z axes and product of inertia about x and z axes, slug-ft^2

J propeller advance ratio, $\frac{U_\infty}{nD}$

L lift, lb

L', M, N rolling, pitching, and yawing aerodynamic moments about stability axes in wind-tunnel results, about body axes in simulator section, ft-lb

L_p' damping in roll, ft-lb/radian/sec

m mass of vehicle, slugs

n propeller angular velocity, rps

P, Q, R rolling, pitching, and yawing angular velocities of body axes, radians/sec

$\dot{P}, \dot{Q}, \dot{R}$ rolling, pitching, and yawing angular accelerations of body axes, radians/sec^2

q_S slipstream dynamic pressure, calculated from $q_\infty + \frac{T}{S_p}$, lb/sq ft

q_∞ free-stream dynamic pressure, lb/sq ft

S wing area, sq ft

S_p	disk area of the two propellers, sq ft
T	thrust of the two propellers, lb
T_{cp}	thrust due to collective pitch, lb
T_{tp}	thrust due to throttle position, lb
u,v,w	longitudinal, side, and normal linear velocities of body axes, ft/sec
$\dot{u},\dot{v},\dot{w}$	longitudinal, side, and normal linear accelerations of body axes, ft/sec^2
U_∞	forward or free-stream velocity, ft/sec or knots
X,Y,Z	longitudinal, side, and normal aerodynamic forces with respect to body axes, lb
α	angle of attack, measured between body axis (horizontal fuselage reference line) and free-stream velocity
β	sideslip angle, deg
β_p	propeller pitch angle, deg
δ_e	elevator deflection, deg, or longitudinal stick position, fraction of full deflection
δ_f	deflection of aft flap, deg
δ_R	rudder deflection, deg
δ_S	lateral stick deflection, fraction of full deflection
δ_{S_L}	left spoiler-aileron deflection, deg
Δ	incremental
ζ	damping ratio
η	propeller efficiency, percent
θ_S	slipstream turning angle measured from thrust axis, deg
ψ,θ,φ	yaw, pitch, and roll angle of body axes relative to arbitrary earth axes, deg

$\dot{\psi},\dot{\theta},\dot{\varphi}$ yawing, pitching, and rolling angular velocities of body axes relative to arbitrary earth axes, radians/sec

ω_n natural frequency

DESCRIPTION OF THE AIRPLANE

Sketches and dimensions of the airplane tested are given in figure 1, table I, and reference 6. Photographs of the airplane in the wind tunnel and on the ground test stand are presented in figure 2. The wing was equipped with double-slotted flaps shown at several deflections in figure 3. The deflection of the rear flap was about twice that of the front flap; it should be noted that the deflection of the rear flap is used as the reference deflection throughout the report. In the fuselage was located an 825-horsepower free-turbine jet engine (Lycoming T-53) which was geared to drive two wooden counterrotating propellers with rotation being down at the wing tips. The pitch angle of the propellers could be either locked in a desired setting or controlled remotely.

Longitudinal control was provided by the elevator and by deflection of the residual thrust of the jet engine. This thrust deflecting device was located on the end of the fuselage (fig. 1), and the thrust was deflected equally upward and downward with no net horizontal force when the reaction control was in a neutral position. This neutral position corresponded to a centered stick and an elevator deflected -5°. Full forward stick deflected the elevator to $+10^\circ$ and deflected all of the gases out of the bottom of the reaction control; full backward stick deflected the elevator to -20° and deflected all of the gases out of the top of the reaction control. Longitudinal trim at forward speed was provided by movement of the stabilizer between 13° and 23° with respect to the fuselage reference line.

Directional control was provided by the rudder and by deflection of the residual thrust of the jet engine through guide vanes on top and bottom of the reaction control. Full deflection of the rudder was 25°.

Lateral control was provided by the spoiler-ailerons shown in figure 3(a). The deflection of the spoiler-ailerons was almost linearly related to the lateral stick movement, with a maximum spoiler deflection of 50°. Additional lateral control was available by means of differential thrust output of the propellers. For this arrangement, the remote control unit of the propeller pitch mechanism was connected to the lateral stick to increase the pitch angle on one propeller while the pitch of the other was decreased, and vice versa. This differential pitch angle was a linear function of stick movement with a maximum pitch angle change of 3° on each propeller.

The moments of inertia of the airplane about each of the axes were obtained from the Ryan Company and are given in table I.

WIND-TUNNEL TESTS

The major portion of the tests was directed toward conditions and forces simulating level unaccelerated flight, that is, lift about equal to the airplane weight (2625 lb) and drag about equal to the horizontal thrust component. This was accomplished by an iterative process wherein angle of attack and thrust were varied to achieve this 1g balance condition for a particular combination of airspeed and flap deflection. Once this condition was obtained, the engine power was unaltered throughout the particular test run for which information was obtained. By this technique data were obtained over an angle-of-attack range of -19° to $+20^\circ$ (with respect to horizontal fuselage reference line), and a sideslip range of -3° to $+12^\circ$. The tests were performed with a range of flap deflections from 0° to 70° over selected ranges of free-stream velocities from 100 knots (q_∞ = 34 lb/sq ft) to 0 knots. The extent of these tests was restricted by structural limitations prescribed by the manufacturer. Initial tests were made without the reaction control installed. Subsequent tests included the reaction control and also the leading-edge slat shown in figure 3(a).

The lateral control system was evaluated with and without differential propeller pitch, and the longitudinal and directional control systems were evaluated with and without the reaction control installed. When the reaction control assembly was not installed, a residual thrust force existed which was roughly proportional to engine power with 100 pounds of force existing at 700 horsepower. This thrust force was not removed from the drag data presented herein but was taken into account during the iterative process to achieve 1g conditions. When the control assembly was installed, the tail-pipe area was decreased and the fuel flow was increased, thus increasing the available thrust for reactive control.

The wind-tunnel tests were for a flap height of about 17 feet above the tunnel floor. The effect of approaching the ground at zero forward speed was investigated outside of the tunnel with the airplane mounted on a strain-gage support system at 0° and 18° angle of attack.

The results of propeller calibrations made with the propellers installed on the airplane are presented in figure 4. These calibrations were made at a fuselage angle of attack of -19° (thrust axis at -6°) with flaps retracted so that zero lift was approximated. The propeller thrust was calculated from the sum of the measured drag with the propellers installed and the measured drag of the airplane with the propellers removed. The power output of the engine was calculated from a torque gage integral with the engine and previously calibrated by the engine manufacturer. Consequently, the power coefficient and efficiency shown in figure 4 include gearbox and transmission losses which were a relatively

small but unknown quantity. No attempt was made to assess interference and interaction effects of flap deflection or angle of attack on the propeller characteristics. The propeller blade pitch was fixed at 11-1/2° for the majority of the tests.

The least count of the wind-tunnel balance system was as follows:

Lift, lb	20
Drag, lb	2
Pitching moment, ft-lb	400
Side force, lb	5
Yawing moment, ft-lb	150
Rolling moment, ft-lb	450

The tunnel dynamic pressure was maintained at least within ±0.2 pound per square foot of the desired value. The effects of this variation and of propeller speed variation on propeller advance ratio resulted in a maximum thrust variation of ±5 percent. Because of these variations, as well as unsteady flow conditions on the wing and flap, data points will be found to scatter considerably beyond the band indicated by the least count of the scales.

The values of lift and drag presented in this report include the direct effects of thrust, that is, $T \sin(\alpha + 13^\circ)$ and $T \cos(\alpha + 13^\circ)$, respectively. No corrections for the influence of the wind-tunnel walls have been applied to the data. Normal wind-tunnel wall corrections are considered to be inapplicable for this test because of the low free-stream velocities and relatively high values of slipstream velocities and deflections. Although this factor would indicate the necessity of relatively large corrections, it would be partially compensated for by the small size of the airplane compared to the tunnel (the ratio of the wing span to tunnel width was 0.29).

No corrections for strut tares or strut interference have been applied to the data. It is expected that these corrections would be insignificant.

DESCRIPTION OF MOVING SIMULATOR AND TESTS

A piloted simulation of the flight of the airplane was made with a six-degree-of-freedom simulation in which the pilot and his cockpit are free to move around two of the axes, pitch and roll.

The information flow, the simulation computing equipment, and the servo drive system for the pitch and roll chair are presented in block diagram form in figure 5. As indicated in this figure, the pilot's control motions, which were converted into appropriate voltages, were the

input to an analog computer. From these inputs and the aerodynamic derivatives, the analog computer simultaneously computed the aerodynamic forces and the resulting vehicle motion. The pilot was presented the simulated six-degree-of-freedom vehicle motions through the moving cockpit and the visual cues of the cockpit display as follows:

Pitch	Pitch motions of the cockpit (-15° to $+40^\circ$)
Roll	Roll motions of the cockpit (-180° to $+180^\circ$)
Yaw	Yaw rate indicator (-10° to $+10^\circ$/sec)
Forward motion	Airspeed indicator (-10 to +60 knots)
Side motion	Side velocity indicator (-15 to +15 ft/sec)
Vertical motion	Rate of climb indicator (-50 to +50 ft/sec)

Figure 6(a) shows an external view of the moving cockpit and figure 6(b) shows the instrument panel and internal layout of the cockpit with the pilot's controls which were similar to the flight article. The pilot's controls shown in figure 6(b) were: a conventional stick, rudder pedals, a throttle, a collective pitch control, a longitudinal trim actuator (located on top of the stick), and a flap actuator (located on top of the throttle).

To simulate an actual control system, stick bungees were used to provide forces proportional to control displacement. The relationships used were 6 pounds of force for the 5 inch maximum longitudinal stick displacement, 18 pounds of force for the 5 inch maximum lateral stick displacement, and 50 pounds for the 1-1/2 inch maximum rudder pedal displacement. These forces were estimated since pertinent data were not obtained in the wind-tunnel tests. The actuation rates for the flaps and adjustable stabilizer used for trim were 5° per second. A first-order time constant of 0.5 second was used to simulate engine response to throttle movement and a first-order time constant of 0.2 second was used to simulate the lag between lateral stick deflection and the development of the rolling moment.

The boundaries of the simulator study were (1) a speed range from 0 to 55 knots, (2) the structural limit speeds denoted by the manufacturer, and (3) the wing stall. The equations used to represent the motions and aerodynamic characteristics of the simulated vehicle are presented in table II. Table II also gives the values of the various terms used in the simulation. The static aerodynamic terms were derived from preliminary wind-tunnel results for the airplane without leading-edge slat, and the damping terms were estimated. Comparison of values calculated from the equations in table II with the preliminary wind-tunnel data showed good agreement within the aforementioned boundaries and for 1g level flight. Subsequent to the simulation, additional data were obtained, and a further examination indicated differences in values from the preliminary results, chiefly in values of pitching moment. It was concluded that the

differences were sufficiently small that they would have only a minor effect on the pilot's comments, and therefore the simulation was not repeated with the corrected data.

An initial period of the study was used to familiarize each pilot with the flight characteristics at speeds near 50 knots, and then the stability and control characteristics were investigated over a speed range at each of several flap settings and power required for level flight. The pilots then "flew" complete transitions to hovering, investigated the characteristics in hovering, and then made the transition back to the higher speeds.

RESULTS AND DISCUSSION

Because of the nature of the study, most of the discussion relates specifically to the testbed aircraft although some implications generally applicable to this type of VTOL aircraft are discussed. Consideration is given the hovering and transition characteristics derived from both the wind-tunnel study and from the piloted ground-simulation studies.

The pilot's rating system and general comments for the complete range of the simulation study are presented in tables III and IV. These comments were made by two Ames test pilots with helicopter experience and are representative of those of the pilots who flew this simulation.

Longitudinal Characteristics

Hovering.- Data at zero forward speed were obtained both in the wind tunnel at an effective height of 17 feet and out of the wind tunnel on a strain-gage support system at ground heights of 2 and 6 feet. The variations of turning angle, θ_S, turning efficiency, F/T, and pitching moment, M/TD_p, with flap deflection out of ground effect (h = 17 feet) are shown in figure 7. It can be seen from the sketch in figure 7 that hovering is possible out of ground effect when the resultant force, F (resultant of lift, thrust, and aerodynamic drag), is rotated to a vertical position, and when sufficient thrust is provided to produce a resultant force equal to the weight of the airplane. Accordingly, the attitude of the thrust axis required to hover at each flap deflection is defined by $90^\circ - \theta_S$, and a reduction in F/T indicates an increase in the ratio of thrust to weight required to hover. At the design point of 70° flap deflection, the thrust axis must be inclined some 35° (a fuselage inclination of 22°), and the thrust required must be 25 percent greater than the weight of the airplane. While the pitching moment required to balance the machine without the reaction control was small, addition of the reaction control in neutral position added a nose-down moment which to overcome required about 60 percent of the available reaction control (the maximum control

available was a value of M/TD_p of about ± 0.08). Based on visual flow observations, a portion of the nose-down moment was traced to the force generated on the horizontal tail by the impingement of the vertical jet from the reactive control. The variations of turning angle, turning efficiency, and pitching moment with ground plane height are shown in figure 8 for several flap deflections and also with a leading-edge slat. It is seen that approaching the ground during hovering had a significant effect on moment but little effect on θ_S or F/T. The increase in pitch-down moment with decreasing height represents a critical control problem since, without the slat, the trim moment required near the ground exceeds the moment that can be provided by the reaction control. This pitch-down moment was decreased by the leading-edge slat. With the slat installed, the nose-down moment could be easily trimmed with the reaction control (about 50 percent of the maximum control required), and practically no reaction control was required to trim when the airplane was out of the ground effect. Reducing flap deflection on the airplane without the slat would also bring the trim moment within the capabilities of the reaction control, but at a cost of increased hover attitude.

The piloted simulation was based on preliminary pitching-moment data obtained in the wind tunnel without leading-edge slat and out of the ground effect. For these conditions, the pitching moment provided by the reaction control was considered to be marginal to satisfactory by the pilot. The maximum pitching moment available for maneuvering after the unbalanced moment was trimmed corresponded to an initial angular acceleration of about 0.7 radian per second squared. It is interesting to note that a value of 1 radian per second squared was suggested for VTOL machines in reference 10; this value was based on control moments considered to be satisfactory for helicopters.

Transition.- The lift, drag, and moment characteristics of the machine at various forward speeds (away from the ground) are shown for various flap deflections in figure 9 (no leading-edge slat) and figure 10 (with leading-edge slat). As noted previously, these data were obtained by adjusting power and attitude to approximate lift equal to weight and drag equal to zero at each flap deflection. Then angle of attack was varied while tunnel speed and engine power were held constant. From the data shown in figures 9 and 10, it is possible to examine the static longitudinal characteristics this machine would have in a transition from hovering to normal flight at an altitude out of the ground effect. To facilitate such an examination, these data are summarized in figures 11 and 12 for 1g level flight. Figure 11 (no leading-edge slat) and figure 12 (with leading-edge slat) present the effect of forward speed on

(a) Fuselage angle of attack

(b) Thrust required

(c) Power required

(d) Change in pitching moment with angle of attack, stick fixed, $(\partial M/\partial \alpha)$ measured at constant airspeed and power

(e) Change in pitching moment with speed, stick fixed, $(\partial M/\partial U_\infty)$ calculated from measurements of the moment change with thrust at constant angle of attack and from the change in thrust with velocity obtained from the propeller calibration

(f) Out-of-trim moment with longitudinal control neutral[1]

(g) Stick position required to trim with reaction control installed, calculated from faired moment curves (f) (Symbol at end of curve denotes flap deflection.)

The relative importance of (d), (e), and (g) has not been assessed in flight for this type of vehicle. For a conventional airplane in which power effects are small, the angle-of-attack stability has been of primary importance and is indicated by the stick position variation with speed.

The results of figure 11 from a transition standpoint show that

(a) The thrust and power required at any airspeed are practically independent of flap deflection; for all cases, the thrust and power variation with airspeed is unstable below 60 knots; that is, thrust and power required for level flight decrease with speed increase.

(b) The stick-fixed pitching-moment change with angle of attack at constant airspeed and power was unstable for some flap configurations at speeds less than 42 knots; increasing flap deflection for a given speed reduced this instability. However, stability was not present for any flap deflection tested below 20 knots at the given center of gravity location. A 30-percent chord forward movement of the center of gravity would be required to provide at least neutral stability at the low forward speeds; such a change could not be tolerated in hovering with the existing reaction control. To obtain maximum stick-fixed longitudinal stability in transition, the maximum possible flap deflection should be scheduled at each airspeed.

(c) Stick-fixed pitching-moment stability with speed did not exist in the speed range tested, that is, a nose-down moment was obtained by increasing forward speed at a constant angle of attack and power.

(d) Out-of-trim pitching moments decrease rapidly (1) with increasing flap deflection at a given speed and (2) as speed is increased above 15 knots with flaps deflected. This latter moment change is undesirable in that increased forward stick deflection is required for trim as forward speed is decreased.

---

[1]These pitching-moment data include data other than shown in figures 9 and 10, and they correspond to a -5° elevator deflection.

Comparison of the data in figures 11 and 12 shows that the addition of the leading-edge slat (used to reduce nose-down moment during hovering near the ground) had only a small effect on the angle of attack, thrust, and power required for 1g level flight. However, this slat increased the nose-up moment near 15 knots to the limit of the longitudinal control, and it increased the angle-of-attack instability throughout the speed range tested.

Figure 13 presents the variation of several basic control parameters of the airplane out of ground effect and without a slat during a transition scheduled to minimize the out-of-trim pitching moments in order to retain a large portion of the control for maneuvering, and for which consideration was also taken of the stick-fixed stability and stick position change with speed and flap deflection. It is seen by examination of the factor $\partial M/\partial \alpha$ that the airplane will exhibit stick-fixed angle-of-attack instability from hovering to a speed of 20 knots, neutral stability until about 40 knots, and stability above 40 knots. During this transition, the attitude will change from 22° nose-up at hover to about -10° at 24 knots and remain at -10° until flap retraction is complete. It should be noted that numerous transitions can be planned with various compromises in the factors considered.

Figure 14(a) summarizes the effectiveness of the stabilizer and elevator without reactive control for conditions corresponding to 1g level flight and also shows a comparison with the theoretical effectiveness calculated from references 7 and 8 with the assumption that the dynamic pressure at the horizontal tail is that of the free stream. Based on these results, it appears that the location of the horizontal tail surface was such that the effective dynamic pressure at the tail was that of the free stream. Figure 14(b) shows the maximum pitching-moment control and the maximum acceleration in pitch available at various forward speeds with and without the reaction control installed. It must be recognized that the moment created by the reaction control results from the residual thrust of the jet engine, and that this thrust is approximately proportional to the power output of the engine. As was noted earlier, the propeller thrust and power required for 1g flight were practically independent of flap deflection at a given speed (fig. 11(b)), and therefore, a single-valued curve for the available control moment versus speed is obtained for 1g flight. As shown in figure 14(b), the minimum control available exists near 25 knots where the power and free-stream dynamic pressure are low and neither reaction nor elevator has much power.

The foregoing discussion of stability and control problems in a transition was based entirely on wind-tunnel results. Doubt exists that experience with conventional aircraft enables a completely valid interpretation of such wind-tunnel results in the case of unconventional VTOL aircraft. In lieu of flight tests, the simulator was used to determine the pilot's reaction to the stability and control characteristics shown to exist in the wind-tunnel tests. In general, the pilot was given the task of slowing the aircraft and determining the minimum speed at which

control could be maintained under specified conditions, for example, fixed flap deflection. After some experience under the specified conditions, the pilot was given free choice of the parameters and then he defined the limiting flight conditions at each speed for which control could be maintained. Figures 15 to 18 show example cases taken from the simulation study; figure 19 shows the summary results of the study and defines the limits within which the pilots concluded the airplane could accomplish transition.

As was noted earlier, for a constant flap setting, decreases in speed will create positive pitching moments. This characteristic requires the pilot to push forward on the stick as he decreases speed at a constant flap setting; in addition to this stick position instability, stick-fixed static instability (pitching-moment variation with angle of attack) existed below about 35 knots. For each flap setting (δ_f less than 60°), there was a critical speed below which there was insufficient longitudinal control to keep the airplane from pitching up out of control. Figure 15 presents a time history of a typical pitch-up taken from the simulation results to illustrate the situation where the rate of increase in moment was large enough to offset the full longitudinal control input of the pilot. The pilots found they could regain control of the vehicle beyond the limitation of available longitudinal control by the reduction of power; this reduced the nose-up pitching moment and allowed the nose to be lowered and speed to be regained. The loss in altitude during this type of recovery was generally from 100 to 300 feet. Figure 16 presents a time history of a moderate pitch-up controlled by the reduction of power. Another method of controlling pitch-up, which resulted in only a small loss in altitude, was to lower the flap. By this method, the airspeed was kept above the minimum control speed for the new flap setting. The pilots found actuation rates of 5° per second were sufficient to control moderate pitch-ups but lower actuation rates were marginal. Figure 17 shows a time history where the pitch-up was controlled by a change in flap setting. The minimum speeds for which the simulated airplane could be controlled by the aforementioned techniques are compared in figure 19 with values of (1) pitching moment (with centered stick), at several speeds and flap deflections, which had to be balanced for level 1g flight and (2) the maximum available longitudinal control used for the simulation.[2] It is seen that the simulated vehicle could be flown at speeds below which there was insufficient longitudinal control to keep the airplane from pitching up. By considering the pitch-up characteristics in relation to the longitudinal control available, the pilots determined minimum comfortable transition speeds for each flap setting as shown in figure 19. The pilots were able to maneuver this vehicle through transition with satisfactory attitude control when the pitching rates were kept low and a sufficient speed margin was maintained to stay out of the pitch-up region. Time histories of typical transitions from 40 knots down to 0 and from 0 up to 40 knots are shown in figure 18. To

[2]It should be pointed out again that differences in the pitching moment shown in figures 19, 11, and 14 are not due to inaccurate simulation (see Description of Simulator and Tests).

avoid the pitch-up problem mentioned above, the pilots would generally "lead" with the flap actuator and then follow up with the throttle to maintain a steady decrease in speed and lead with the throttle and follow with the flap when increasing speed. The increase in throttle or corresponding increase in thrust required at the lower speeds is shown in figure 11(a). For this simulation, where only a rate-of-climb indicator was used, this type of transition led the pilot to lose altitude when decreasing speed and to gain altitude when increasing speed as shown on the time history. The pilots feel that altitude control for this vehicle was very good, as indicated by the rate-of-climb indicator, and that if they were given an absolute altitude reference they would have had little difficulty in maintaining altitude during transition. Comparison of the flap-speed relation of comfortable piloted transitions (fig. 19) with that prepared on the basis of wind-tunnel data (fig. 13) show general agreement.

Figure 19 also presents the angles of attack corresponding to the control boundaries in balanced 1g flight conditions. As this figure indicates, the structure limit and controllable limit form a corridor where transition is possible, and the structure limit and the minimum comfortable transition speed form a corridor where transition is most easily controlled by the pilot. The width of the corridor, it will be noted, can be expanded by raising the structural limit speeds for each flap deflection. The other boundary of the corridor may be expanded by moving the center of gravity forward to increase the longitudinal stability and to reduce the nose-up moment. However, on this particular airplane, longitudinal trim capabilities in hovering flight would prevent utilization of this latter change.

The pilots found the response to longitudinal control sluggish, especially in the speed region near 20 knots. Figure 20 shows the longitudinal and lateral dynamic stability characteristics which were calculated from the static tunnel data, and figure 21 shows these longitudinal characteristics in relationship to the results of flight tests of a fighter-type airplane (ref. 9). Reference 9 indicates that the dynamic longitudinal characteristics fall in a region where the pilot opinion indicated slow, sluggish response. Table IV indicates that the pilot's opinion of the longitudinal stability being unsatisfactory is in agreement with the results of reference 9. It must be noted that the pilot opinions for reference 9 were based on fighter-type airplanes with a constant stick force per g; whereas, for the VTOL simulation, the pilot has restricted his opinion to a less maneuverable type of vehicle with altogether different stick force control characteristics. A preliminary estimation of desired control for VTOL machines was presented in reference 10 where an initial acceleration in pitch of 1 radian per second squared was suggested for a vehicle of 2600 pounds, presuming that artificial damping could be provided at a level required from flight tests. This criterion appears to be of the right order of magnitude since the pilots considered the longitudinal control marginal below 30 knots and

satisfactory above 30 knots - speed ranges where the initial acceleration fell below 0.8 radian per second squared and above 0.8 radian per second squared, respectively.

Lateral-Directional Stability

The variations of rolling moment, yawing moment, side force, lift, drag, and pitching moment with sideslip angle are presented in figure 22 for several flap deflections at various forward speeds. These data were obtained in the wind tunnel for the airplane without reaction control and without a leading-edge slat. The effect of forward speed on the lateral and directional stability derivatives, $dL'/d\beta$ and $dN/d\beta$, at 0° angle of sideslip is shown in figure 23. As a reference, curves for $dC_n/d\beta$ of 0.005 and $dC_l/d\beta$ of -0.005 are included in this figure. Based on the simulation, the pilots considered the lateral-directional stability to be unsatisfactory at the lower speeds and marginal at the higher speeds.[3]

Lateral-Directional Control

The lateral control characteristics measured in the tunnel tests are shown in figure 24 for several flap deflections at various forward speeds. The maximum rolling moment and the maximum initial rolling acceleration calculated for full stick deflection are presented in figure 25 for various forward speeds at conditions corresponding to 1g level flight. The use of spoiler alone provided rolling moments throughout the speed range because it was located in the propeller slipstream; however, this control produced adverse yawing moments at the lower speeds. Addition of the differential propeller pitch approximately doubled the rolling moment at the lower speeds, and the adverse yawing moments were greatly reduced.

The effectiveness of the rudder at various speeds without reaction control is summarized in figure 26(a). This effectiveness was maintained over the 25° rudder deflection range that was tested. The yawing moment is proportional to the free-stream dynamic pressure, indicating that the slipstream is below the rudder. It is also evident that rudder effectiveness was unaffected by 12° of sideslip. The effect of forward speed on the yawing moment and calculated maximum yawing acceleration obtained

[3]In the early stages of the simulation, the pilot was given either the yaw rate indicator or the side velocity indicator separately. Neither arrangement was considered satisfactory by the pilots and both instruments were installed together for the remainder of the study. The pilots felt this display of directional motion was only marginal and therefore they could not evaluate the directional stability characteristics with complete confidence.

with full directional control deflection (25° rudder) with and without reactive control is presented in figure 26(b). It is seen that the variation of maximum control with speed is similar to that of the elevator plus reaction control in that a minimum value is obtained around 25 knots, a speed where minimum engine power is required and the free-stream dynamic pressure is low.

During the simulation, the pilots found the lateral control generally marginal when the spoiler only was used and they found the previously mentioned adverse yaw to be bothersome. When the spoilers were combined with the differential pitch, the lateral control was considered to be satisfactory but the nonlinear yaw versus stick variations (fig. 24) would sometimes cause the pilot to induce directional oscillations which were difficult to damp out, especially at the higher speeds. In the hovering region the lateral-directional control operation was like that of a helicopter. If the pilot wanted to turn the vehicle, he would keep the wings level and yaw about the same point on the ground using only rudder control. For this configuration, the pilots could turn the vehicle with yaw rates of 5° to 10° per second, the highest rates tested, with no difficulties. If the pilot wanted to induce side velocities or correct for side velocity variations, he would have to bank the vehicle using the lateral control. The pilots found that with the spoiler and differential propeller pitch combination they could handle side velocities over 10 knots. With only the spoiler for lateral control, they found they could handle side velocities only up to 5 knots, because the adverse dihedral effect would cause rolling moments greater than the available lateral control. The pilots found that if they did get into trouble in the hovering condition as a result of the vehicle rolling off and the side velocity increasing, they were able to recover by using the rudder to turn into the roll and thus convert side velocity into forward velocity as in helicopter operation. This recovery procedure is opposite to that which the pilot is used to in the relatively high-speed region where, with positive dihedral effect, he will put in opposite rudder to offset rolling off on one wing. In the investigation of lateral control in the hovering condition the relative dihedral effect (dL'/dv) was varied because of uncertainties in the wind-tunnel data at low speeds. Figure 27 shows the pilot ratings of the two lateral control systems for a neutral dihedral effect, and for a large amount of negative dihedral effect; the values used represented the extremes of the reasonable fairings through the wind-tunnel data. As would be expected, the pilots felt the controls to be more satisfactory with increases in dihedral effect, but the increases fall within the scatter of ratings for the two pilots.

The rolling moment obtained by deflecting the stick from neutral to full deflection and the calculated maximum rolling acceleration were presented previously at various forward speeds in figure 25 for conditions corresponding to 1g level flight. These values are shown in figure 28 in relation to control ratings of fighter-type airplanes as proposed in reference 11. Comparison of the ratings that would be predicted by this method with those obtained during the simulation show that a good correlation was obtained with the roll time constant of 0.7 which was obtained

from an estimated value of roll damping. Also included in figure 28 are the values of rolling acceleration proposed for VTOL vehicles in reference 10 and the roll-damping requirements equivalent to the steady-state rolling velocity necessary to satisfy military specifications for helicopters (ref. 12). These criteria were satisfied by the use of spoilers plus differential propeller pitch. Under these conditions the pilots considered the controls to be marginal to satisfactory. With spoilers only, these criteria were not satisfied and the pilots considered the controls less acceptable. Although good correlation was obtained with all three criteria, it should be pointed out that this would not necessarily be possible with a different value of the roll time constant or maximum roll control power in figure 28.

The yawing acceleration required for military helicopters is 0.4 radian per second squared (ref. 12). Comparison of this value with those calculated for the airplane (fig. 26) shows that the available acceleration is less than that specified throughout the transition speed range; however, the pilots found the directional control satisfactory throughout the speed range. It should be noted, however, for this simulation, the pilots' "feel" for directional reference was considered only marginal.

Analysis in Dimensionless Form

It was noted earlier that the primary purpose of the investigation was directed toward obtaining data to examine transition flight of a specific VTOL machine. Consequently, insufficient data were obtained to provide a comprehensive analysis in a coefficient form; however, it was felt worthwhile to present the available data in the manner suggested for VTOL vehicles by references 1 and 13. This method proposed the use of a calculated dynamic pressure in the slipstream rather than the dynamic pressure of the free stream, thereby avoiding infinite coefficients at hovering speeds. The lift, drag, and pitching-moment data are presented in this manner in figure 29 for several flap deflections. The reader should be reminded that the thrust used for the calculation of slipstream dynamic pressure was obtained at one angle of attack in the presence of the airplane and that no corrections for interference or angle of attack have been applied. A chart used for the conversion of thrust to slipstream dynamic pressure and to thrust coefficient is given in figure 30 for the various free-stream velocities of the investigation. The effect of slipstream thrust coefficient on lift and drag (based on the slipstream dynamic pressure) at a given angle of attack is given in figure 31 and is also compared with the variation predicted by the semiempirical method of reference 13. Since considerable separation existed at high flap deflections with low thrust, it is surprising that such good agreement is obtained with a method that was to be limited to flow conditions where air-flow separation does not exist. The degree of separation existing for $C_{T,S} = 0$ (props off) is indicated by the fact that the theoretical flap lift increment is two to three times the value measured. Comparison

of the data at $C_{T,S} = 1.0$ (zero forward speed) with those of comparable small-scale semispan data (refs. 2, 3, and 14) shows that lower turning angles and efficiencies were obtained with the full-scale vehicle.

CONCLUDING REMARKS

Wind-tunnel tests and a piloted-motion simulation were conducted with an airplane designed to take off and land vertically by deflecting the propeller slipstream with large chord flaps. The major portion of the investigation was directed toward flight during transition (from 0 to 60 knots) out of ground effect.

The wind-tunnel tests made out of ground effect showed that the airplane could hover with a 70° flap deflection when the thrust axis was inclined 35° and a thrust-to-weight ratio of 1.25 was applied. Transition from hovering to a flaps-up speed was indicated to be possible with several combinations of flap deflection and angle of attack for each forward speed. For all cases, the variation of thrust and power required with forward speed was unstable below 60 knots, that is, thrust and power decreased with increasing forward speed. Stick-fixed angle-of-attack instability existed for some flap deflections at speeds less than 42 knots. Increasing flap deflection at a given speed reduced this instability; however, longitudinal stability was impossible to realize below 25 knots with the existing center-of-gravity location. In addition, the stick had to be moved forward to trim the airplane as the speed was decreased with flaps deflected.

In spite of these undesirable static longitudinal characteristics, the pilots that flew the simulation could control the vehicle throughout the transition speed range; this was possible within certain boundary conditions governed by the previously mentioned pitch-up characteristics and by structural limitations defined by the airframe manufacturer. When the pitch-up boundary was approached, the pilots found it necessary to keep low pitch rates; longitudinal control could be regained after moderate pitch-ups by throttle control with a loss in altitude of from 100 to 300 feet or by increasing to flap deflection with a much smaller loss in altitude. The pilots were able to fly this vehicle comfortably through transition by the use of throttle and by the choice of flap deflection and angle of attack where a large portion of the longitudinal control was available for maneuvering.

The lateral-directional stability and control characteristics of this machine were not greatly affected by flap deflection at a given speed. The pilots found the lateral control to be marginal with only wing spoilers, and to be satisfactory with the spoilers in combination with differential propeller pitch.

The handling characteristics of the vehicle as rated by the pilots that flew the simulation compared moderately well with those predicted

by existing criteria based either on conventional fighters or on helicopters, where applicable. Although these results are encouraging, it should be pointed out, however, that more research is needed, especially in the areas correlating simulation and flight results and in the measurements of basic handling characteristics of VTOL aircraft.

Limited force and moment measurements at zero forward speed, out of the wind tunnel, showed that proximity to the ground created a large pitch-down moment with practically no change in the turning angle or turning efficiency. This pitch-down moment was beyond the trimming capability of the existing longitudinal control; however, the addition of a leading-edge slat reduced pitching moment sufficiently that it could be trimmed both in and out of ground effect. The effect of hovering either in or out of ground effect was not investigated in the piloted simulation.

Ames Research Center
National Aeronautics and Space Administration
Moffett Field, Calif., July 7, 1959

REFERENCES

1. Kuhn, Richard E., and Draper, John W.: An Investigation of a Wing-Propeller Configuration Employing Large-Chord Plain Flaps and Large-Diameter Propellers for Low-Speed Flight and Vertical Take-Off. NACA TN 3307, 1954.

2. Kuhn, Richard E., and Draper, John W.: Investigation of Effectiveness of Large-Chord Slotted Flaps in Deflecting Propeller Slipstreams Downward for Vertical Take-Off and Low-Speed Flight. NACA TN 3364, 1955.

3. Kuhn, Richard E., and Hayes, William C., Jr.: Wind-Tunnel Investigation of Effect of Propeller Slipstreams on Aerodynamic Characteristics of a Wing Equipped with a 50-Percent-Chord Sliding Flap and a 30-Percent-Chord Slotted Flap. NACA TN 3918, 1957.

4. Tosti, Louis P., and Davenport, Edwin E.: Hovering Flight Tests of a Four-Engine-Transport Vertical Take-Off Airplane Model Utilizing a Large Flap and Extensible Vanes for Redirecting the Propeller Slipstream. NACA TN 3440, 1955.

5. Tosti, Louis P.: Transition-Flight Investigation of a Four-Engine-Transport Vertical-Takeoff Airplane Model Utilizing a Large Flap and Extensible Vanes for Redirecting the Propeller Slipstream. NACA TN 4131, 1957.

6. Price, H. S., and Parks, W. C.: Estimated Performance, Stability and Control Ryan Model 92 Vertical Take-Off Airplane. Ryan Rep. 9220-2, Oct. 1, 1957.

7. DeYoung, John, and Harper, Charles W.: Theoretical Symmetric Span Loading at Subsonic Speeds for Wings Having Arbitrary Plan Form. NACA Rep. 921, 1948.

8. DeYoung, John: Theoretical Symmetric Span Loading Due to Flap Deflection for Wings of Arbitrary Plan Form at Subsonic Speeds. NACA Rep. 1071, 1952.

9. Harper, Robert P., Jr.: Flight Evaluation of Various Longitudinal Handling Qualities in a Variable-Stability Jet Fighter. WADC TR 55-299, July 1955.

10. Crim, Almer D.: Hovering and Low-Speed Controllability of VTOL Aircraft. Jour. of Amer. Helicopter Soc., vol. 4, no. 1, Jan. 1959.

11. Creer, Brent Y., Stewart, John D., Merrick, Robert B., and Drinkwater, Fred J., III: A Pilot Opinion Study of Lateral Control Requirements for Fighter-Type Aircraft. NASA MEMO 1-29-59A, 1959.

12. Anon.: Military Specification. Helicopter Flying Qualities, Requirements for. MIL-H-8501, Nov. 5, 1952.

13. Kuhn, Richard E.: Semi-Empirical Procedure for Estimating Lift and Drag Characteristics of Propeller-Wing-Flap Configurations for Vertical- and Short-Take-Off-and-Landing Airplanes. NASA MEMO 1-16-59L, 1959.

14. Cincotta, G. A., and Dunn, H. S.: The Static and Dynamic Stability of a Deflected Slipstream Vehicle. Princeton University Report No. 407, Mar. 1958.

TABLE I.- GEOMETRIC DATA OF AIRPLANE

Wing	
Area, sq ft	125
Span, ft	23.4
Aspect ratio	4.40
Taper ratio	1.0
Mean aerodynamic chord, ft	5.33
Sweepback, deg	0
Incidence, deg	22
Twist, deg	0
Airfoil section	NACA 4418
Flap	
Span of one flap, ft	10.0
Distance from fuselage center line to inboard end, ft	1.25
Chord	
Fore flap, ft	3.29
Aft flap, ft	3.05
Leading-edge slat	
Span of one slat, ft	10.0
Distance from fuselage center line to inboard end, ft	1.25
Chord, ft	1.67
Horizontal tail	
Area, sq ft	52.0
Span, ft	12.75
Aspect ratio	3.13
Taper ratio	1.0
Mean aerodynamic chord, ft	4.18
Sweepback, deg	0
Dihedral, deg	0
Tail length (wing $\bar{c}/4$ to tail $\bar{c}/4$)	13.76
Vertical tail, sq ft	18.8
Fuselage	
Length, ft	28.0
Frontal area, sq ft	13.3
Maximum width, ft	2.5
Engine	Lycoming T53
Propeller	3-bladed wooden Hartzell
Diameter, ft	9.167
Thrust axis inclination, relative to fuselage reference line, deg	13
Moments of inertia (weight = 2689 lb)	
I_X, slug-ft^2	1442
I_Y, slug-ft^2	2571
I_Z, slug-ft^2	3398
I_{XZ}, slug-ft^2	107

TABLE II.- EQUATIONS OF MOTION

(a) The equations of motion of the simulated vehicle for the six degrees of freedom about the body axes

Applied aerodynamic forces		Gravitational forces		Rates of change of linear momentum
X	$-$	$mg \sin \theta$	$=$	$m(\dot{u} - vR + wQ)$
Y	$+$	$mg \cos \theta \sin \varphi$	$=$	$m(\dot{v} - wP + uR)$
Z	$+$	$mg \cos \theta \cos \varphi$	$=$	$m(\dot{w} - uQ + vP)$

Applied aerodynamic moments		Rates of change of angular momentum
L'	$=$	$I_X\dot{P} - I_{XZ}(\dot{R} + PQ) + (I_Z - I_Y)QR$
M	$=$	$I_Y\dot{Q} + I_{XZ}(P^2 - R^2) + (I_X - I_Z)PR$
N	$=$	$I_Z\dot{R} + I_{XZ}(-\dot{P} + QR) + (I_Y - I_X)PQ$

Rates of changes of orientation angles		Functions of angular velocities
$\dot{\varphi}$	$=$	$P + (Q \sin \varphi + R \cos \varphi)\tan \theta$
$\dot{\theta}$	$=$	$Q \cos \varphi - R \sin \varphi$
$\dot{\psi}$	$=$	$(Q \sin \varphi + R \cos \varphi)\sec \theta$

TABLE II.- EQUATIONS OF MOTION - Concluded

(b) Aerodynamic terms relative to the body axes

$$X = -15u + 70q_\infty + (1.09 - 0.0105\delta_f - 0.0014q_\infty\delta_f)T + (-30 + 4q_\infty)w$$

$$Y = -25v - (0.232q_\infty + 0.000885T)\delta_R$$

$$Z = 400 - 215q_\infty - 0.52\delta_f u - 63w - (0.80 + 0.025q_\infty)T - (1.33q_\infty + 0.00375T)\delta_e$$

$$L' = (150 - 2.1u - 0.024\delta_f)v + (-1000 + 42.4\delta_f + 320q_\infty + 4.7\delta_f q_\infty)\delta_S - 2100P + (200 + 8u)R + \left\{42.4\delta_f\delta_S \quad \begin{array}{l}\text{when differential propeller pitch}\\ \text{augments spoiler lateral control}\end{array}\right\}$$

$$M = -2800 + 53.5u + (4.28 - 0.316q_\infty - 0.047\delta_f)T - (11q_\infty + 0.048T)\delta_e - 38q_\infty(i_t - 13) + (35 - 8.5q_\infty)w - (840 + 16u)Q$$

$$N = (0.6u + 0.024\delta_f u)v + (2.9q_\infty + 0.011T)\delta_R - (5.6\delta_f + 3.3q_\infty)\delta_S + (1500 - 15u)P - (800 + 2.5u)R + \left\{\begin{array}{ll}(1600)(\delta_S - 0.3) & \text{for } \delta_S > 0.3\\ 0 & \text{for } -0.3 < \delta_S < 0.3\\ (1600)(\delta_S + 0.3) & \text{for } \delta_S < -0.3\end{array}\right\} \quad \begin{array}{l}\text{when differential}\\ \text{propeller pitch augments}\\ \text{spoiler lateral control}\end{array}$$

where,

$\delta_e = \pm 15^\circ$

$\delta_R = \pm 25^\circ$

$\delta_S = \pm 1$ (Limit at 0.8 for above equations)

$\delta_f = 0^\circ$ to 70°

$i_t = 13^\circ$ to 23°

$T = (600 < T_{tp} < 4000) + (-2000 < T_{cp} < 2000) - 9.5u$

TABLE III.- PILOT OPINION RATING SYSTEM

	ADJECTIVE RATING	NUMERICAL RATING	DESCRIPTION	PRIMARY MISSION ACCOMPLISHED?	CAN BE LANDED
NORMAL OPERATION	Satisfactory	1	Excellent, includes optimum	Yes	Yes
		2	Good, pleasant to fly	Yes	Yes
		3	Satisfactory, but with some mildly unpleasant characteristics	Yes	Yes
EMERGENCY OPERATION	Unsatisfactory	4	Acceptable, but with unpleasant characteristics	Yes	Yes
		5	Unacceptable for normal operation	Doubtful	Yes
		6	Acceptable for emergency condition only*	Doubtful	Yes
NO OPERATION	Unacceptable	7	Unacceptable even for emergency condition *	No	Doubtful
		8	Unacceptable - dangerous	No	No
		9	Unacceptable - uncontrollable	No	No
	Catastrophic	10	Motions possibly violent enough to prevent pilot escape	No	No

*(Failure of a stability augmenter)

A-22255-3.1

TABLE IV.- PILOT OPINION

(a) Pilot rating of stability and control

Flap setting, deg	Task	Rating		Remarks
		Pilot		
		A	B	
20	Longitudinal stability		5	Unsatisfactory
	Longitudinal control		3	Satisfactory
	Lateral-directional stability		4	Marginal
	Lateral control		4	Marginal
	Directional control		3	Satisfactory
40	Longitudinal stability	5	5	Unsatisfactory
	Longitudinal control	4	4	Marginal
	Lateral-directional stability	4	4	Marginal
	Lateral control	4	4	Marginal
	Directional control	3	3	Satisfactory
70 (Hovering)	Longitudinal stability	---	---	No apparent stability
	Longitudinal control	4		Marginal
	Lateral-directional stability	---	---	No apparent stability
	Lateral control			
	Spoiler plus differential propeller pitch with $\partial L'/\partial v = 150$	3	3.5	Satisfactory
	Spoiler only with $\partial L'/\partial v = 150$	4	5	Marginal for small roll rates
	Spoiler plus differential propeller pitch with $\partial L'/\partial v = 0$	3.5	3	Satisfactory
	Spoiler only with $\partial L'/\partial v = 0$	3.5	4.5	Satisfactory for small roll rates
	Directional control	3	4	Satisfactory

TABLE IV.- PILOT OPINION - Concluded

(b) Pilot determined minimum comfortable and controllable speeds

Flap setting, deg	Minimum comfortable speed, knots		Minimum controllable speed, knots	
	Pilot		Pilot	
	A	B	A	B
20	---	45	31	---
40	30	35	22	20
50	20	---	15-18	---
60	20	24	None	None
70	0	5	None	None

Areas	
Wing, sq ft	125
Horizontal tail, sq ft	52
Vertical tail, sq ft	18.8
Aspect ratio	
Wing	4.40
Horizontal tail	3.13

Dimensions in inches
unless otherwise noted

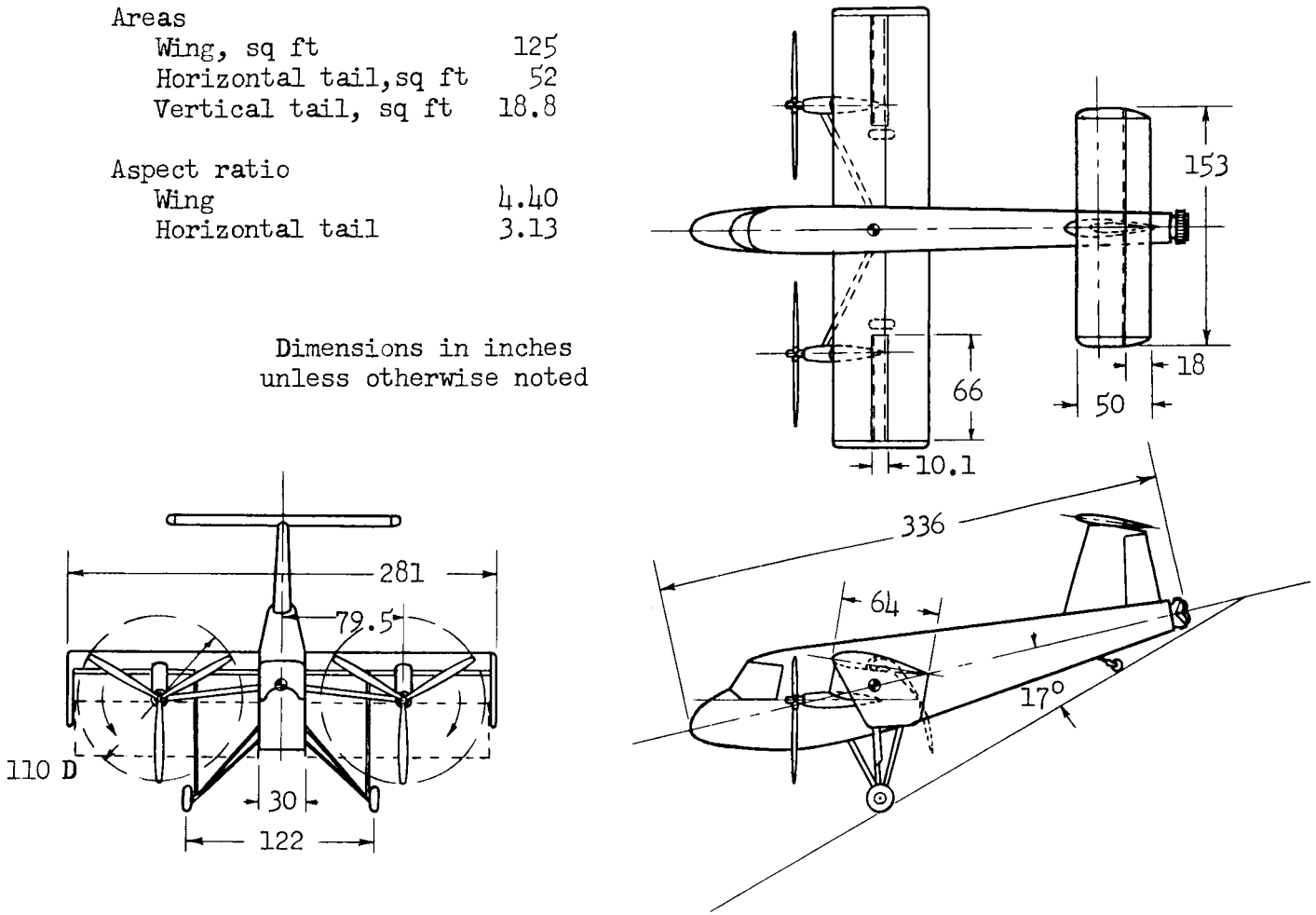

(a) General layout.

Figure 1.- Geometry of the airplane.

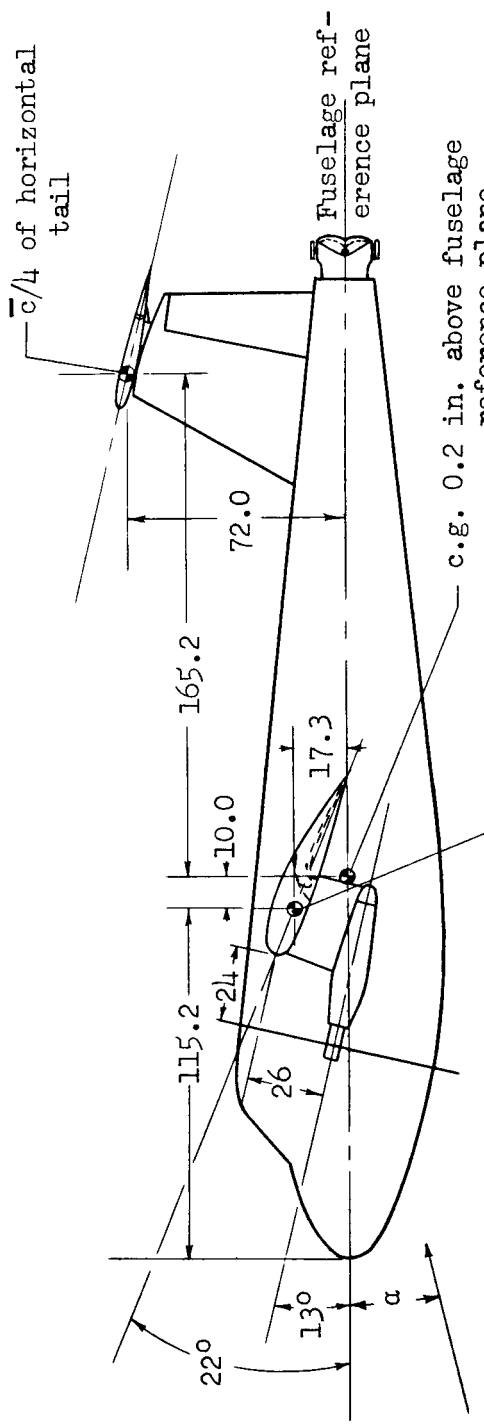

(b) Moment center relationship.

Figure 1.- Concluded.

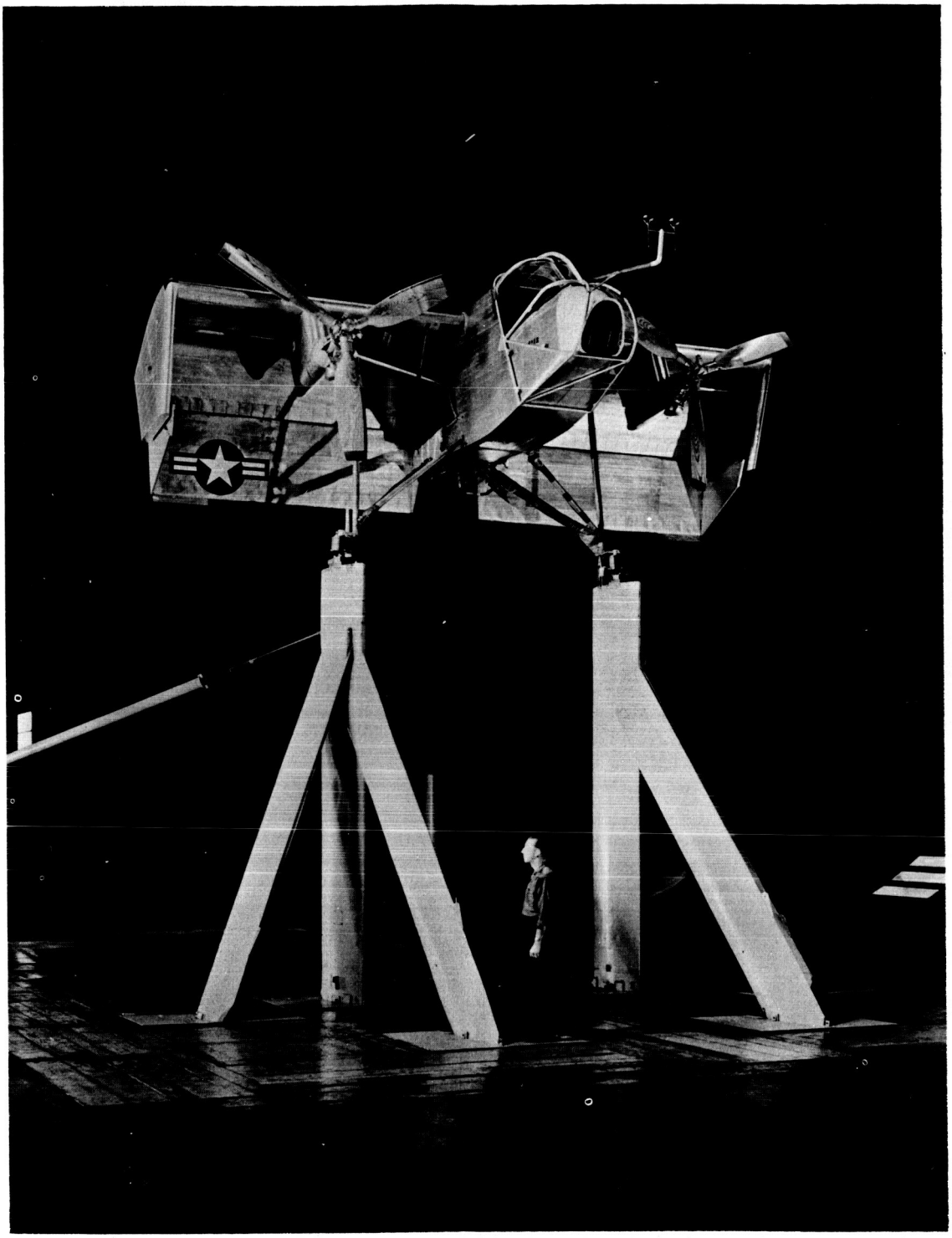

A-23991

(a) With flaps fully deflected.

Figure 2.- The airplane mounted in the Ames 40- by 80-foot wind tunnel.

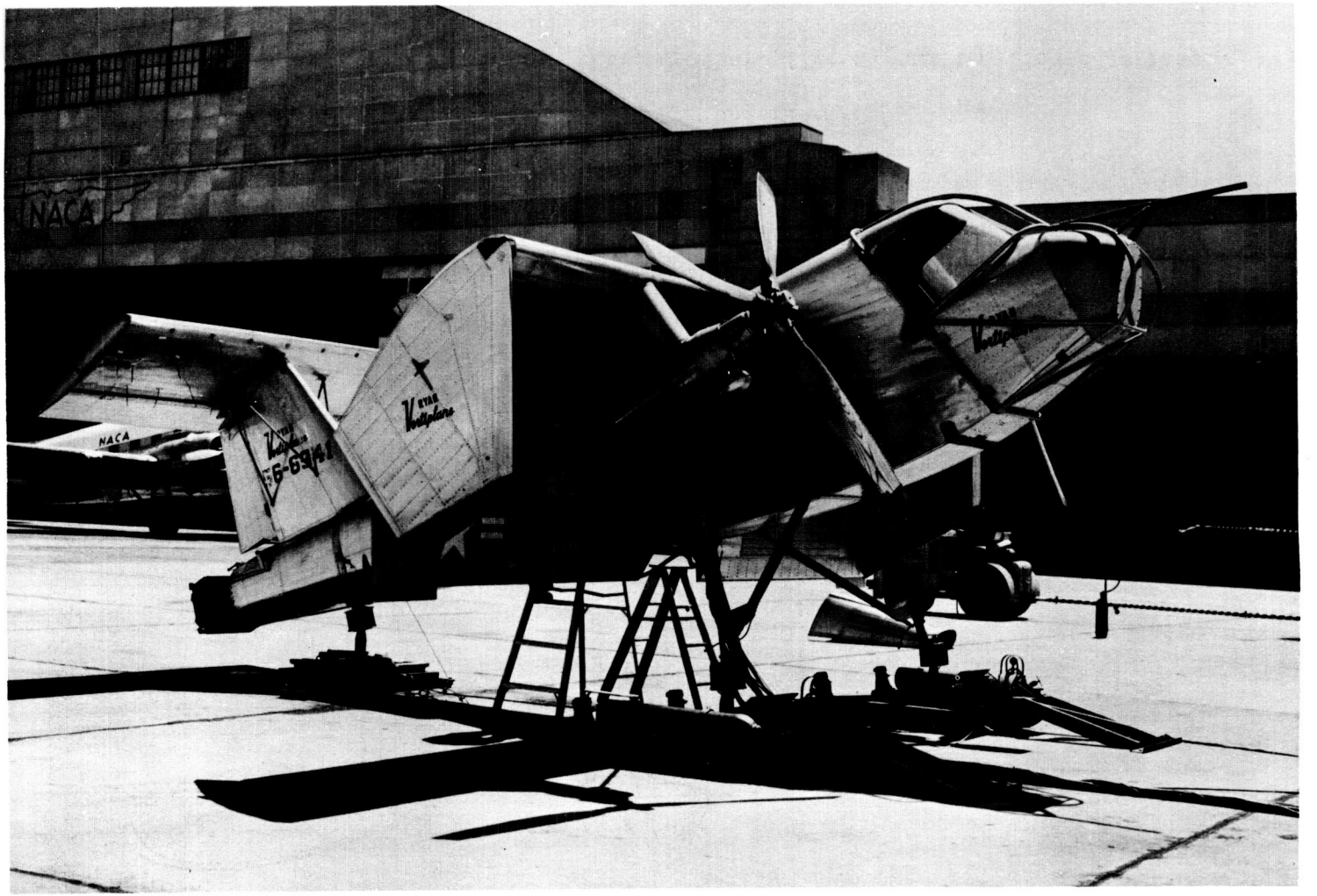

A-24102

(b) The airplane on the ground test stand with flaps deflected 50° and $\theta = 17°$.

Figure 2.- Concluded.

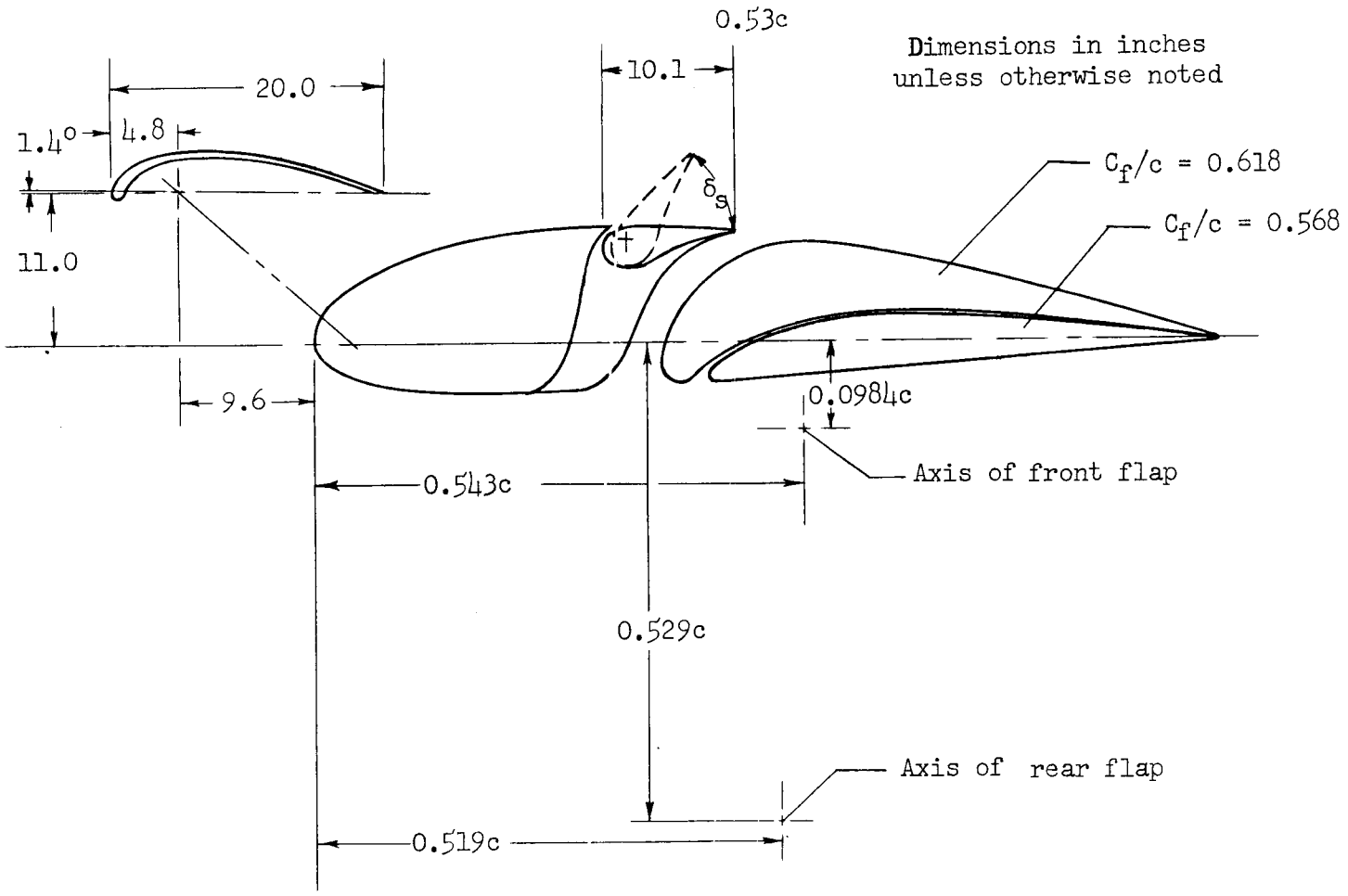

(a) Trailing-edge flaps undeflected.

Figure 3.- Details of the leading-edge slat, spoiler-aileron, and trailing-edge flaps.

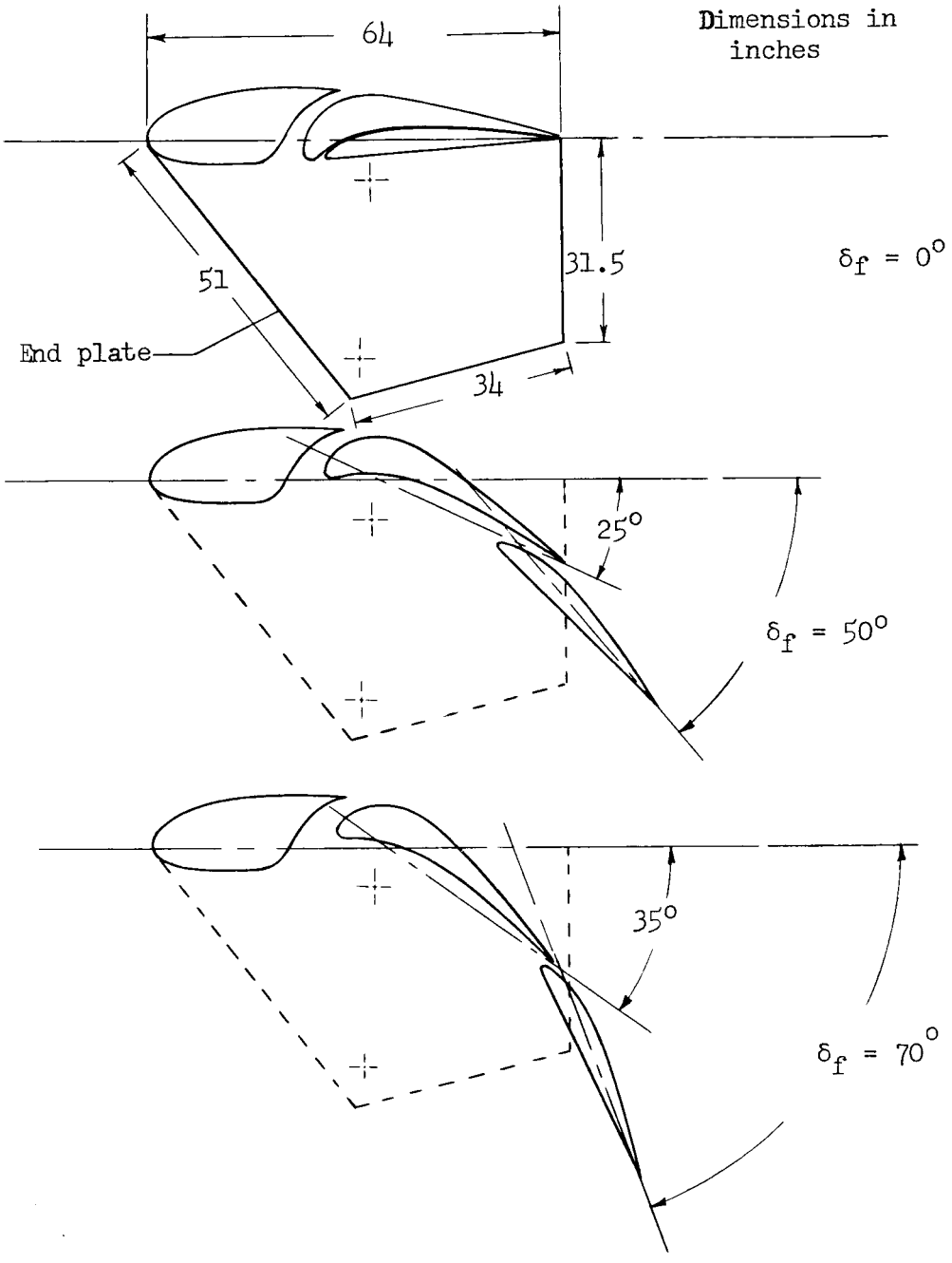

(b) Trailing-edge flaps deflected.

Figure 3.- Concluded.

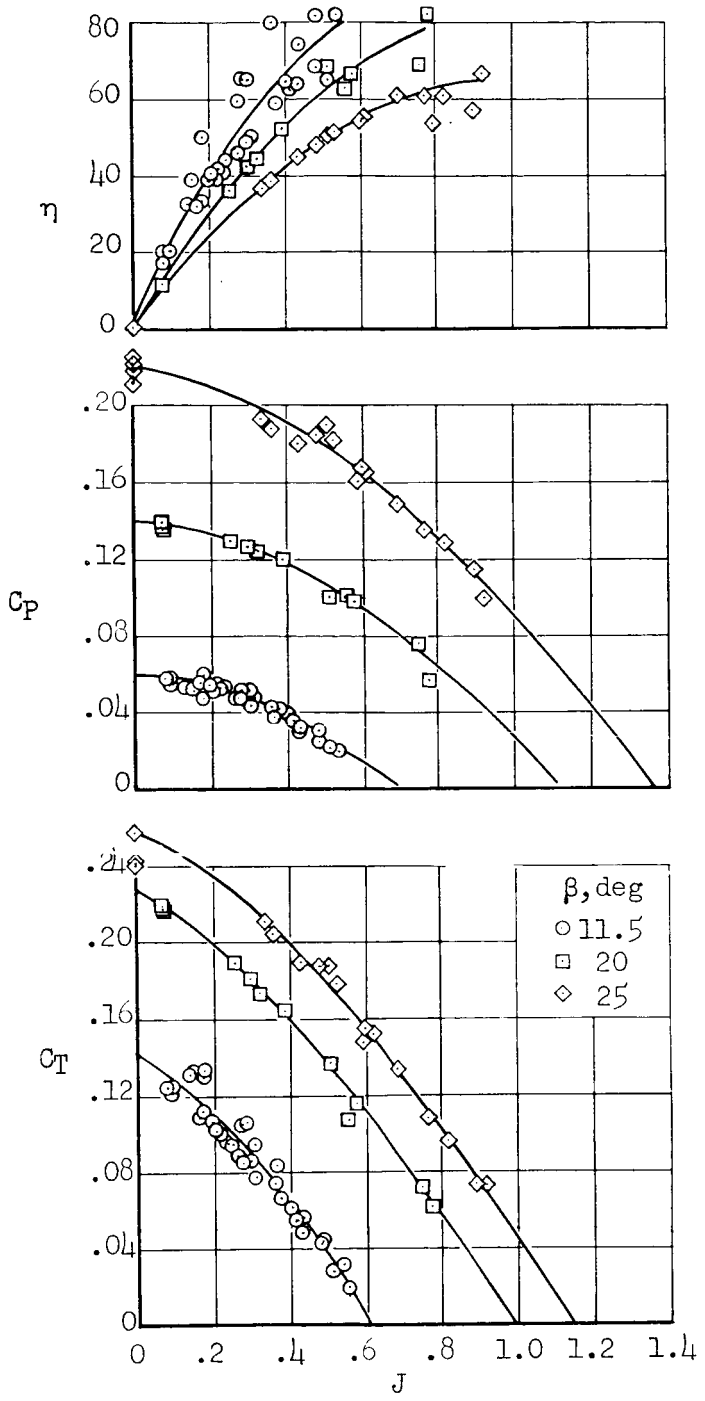

Figure 4.- Propeller characteristics.

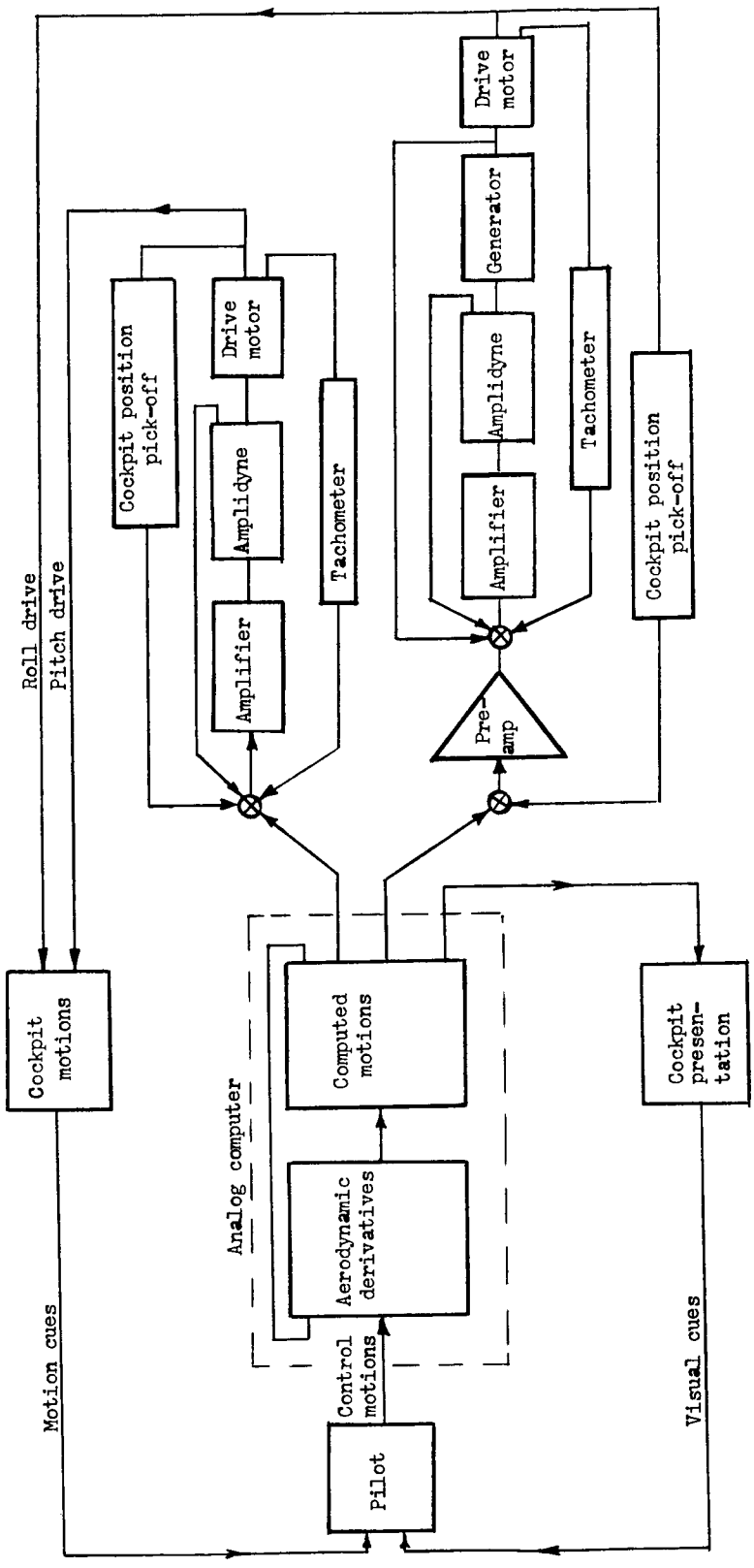

Figure 5.- Block diagram of simulator.

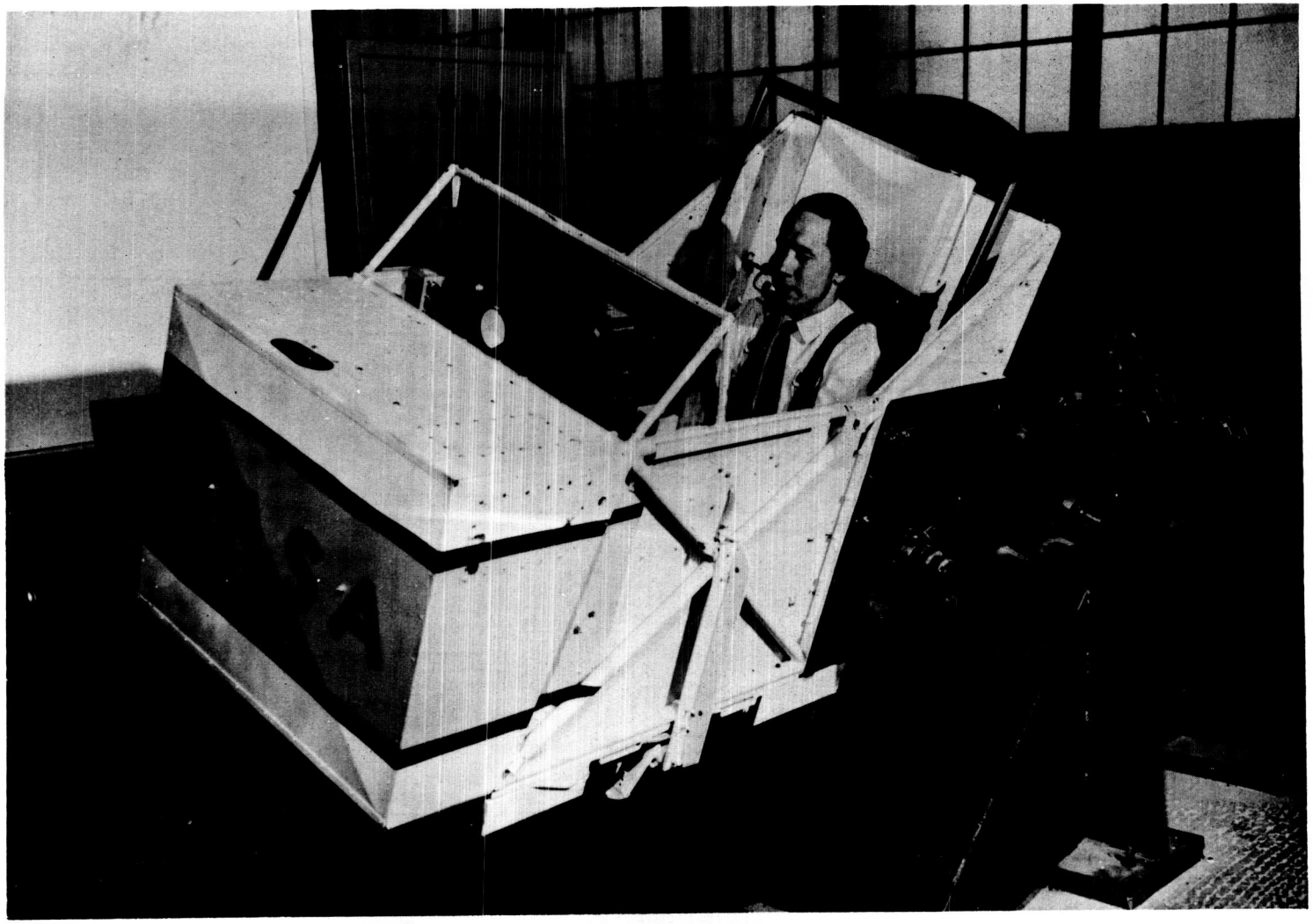

A-25229

(a) Exterior view, 0° of pitch, 20° of roll.

Figure 6.- Photograph of simulator.

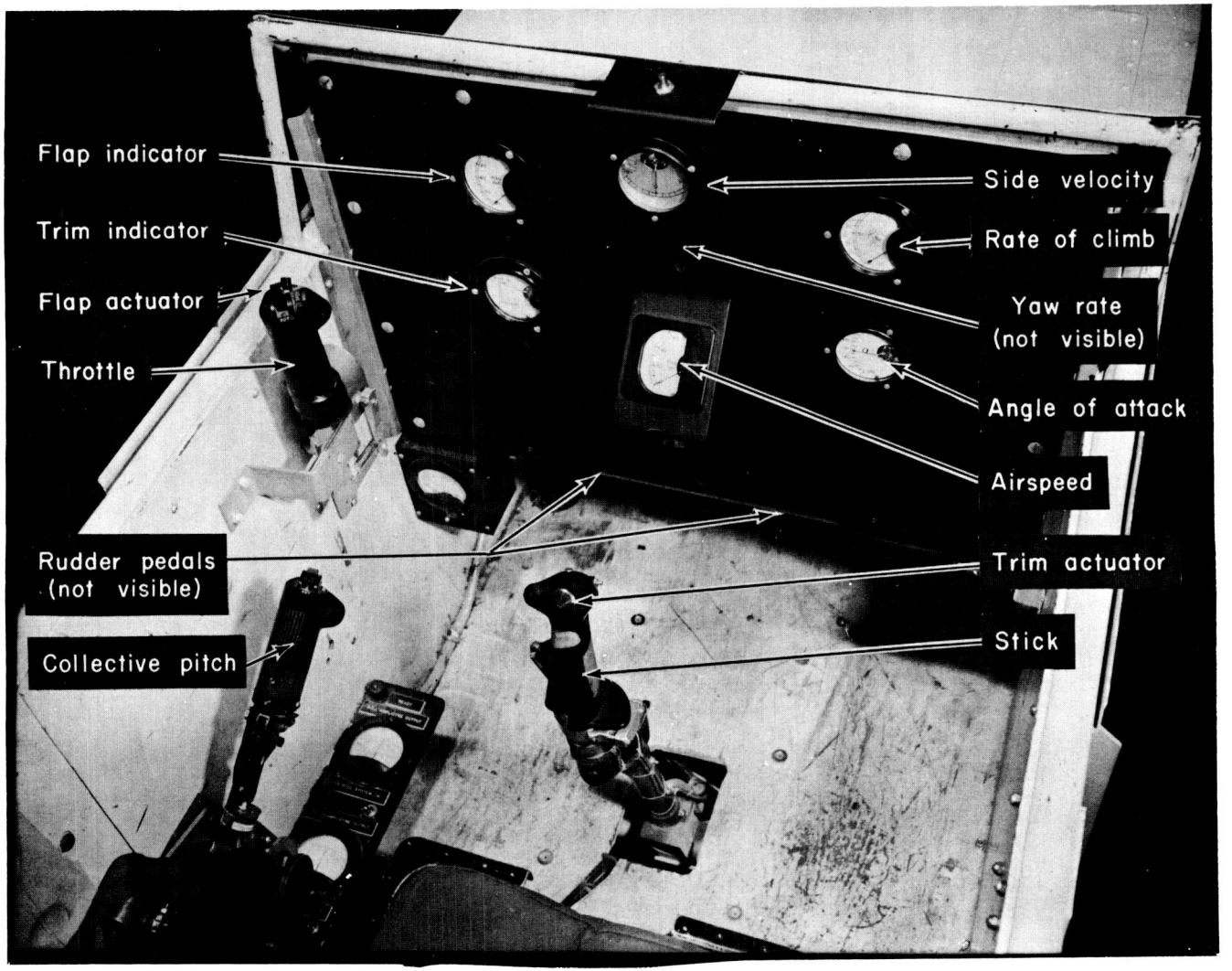

(b) Interior view.

A-24431.1

Figure 6.- Concluded.

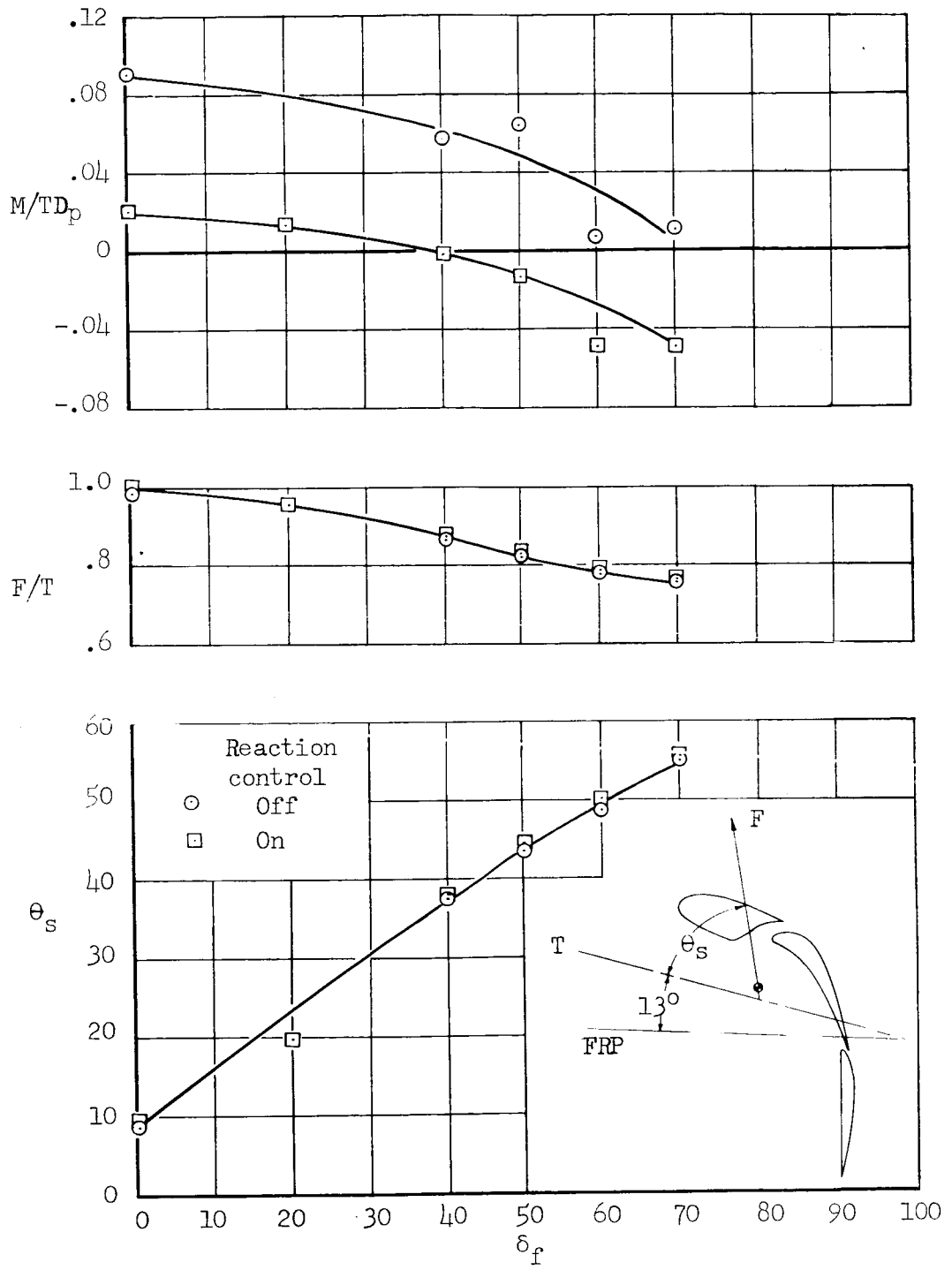

Figure 7.- Effect of flap deflection on turning effectiveness and pitching moment at $U_\infty = 0$, h = 17 feet.

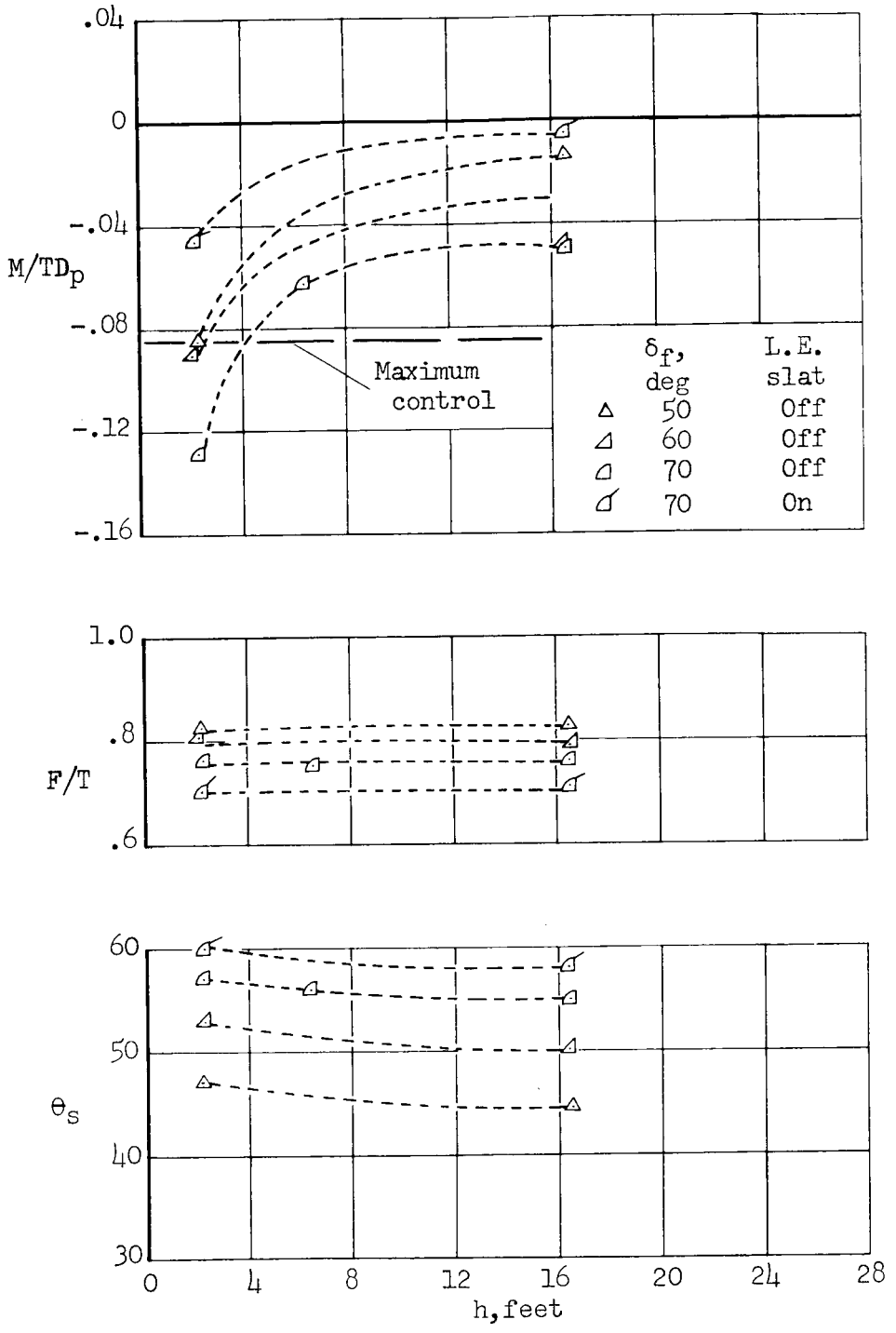

Figure 8.- Effect of height from ground on turning effectiveness and pitching moment for various flap deflections, with and without leading-edge slat; reaction control on, $U_\infty = 0$, thrust approximately 3,000 pounds.

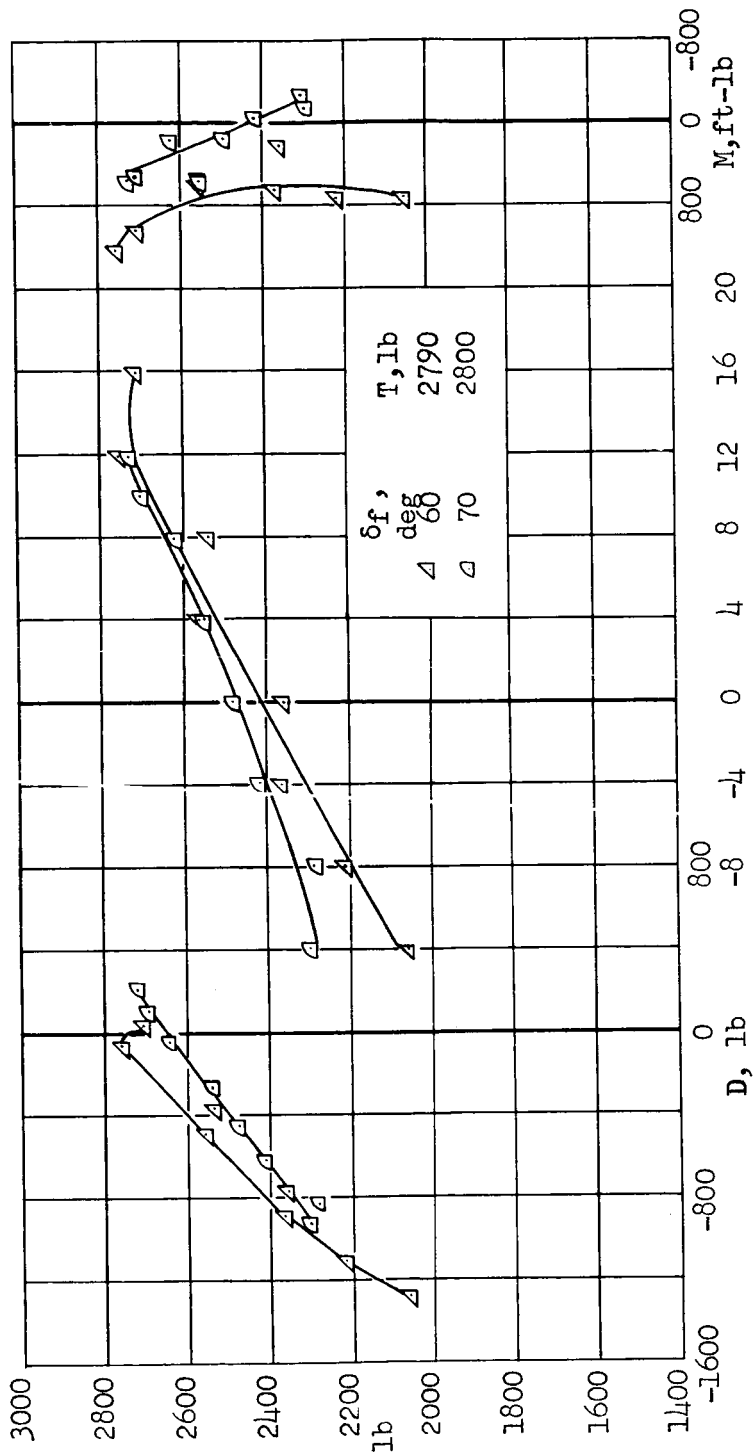

(a) U_∞ = 12.2 knots.

Figure 9.- Lift, drag, and pitching-moment characteristics with various flap deflections and airspeeds; leading-edge slat off, reaction control off, $i_t = 23^\circ$, $\delta_e = 0^\circ$.

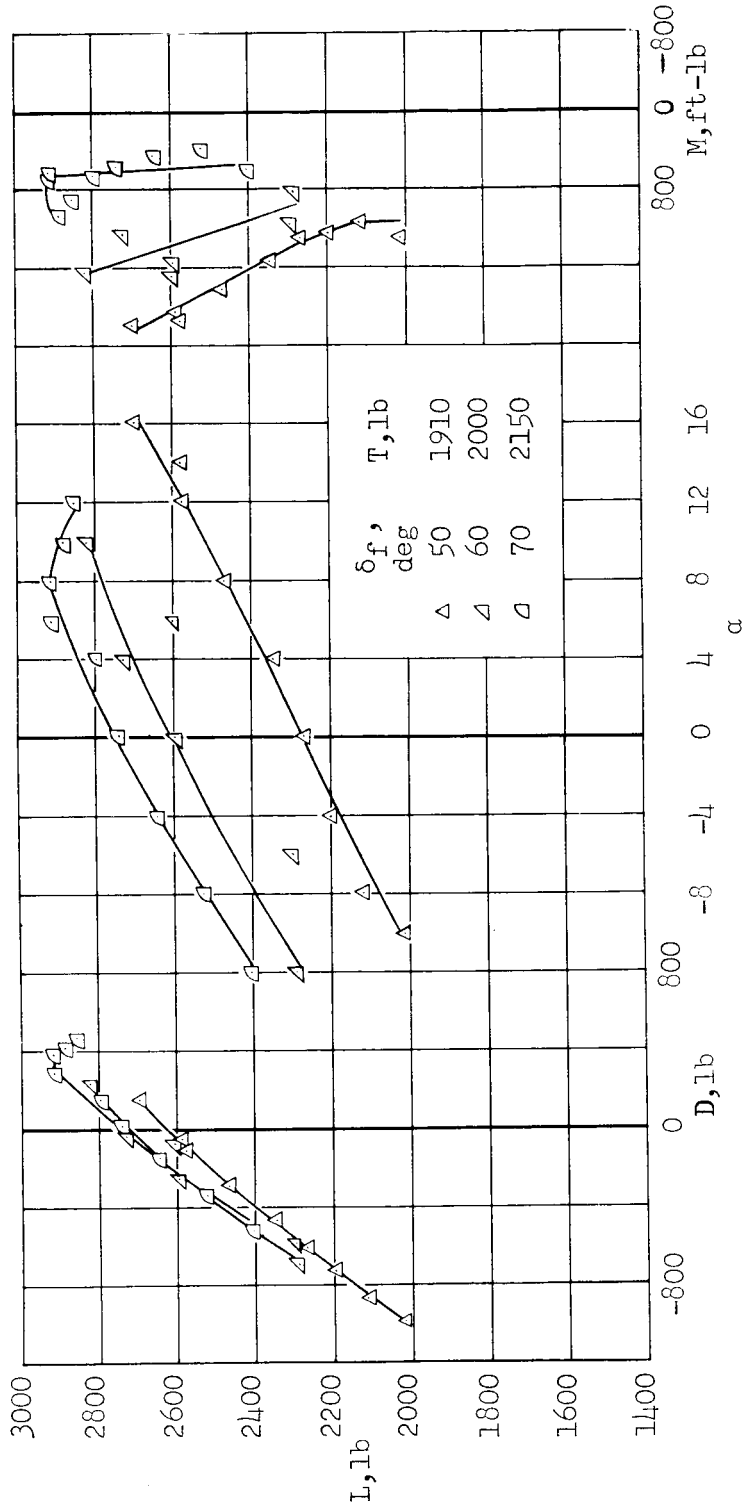

(b) U_∞ = 19.2 knots.

Figure 9.- Continued.

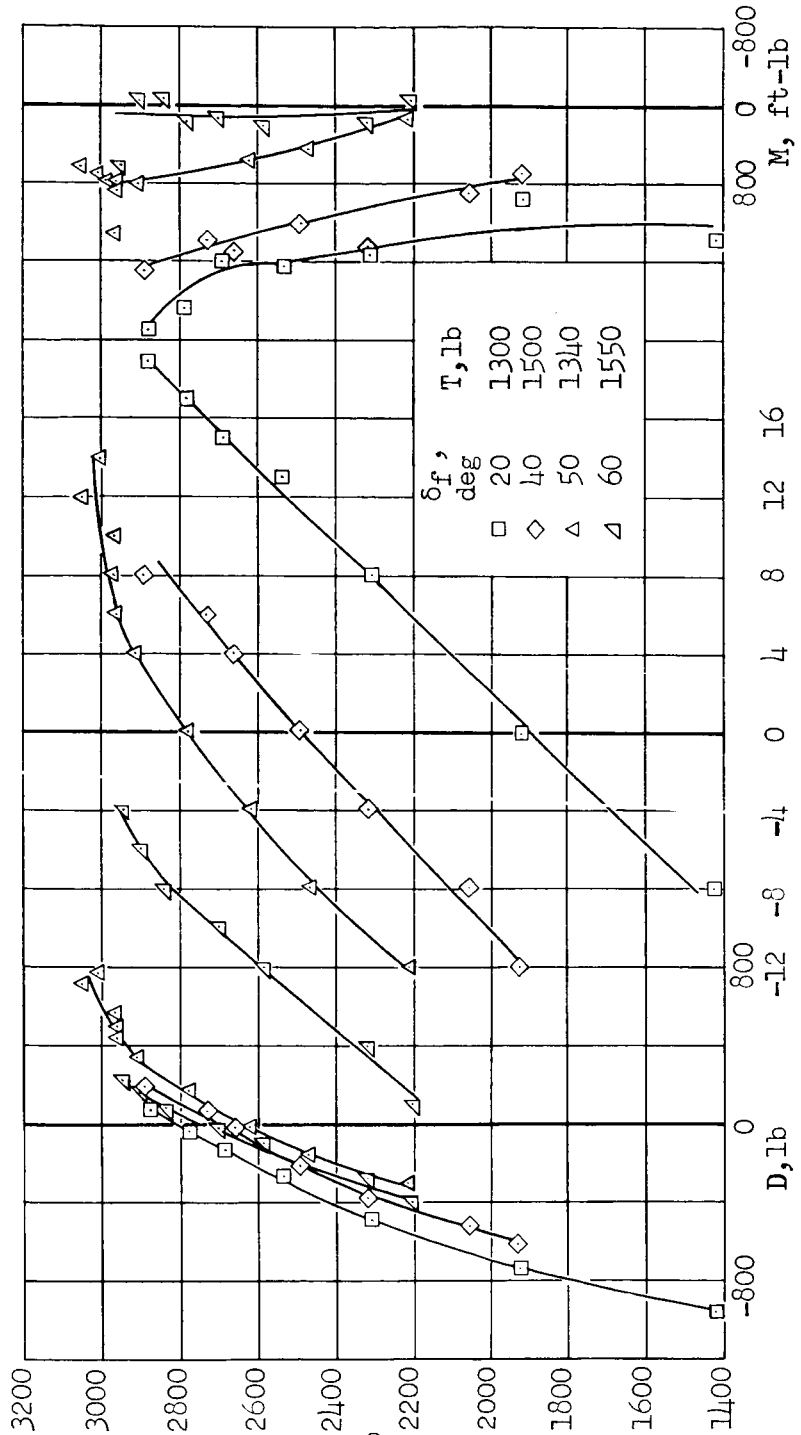

(c) U_∞ = 29.9 knots.

Figure 9.- Continued.

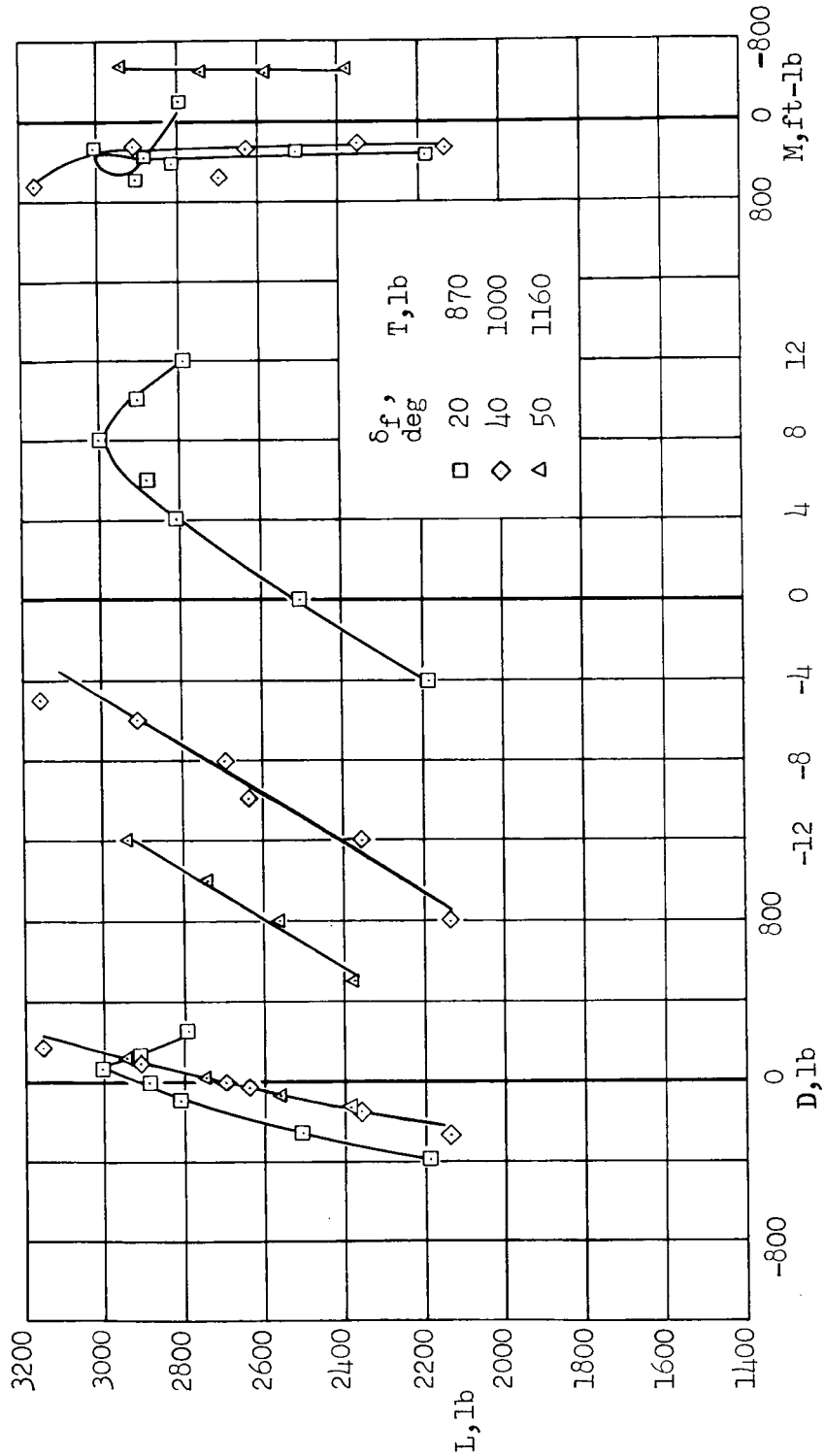

(d) U_∞ = 42.2 knots.

Figure 9.- Continued.

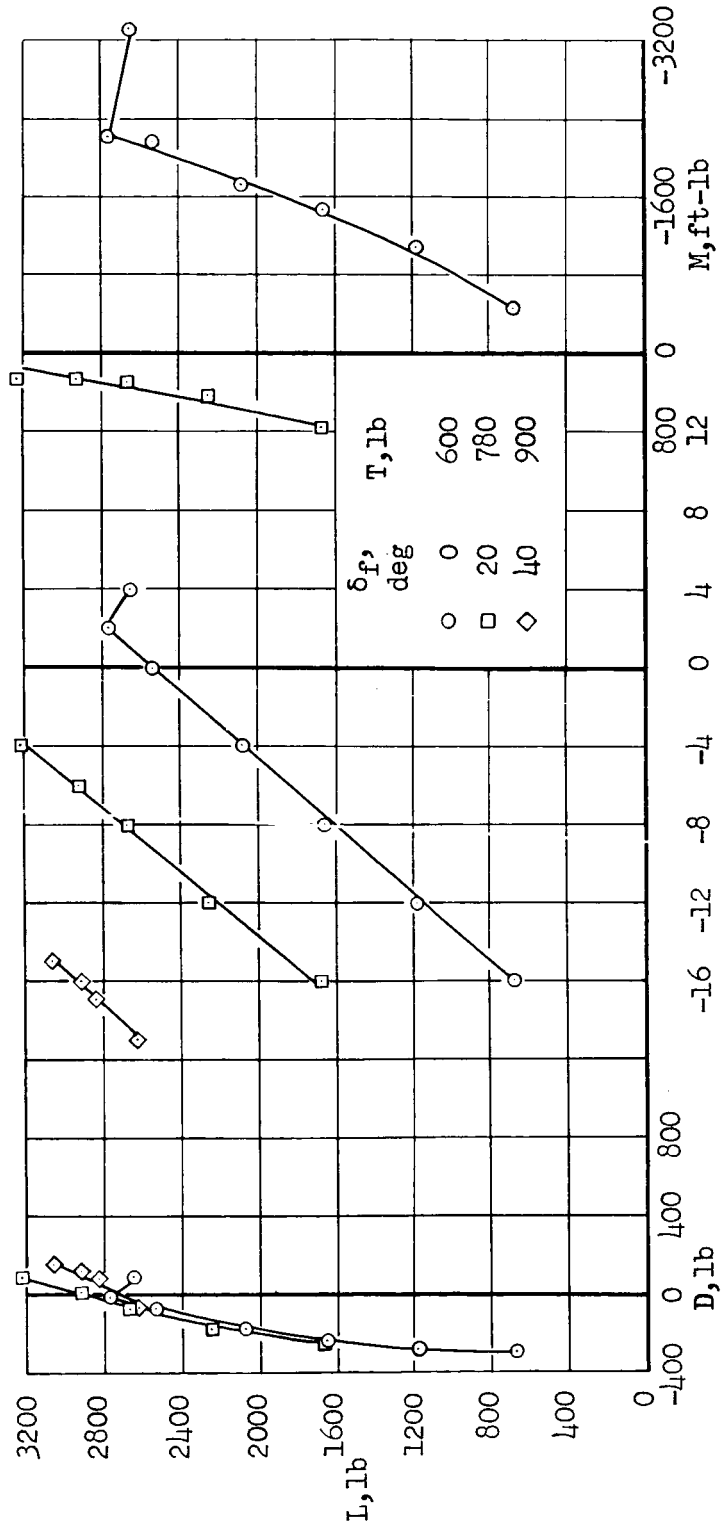

(e) U_∞ = 54.5 knots.

Figure 9.- Continued.

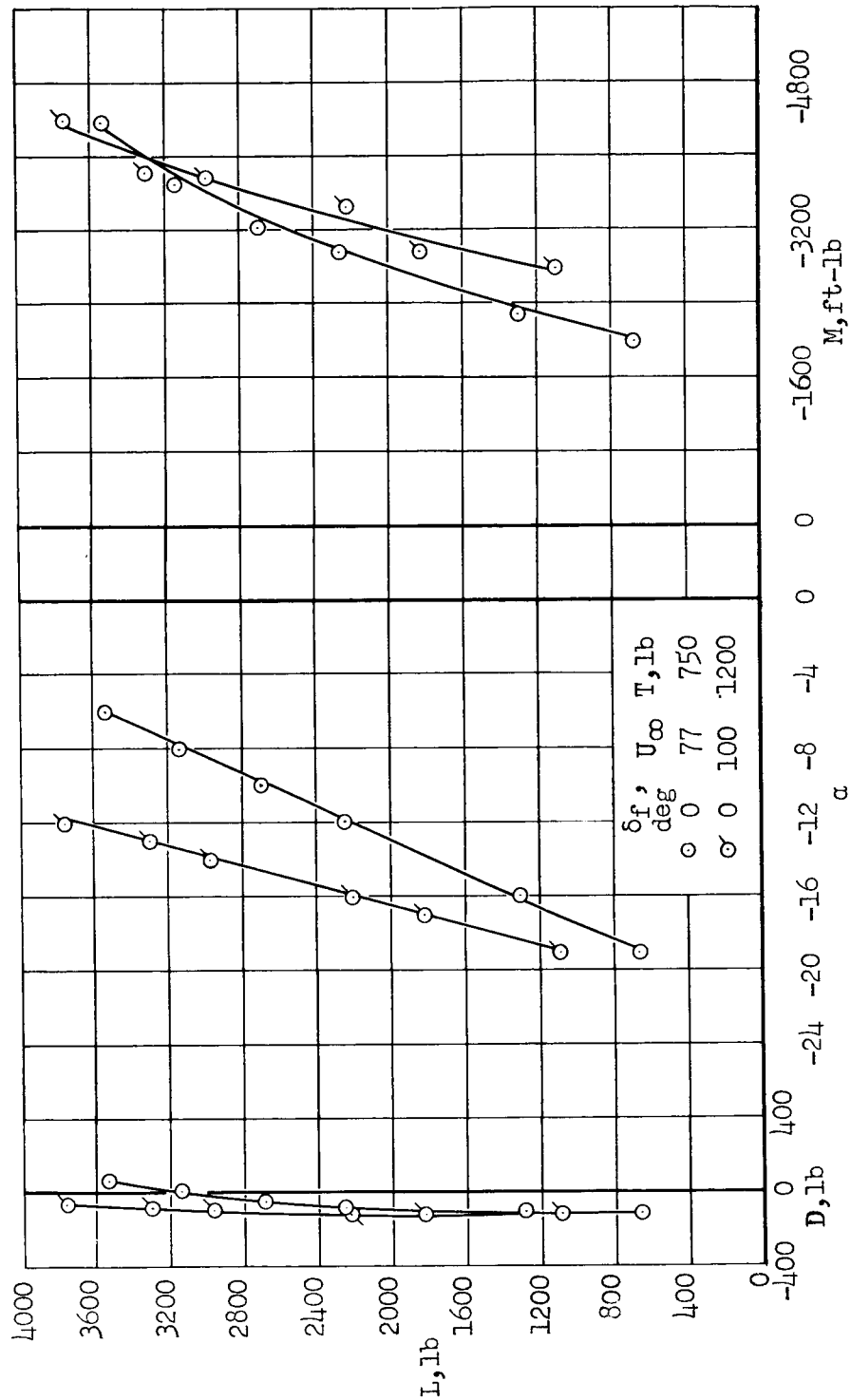

(f) U_∞ = 77 and 100 knots.

Figure 9.- Concluded.

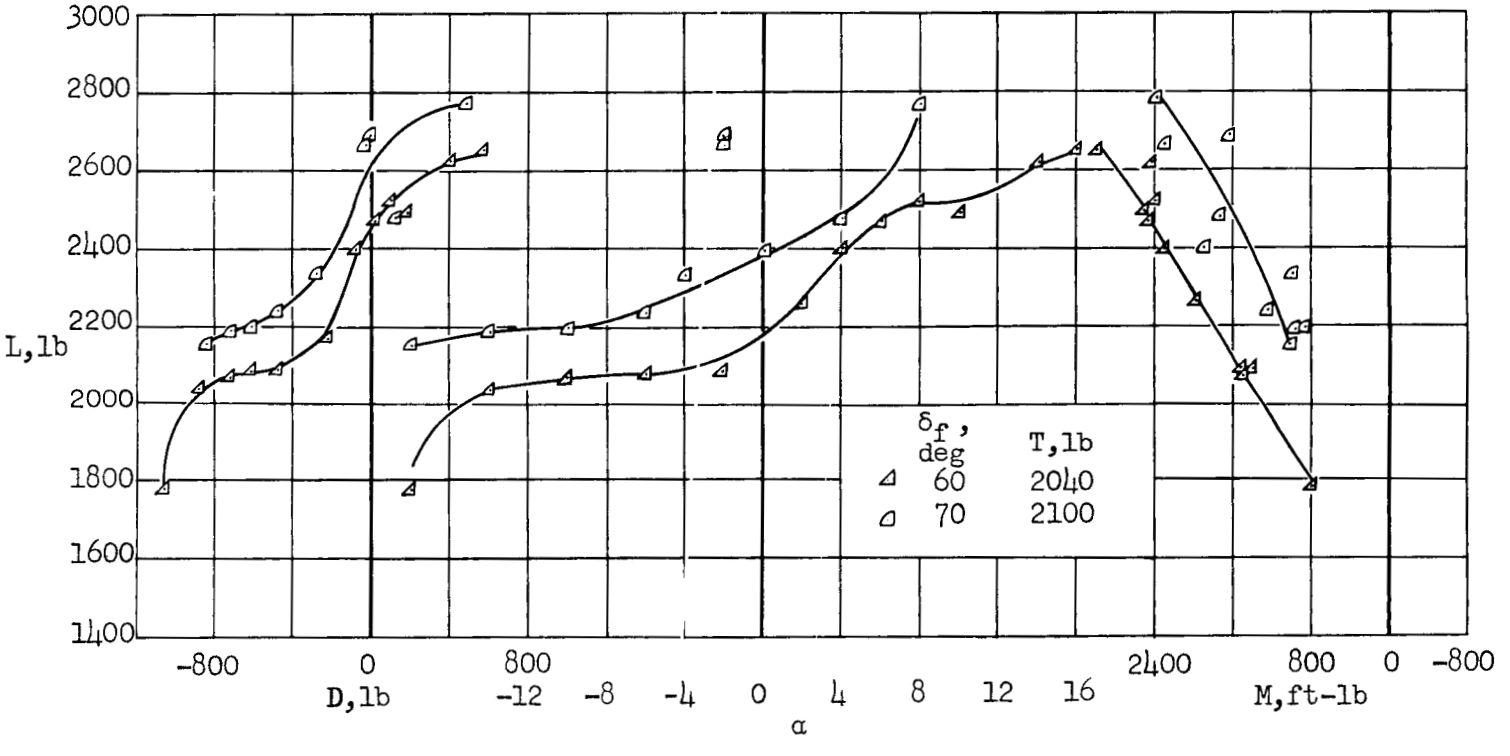

(a) V_∞ = 12.2 knots.

Figure 10.- Lift, drag, and pitching-moment characteristics with various flap deflections and airspeeds; leading-edge slat on, reaction control on, $i_t = 23^\circ$, $\delta_e = -5^\circ$.

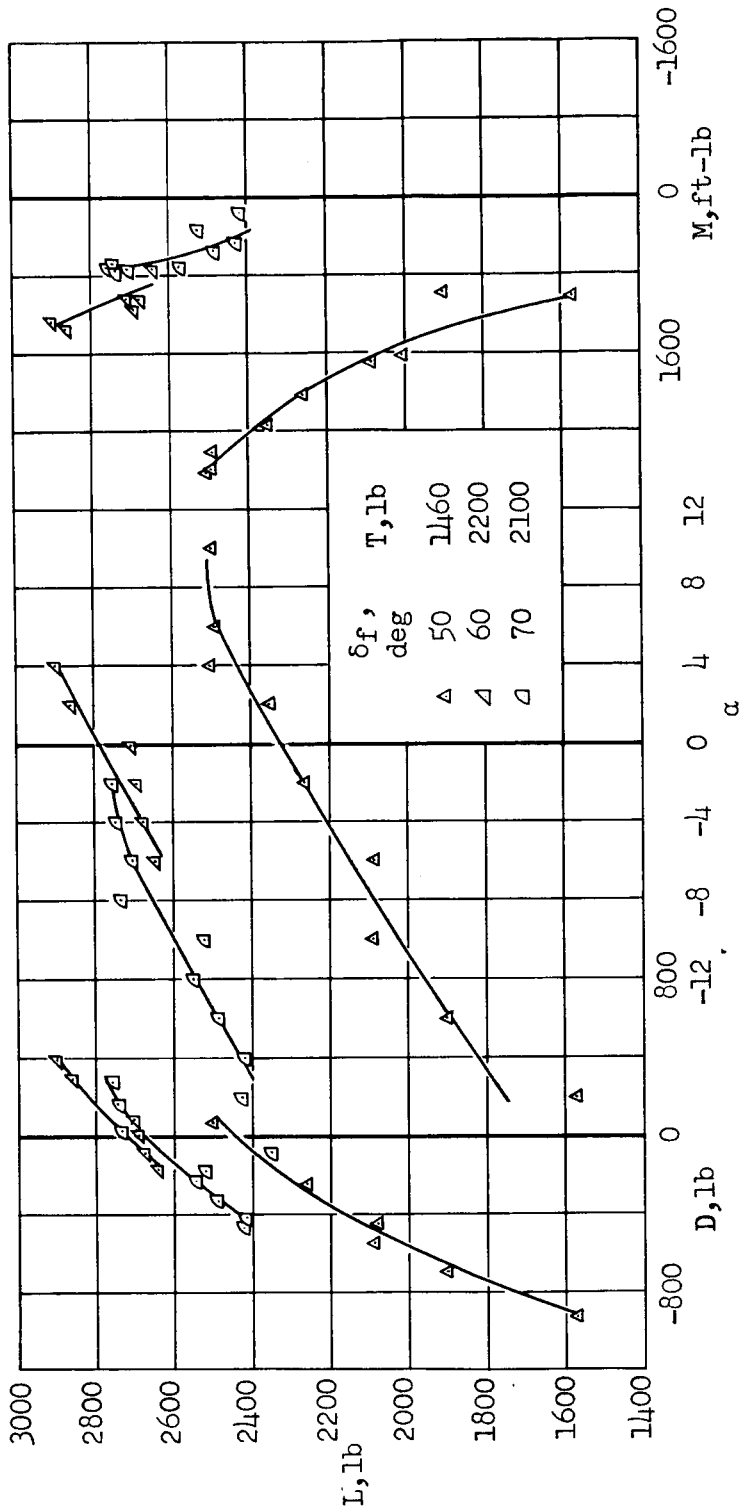

(b) U_∞ = 19.2 knots.

Figure 10.- Continued.

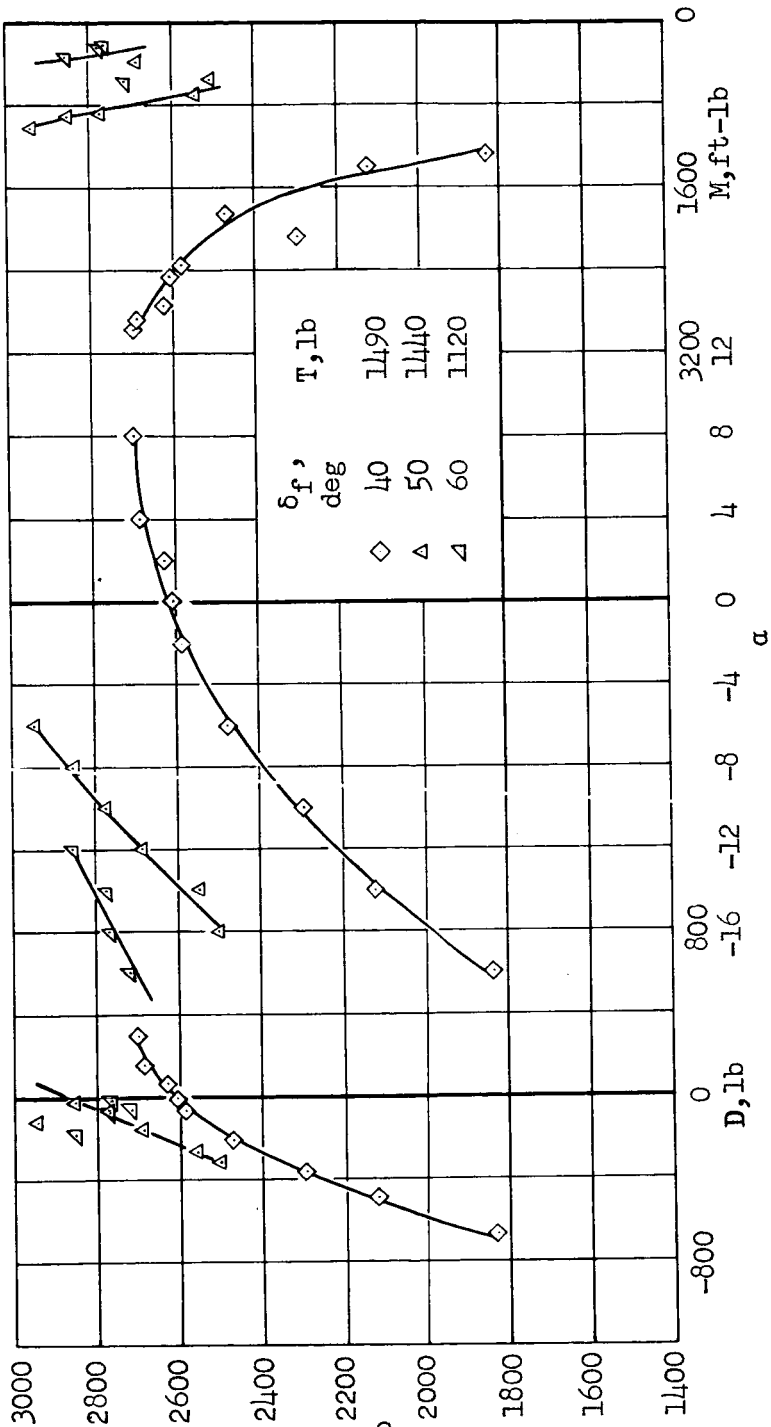

(c) U_∞ = 29.9 knots.

Figure 10.- Continued.

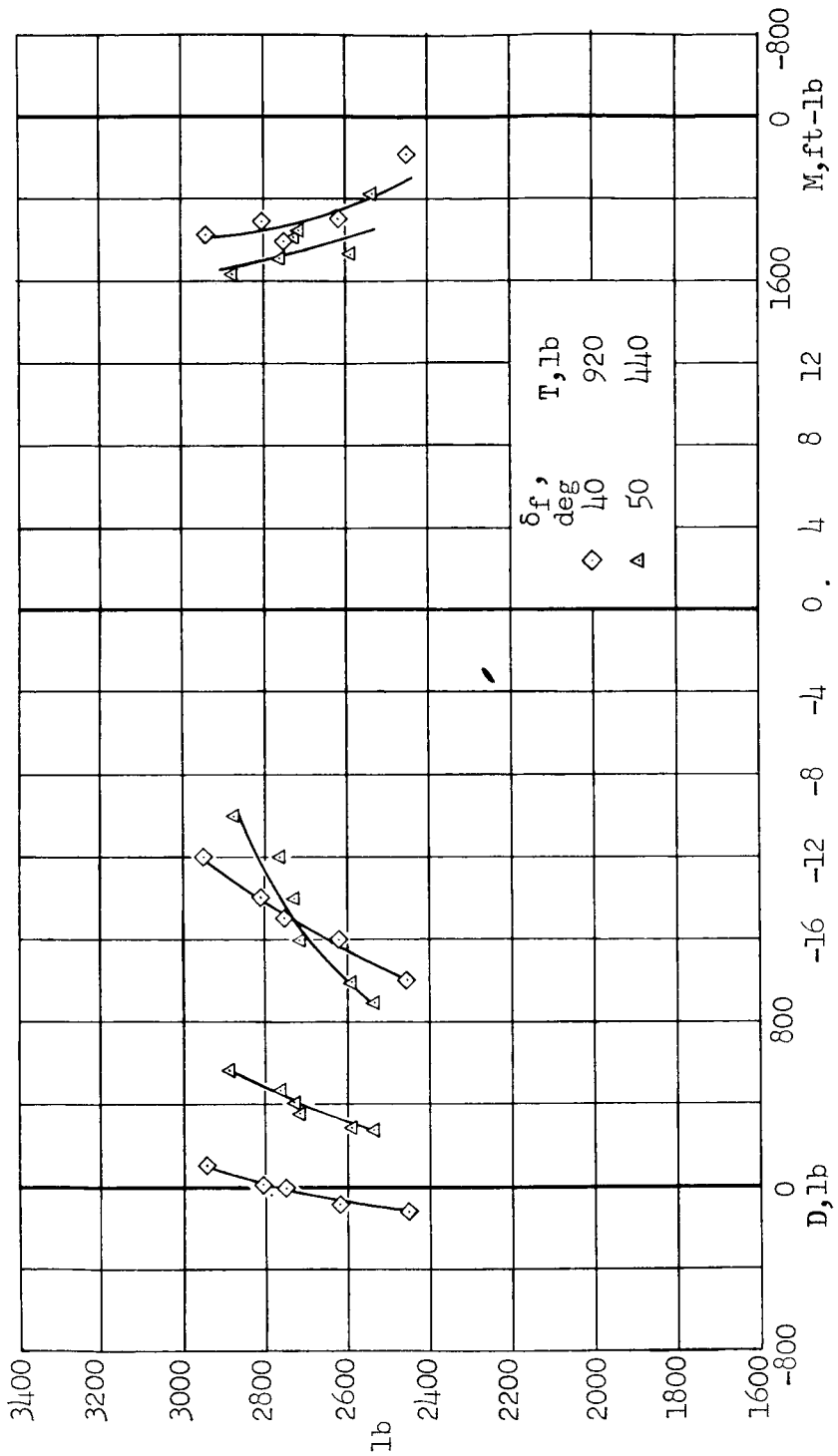

(d) U_∞ = 42.2 knots.

Figure 10.- Concluded.

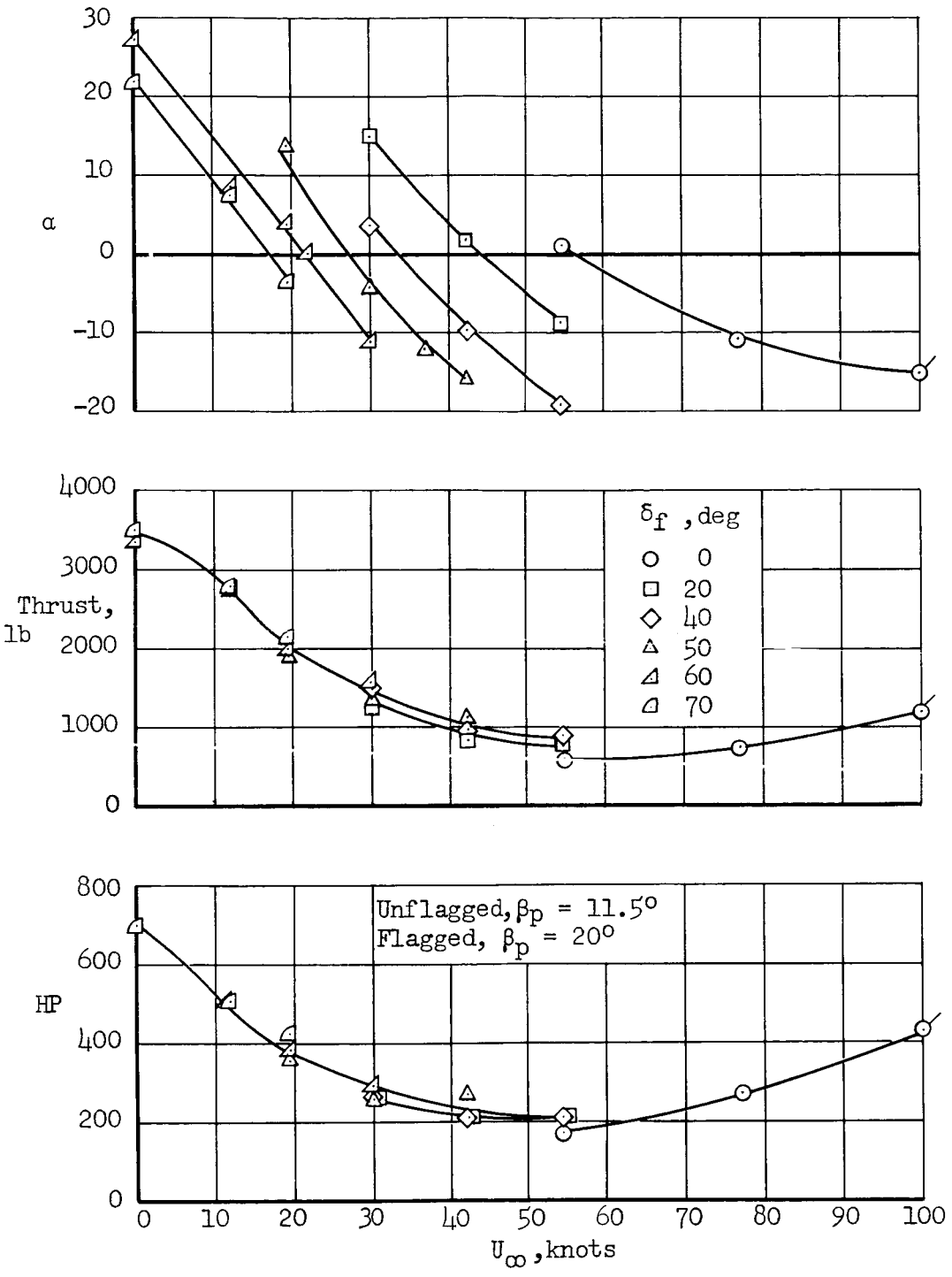

(a) Fuselage angle of attack, thrust, and power required.

Figure 11.- Summary of longitudinal characteristics for 1g level flight; leading-edge slat off, $i_t = 23^\circ$.

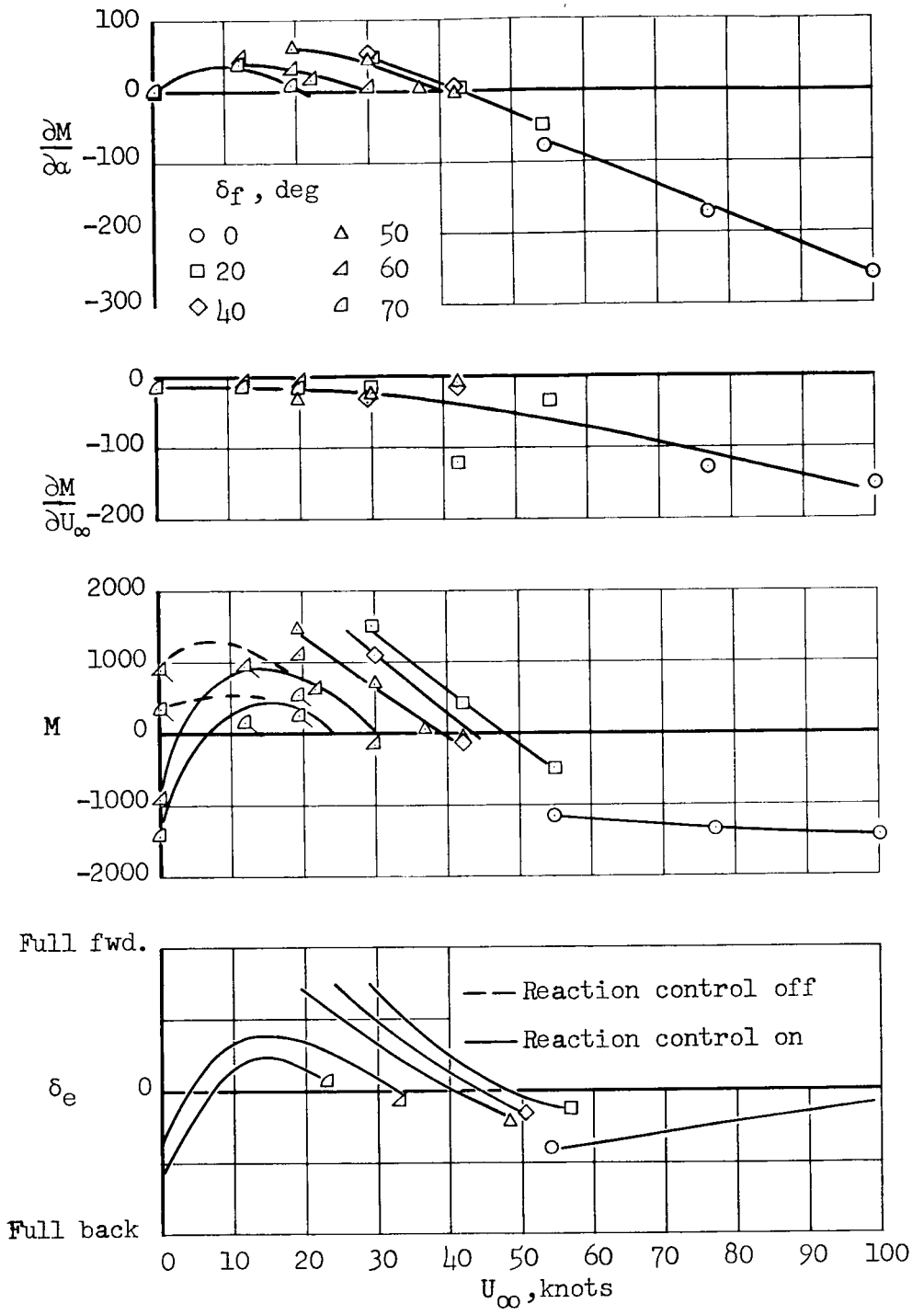

(b) Stability, foot-pounds per degree and foot-pounds per knot; pitching moment with neutral stick, foot-pounds with $\delta_e = -5^o$; and stick position to trim.

Figure 11.- Concluded.

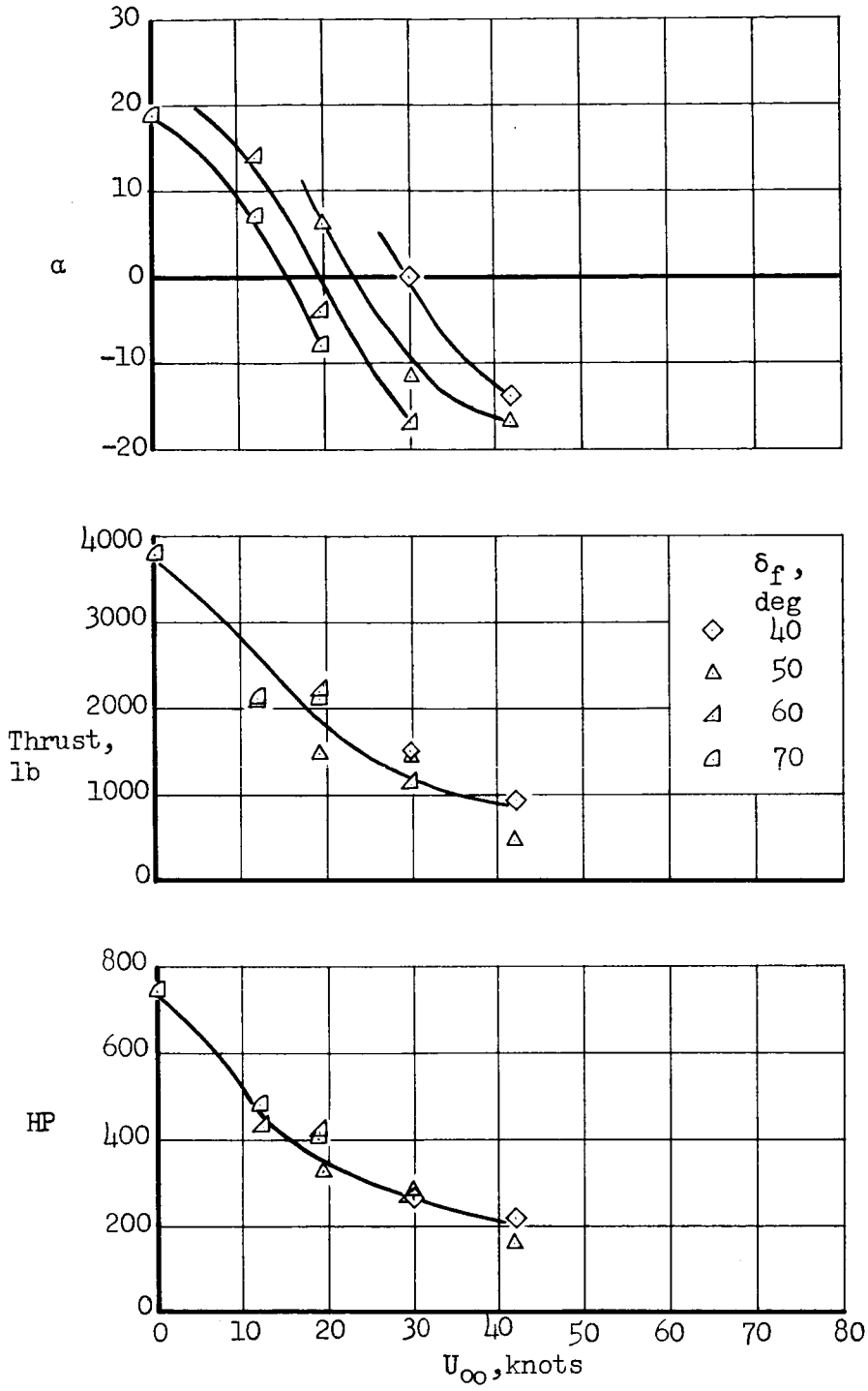

(a) Fuselage angle of attack, thrust, and power required.

Figure 12.- Summary of longitudinal characteristics for 1g level flight; leading-edge slat on, $i_t = 23^{\circ}$.

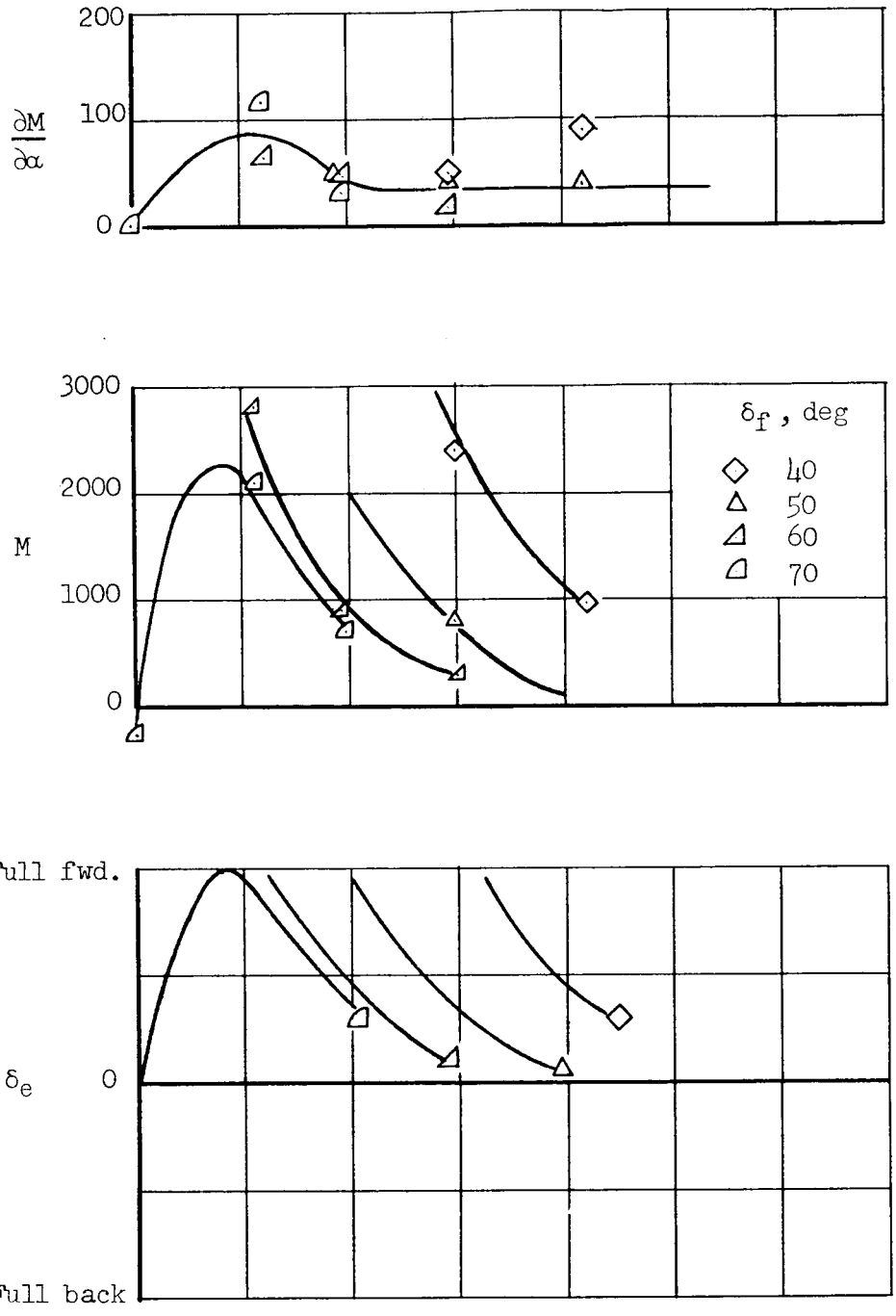

(b) Stability; pitching moment with neutral stick ($\delta_e = -5^\circ$); stick position to trim; reaction control on.

Figure 12.- Concluded.

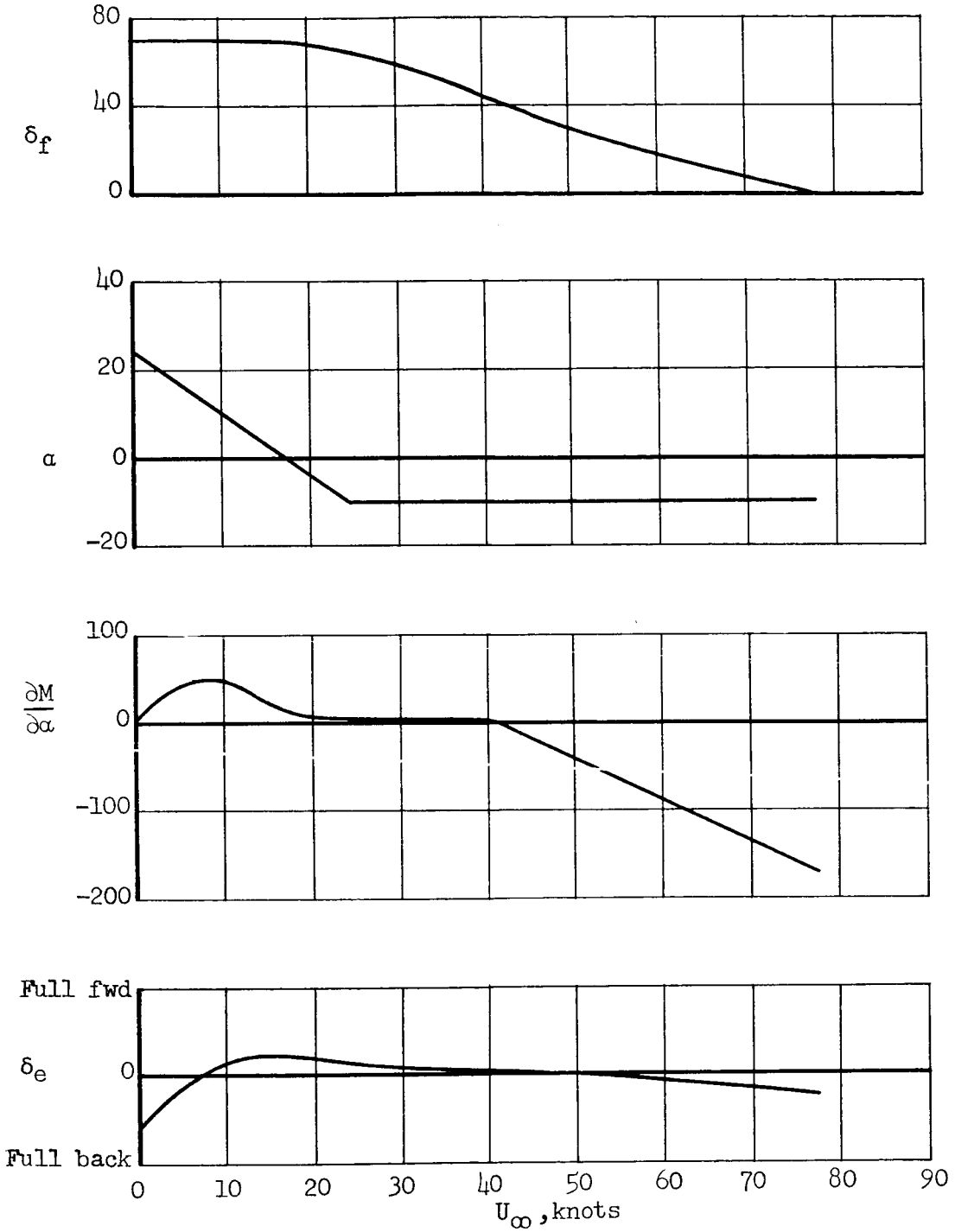

Figure 13.- Example of a transition program for the airplane with reaction control on; leading-edge slat off, $i_t = 23^\circ$.

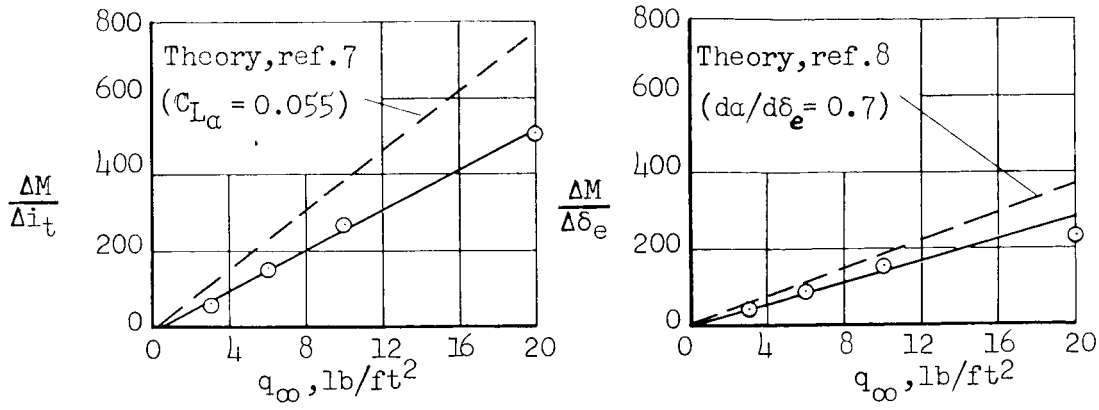

(a) Stabilizer and elevator effectiveness without reaction control.

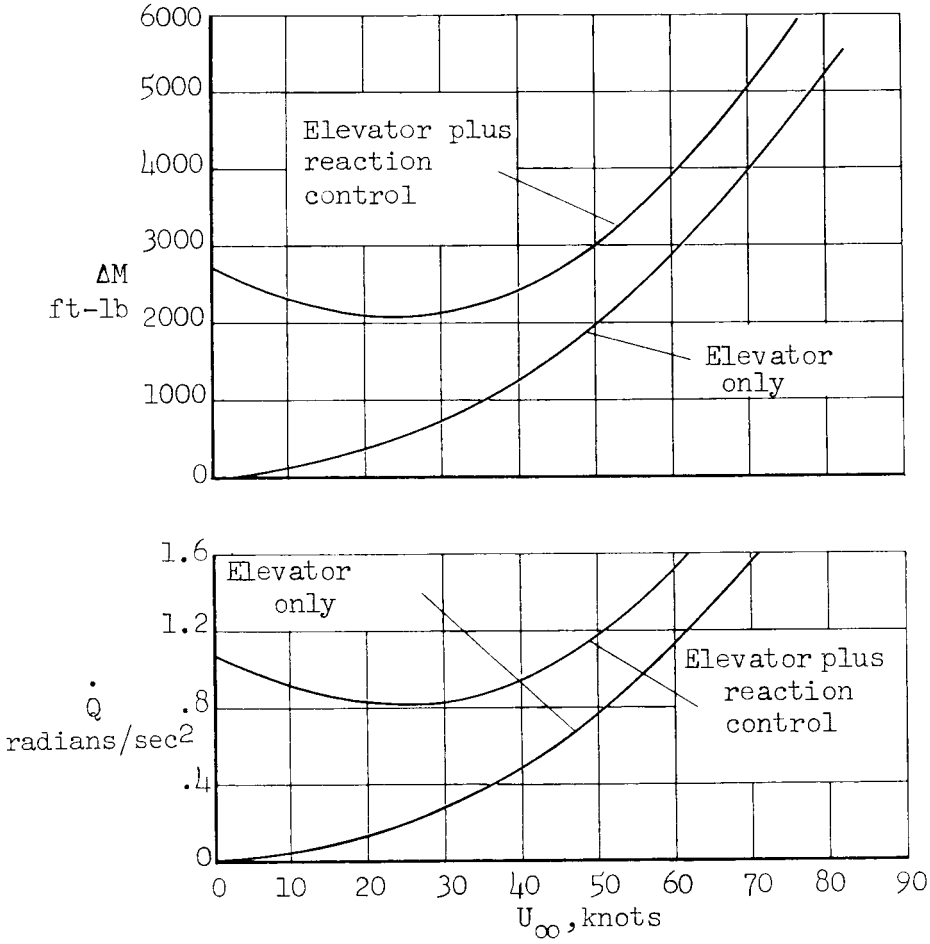

(b) Pitching moment and calculated maximum pitching acceleration obtained with full stick movement from neutral position; $\Delta\delta_e = 15^\circ$.

Figure 14.- Longitudinal control characteristics for level flight.

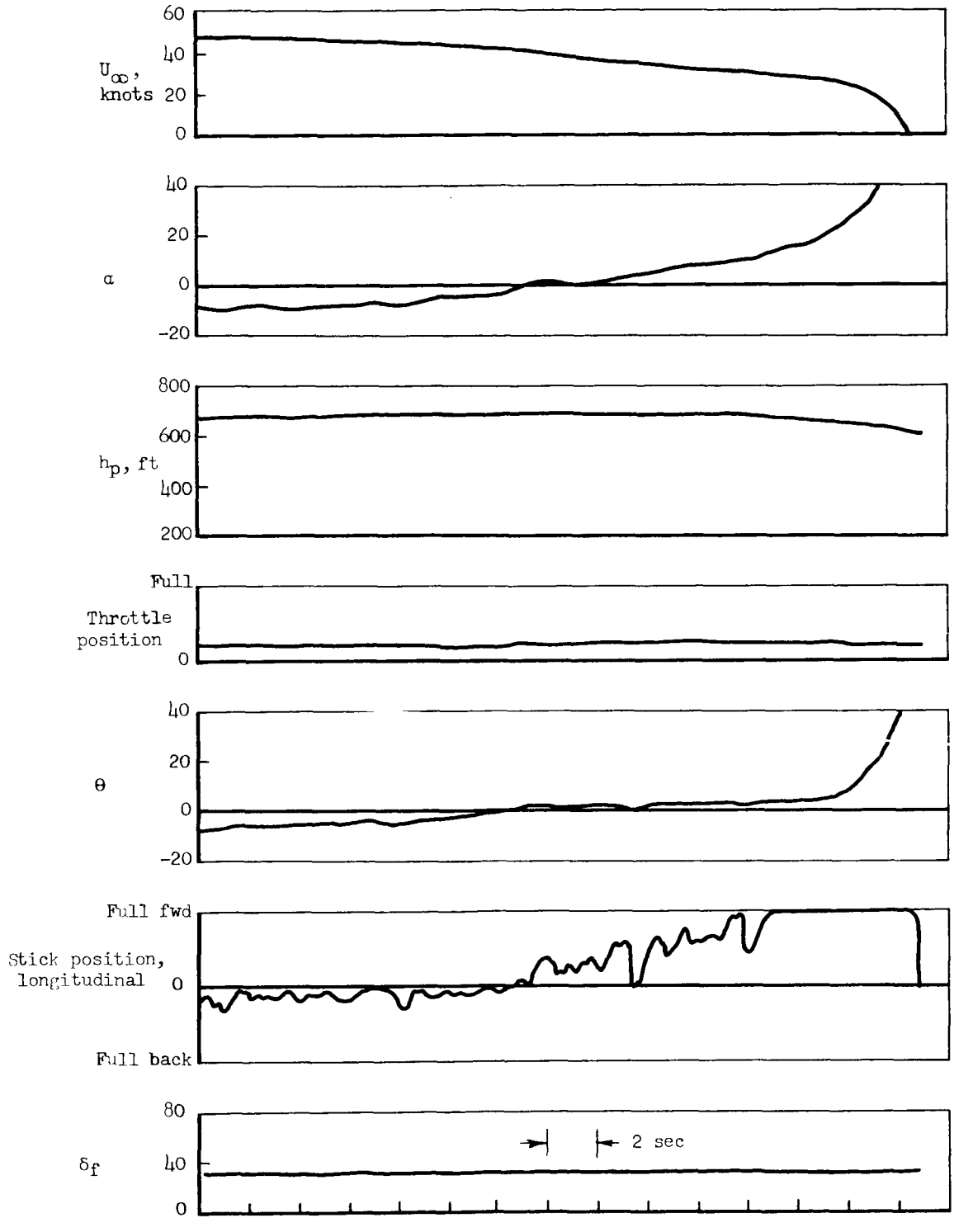

Figure 15.- Time history of an uncontrolled pitch-up in the simulation.

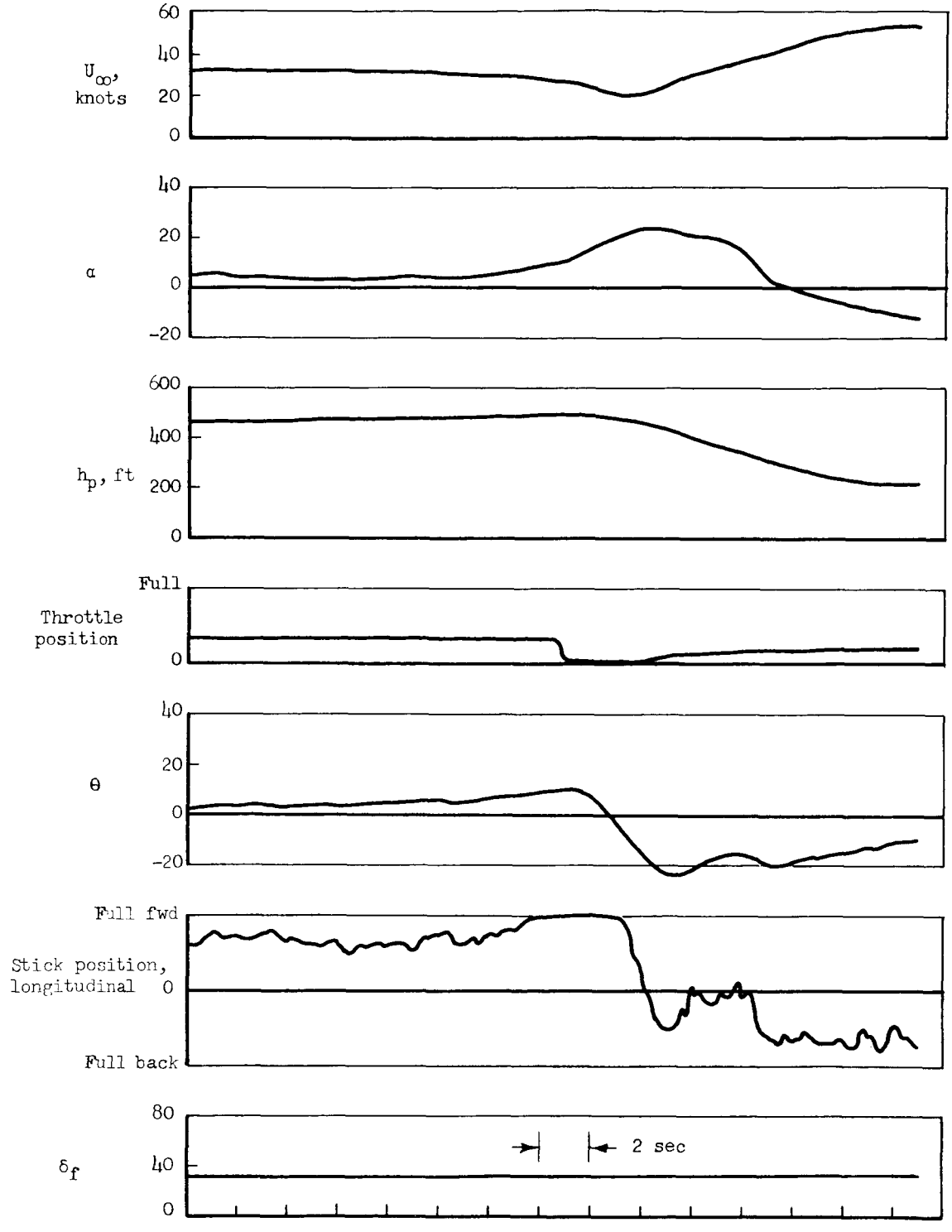

Figure 16.- Time history of a controlled pitch-up using throttle control in the simulation.

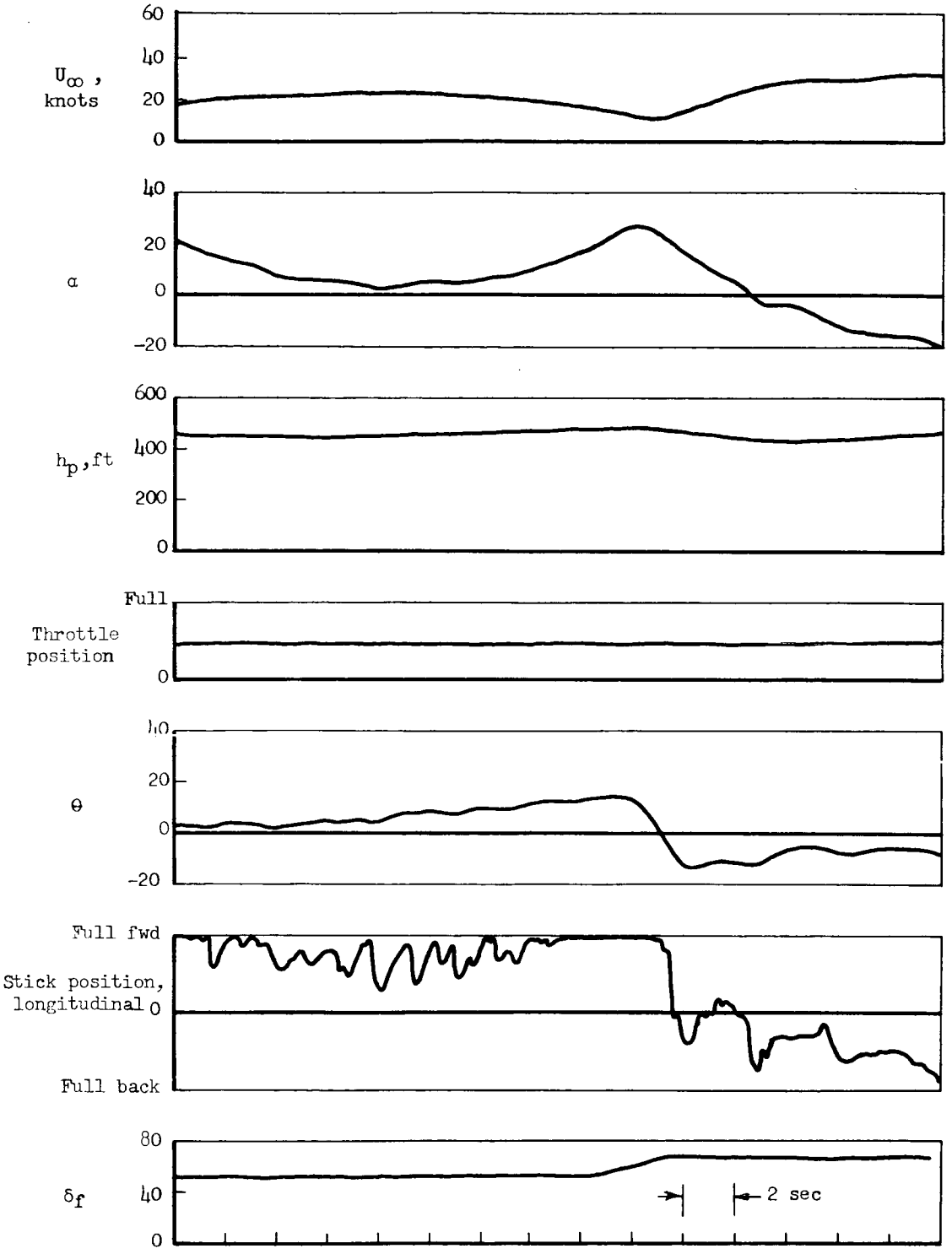

Figure 17.- Time history of a controlled pitch-up using flap control in the simulation.

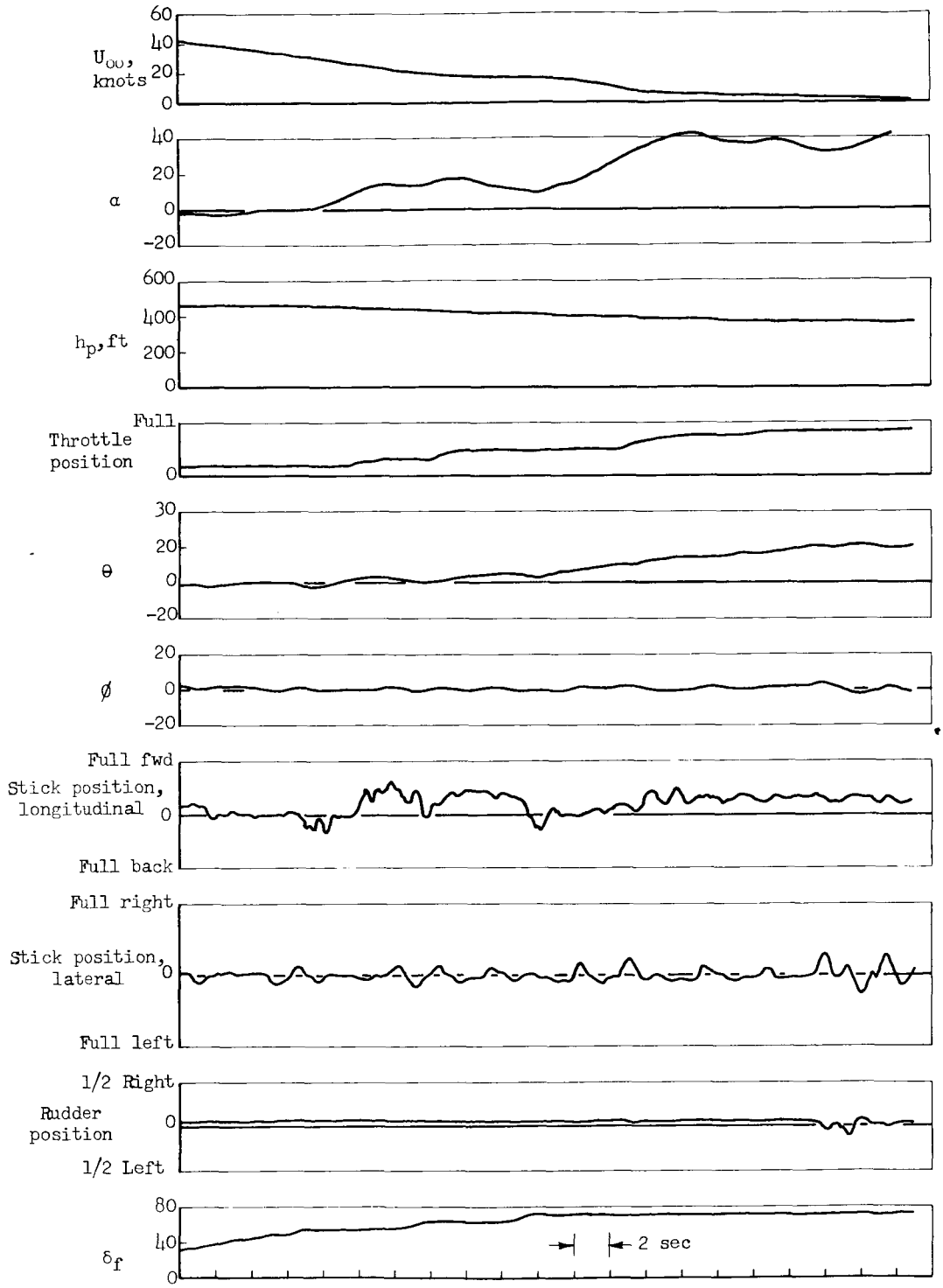

(a) Decreasing speed.

Figure 18.- Time histories of typical transitions in the simulation.

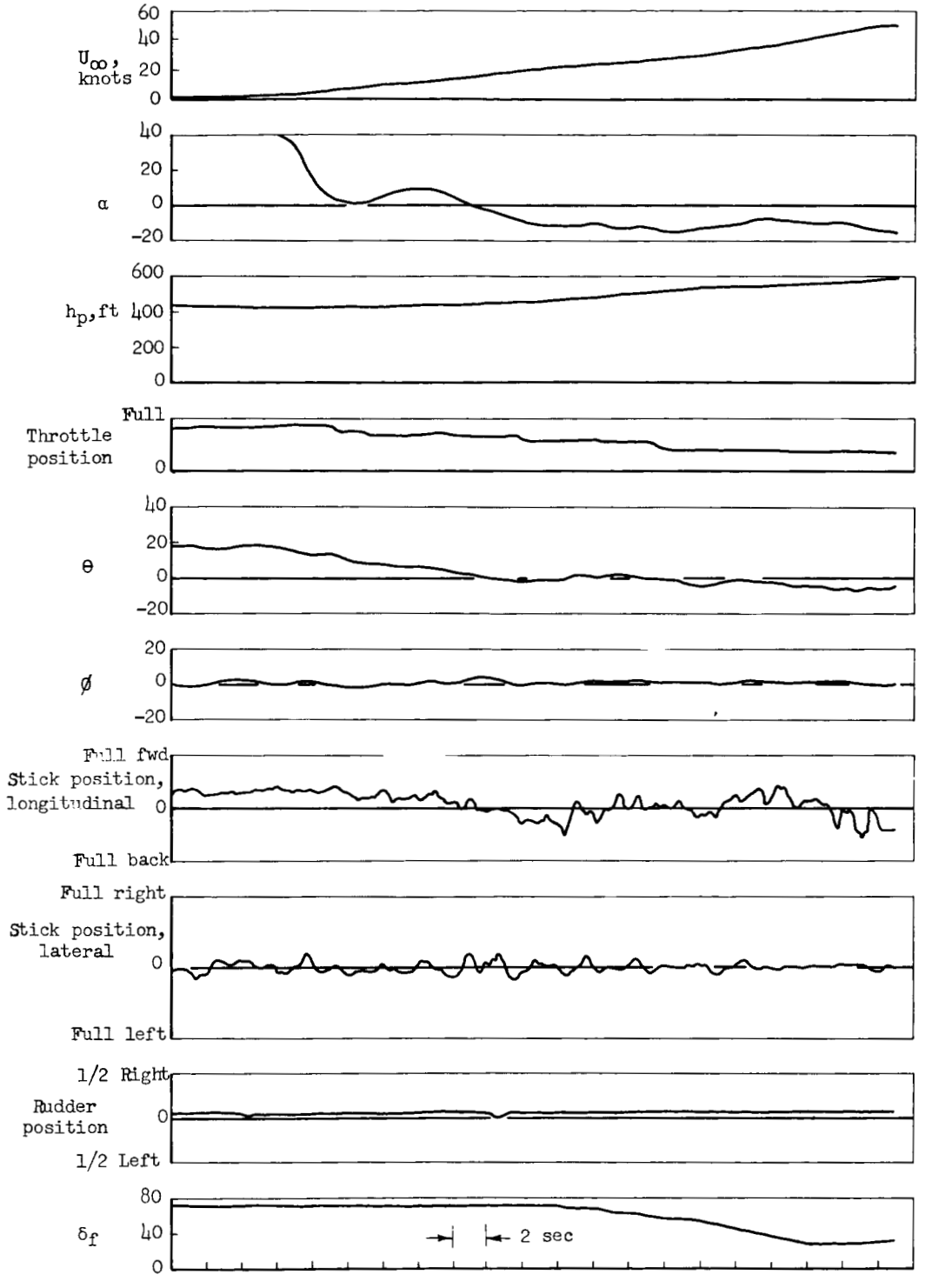

(b) Increasing speed.

Figure 18.- Concluded.

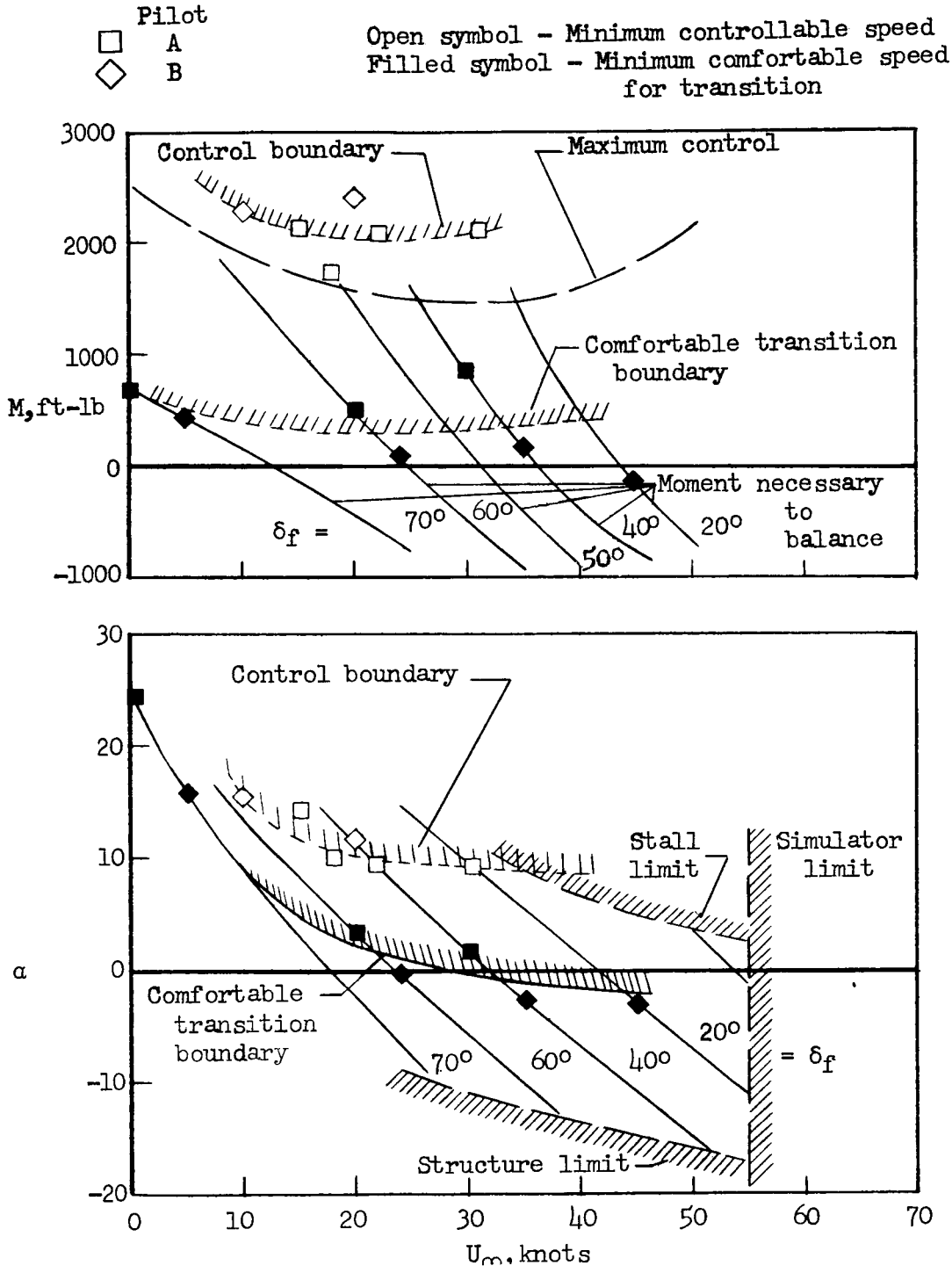

Figure 19.- Boundaries selected by the pilot in the simulation; leading-edge slat off, $i_t = 23^\circ$.

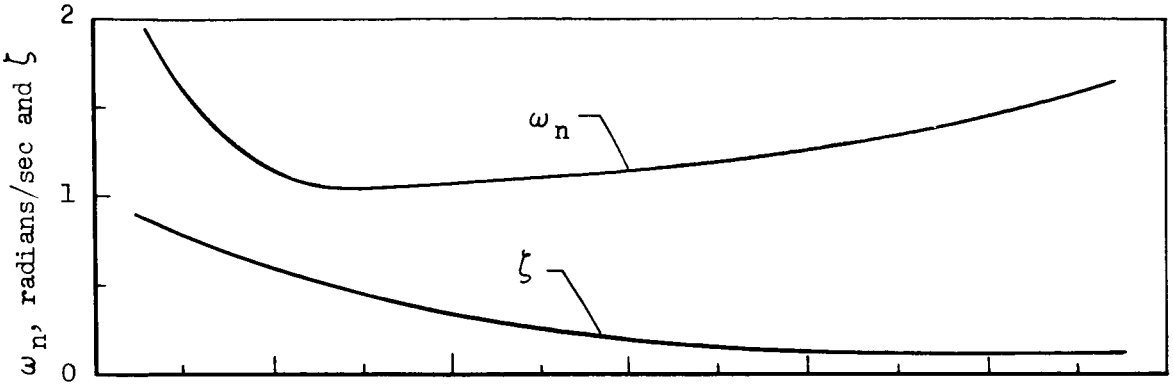

(a) Lateral-directional dynamic characteristics for three degrees of freedom.

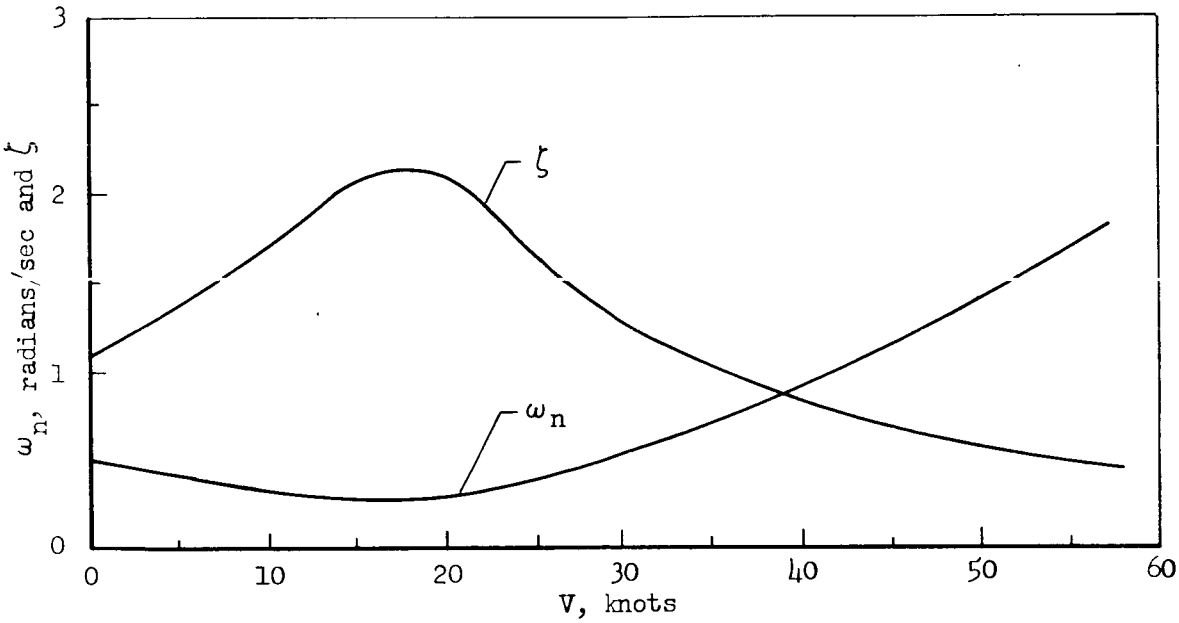

(b) Longitudinal dynamic characteristics for two degrees of freedom.

Figure 20.- Short period longitudinal and lateral-directional dynamic characteristics.

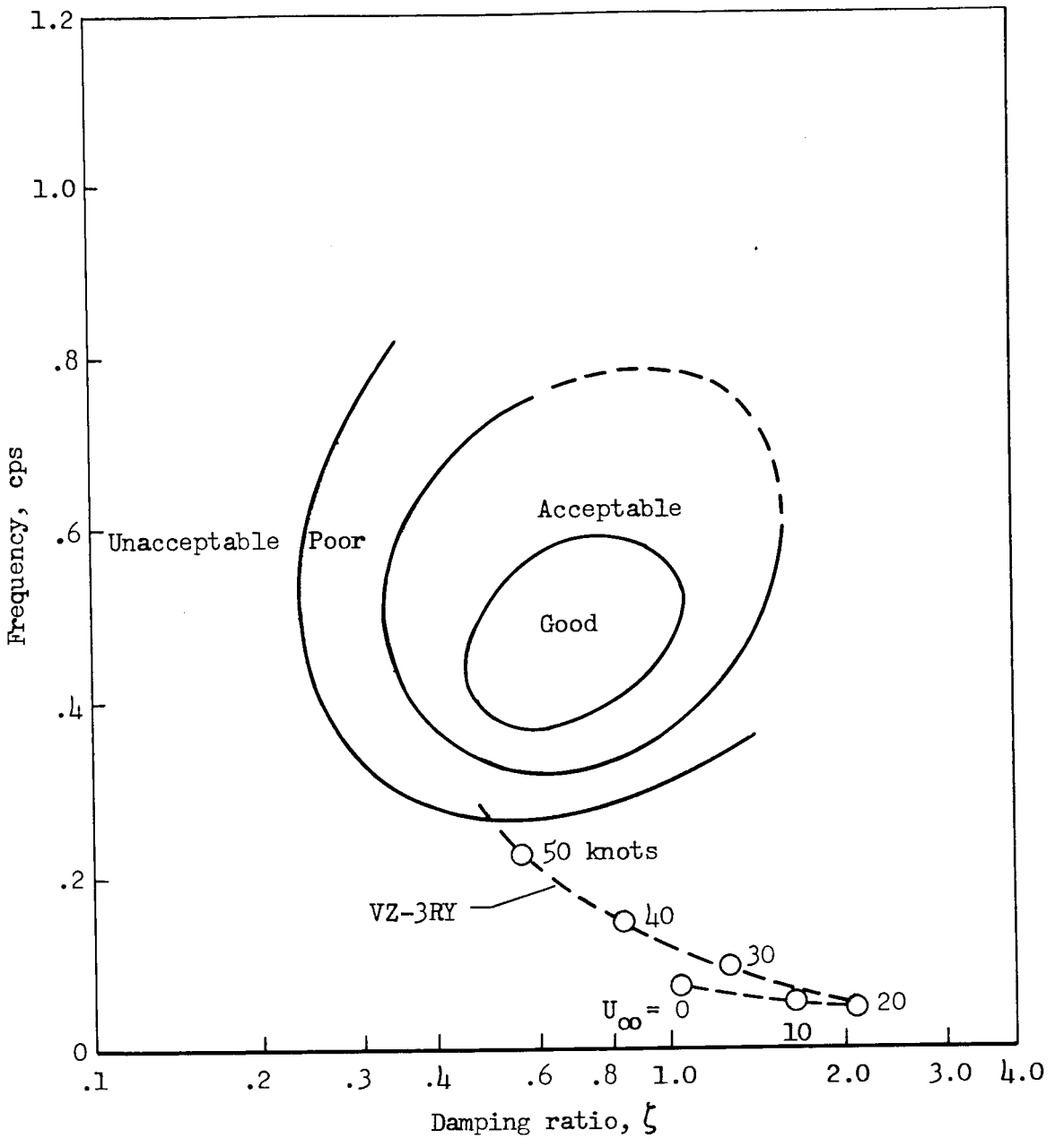

Figure 21.- Natural longitudinal damping characteristics compared with general airplane studies (ref. 9).

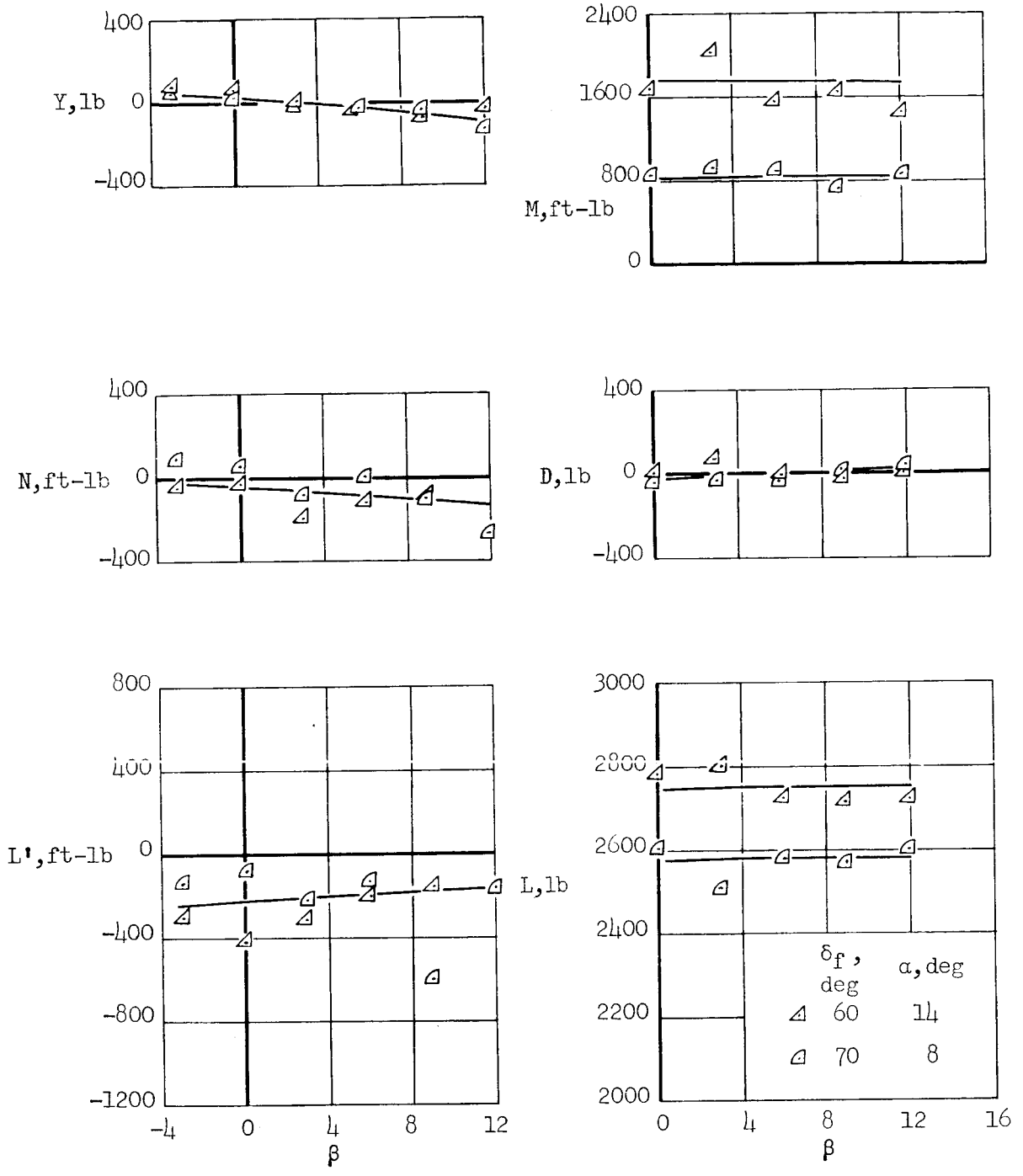

(a) U_∞ = 12.2 knots.

Figure 22.- Effect of sideslip on the force and moment characteristics of the airplane at 1g balance angles of attack and thrust; leading-edge slat off, reaction control off, $i_t = 23^\circ$, $\delta_e = 0^\circ$.

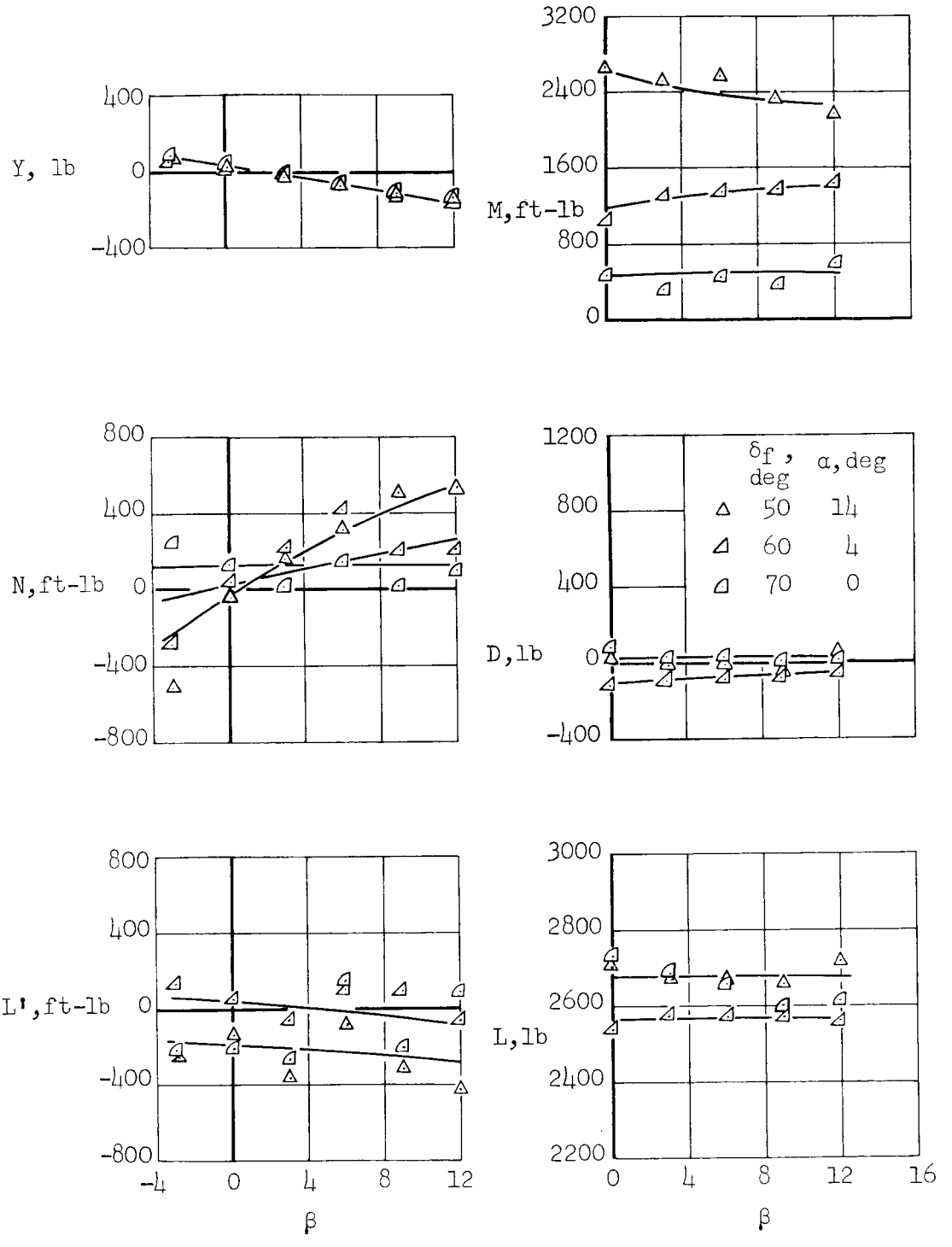

(b) U_∞ = 19.9 knots.

Figure 22.- Continued.

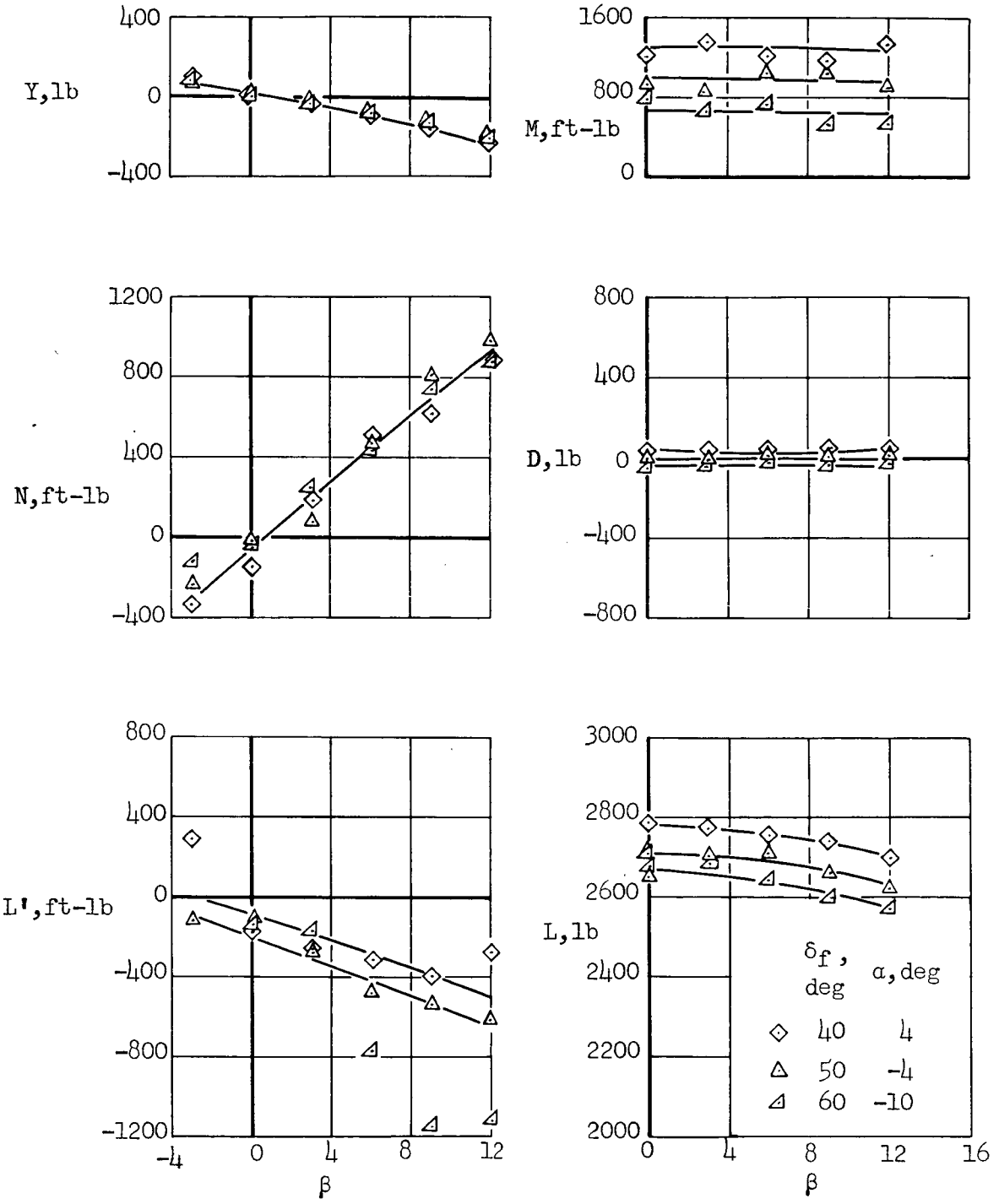

(c) U_∞ = 29.9 knots.

Figure 22.- Continued.

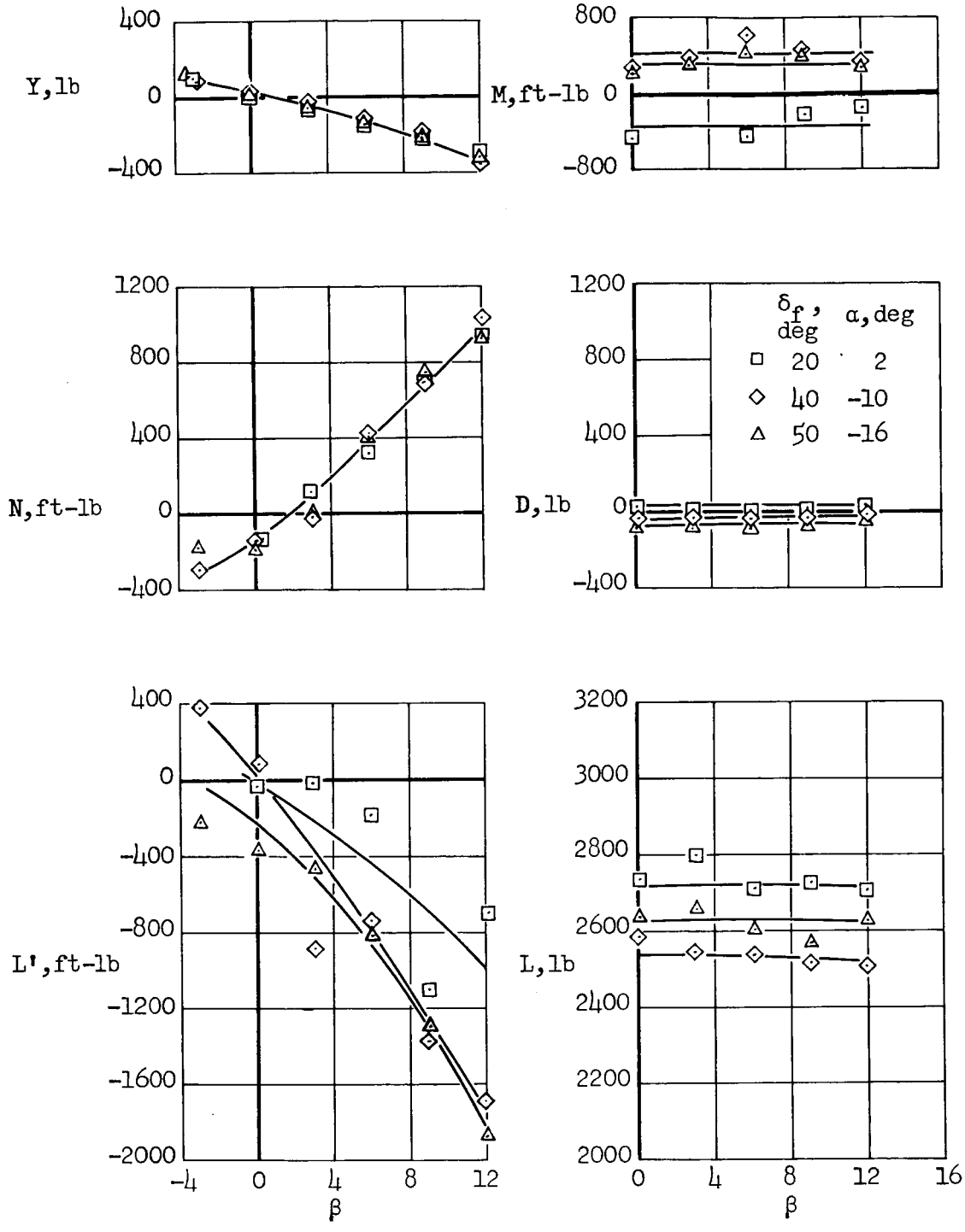

(d) U_∞ = 42.2 knots.

Figure 22.- Continued.

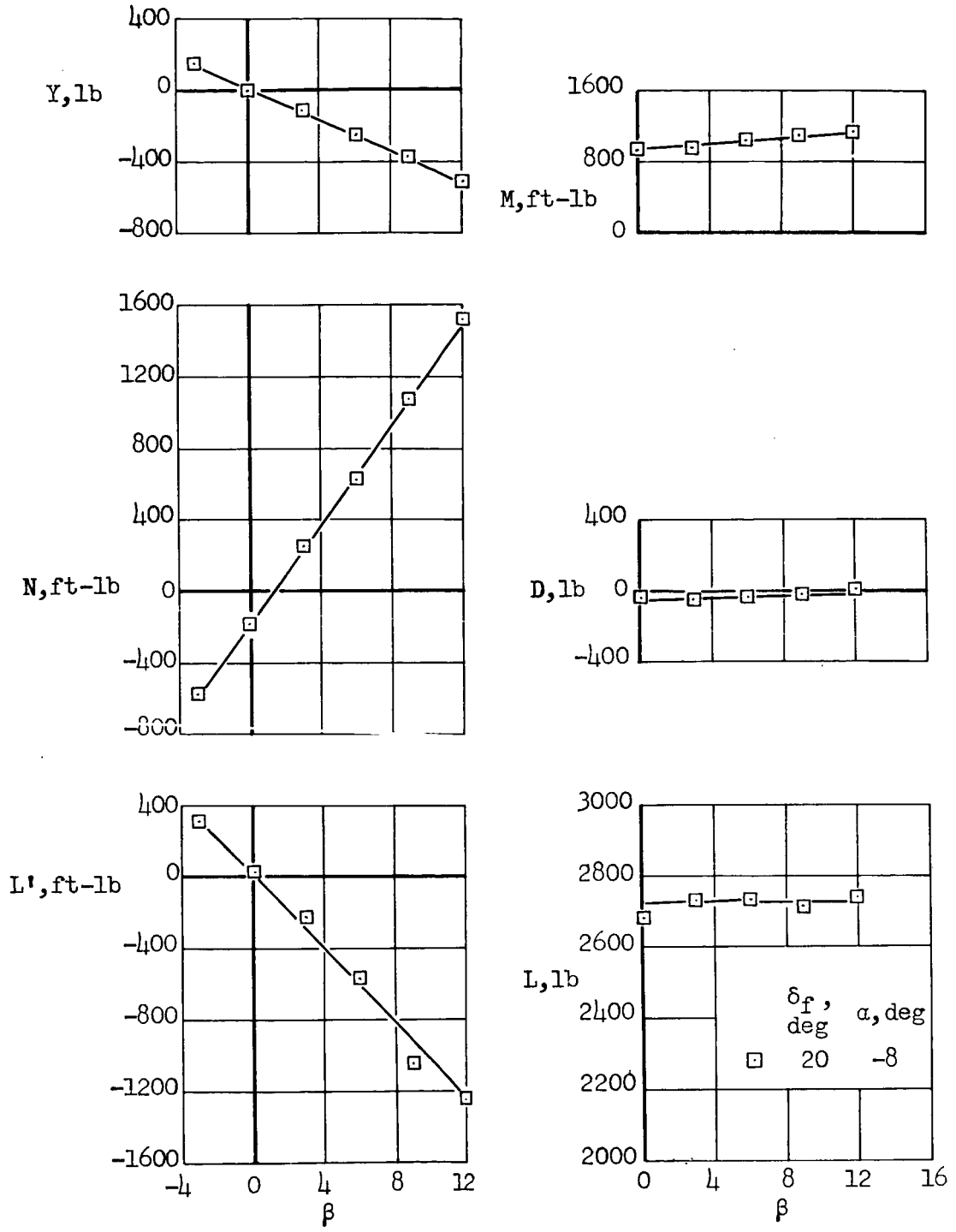

(e) U_∞ = 54.4 knots.

Figure 22.- Concluded.

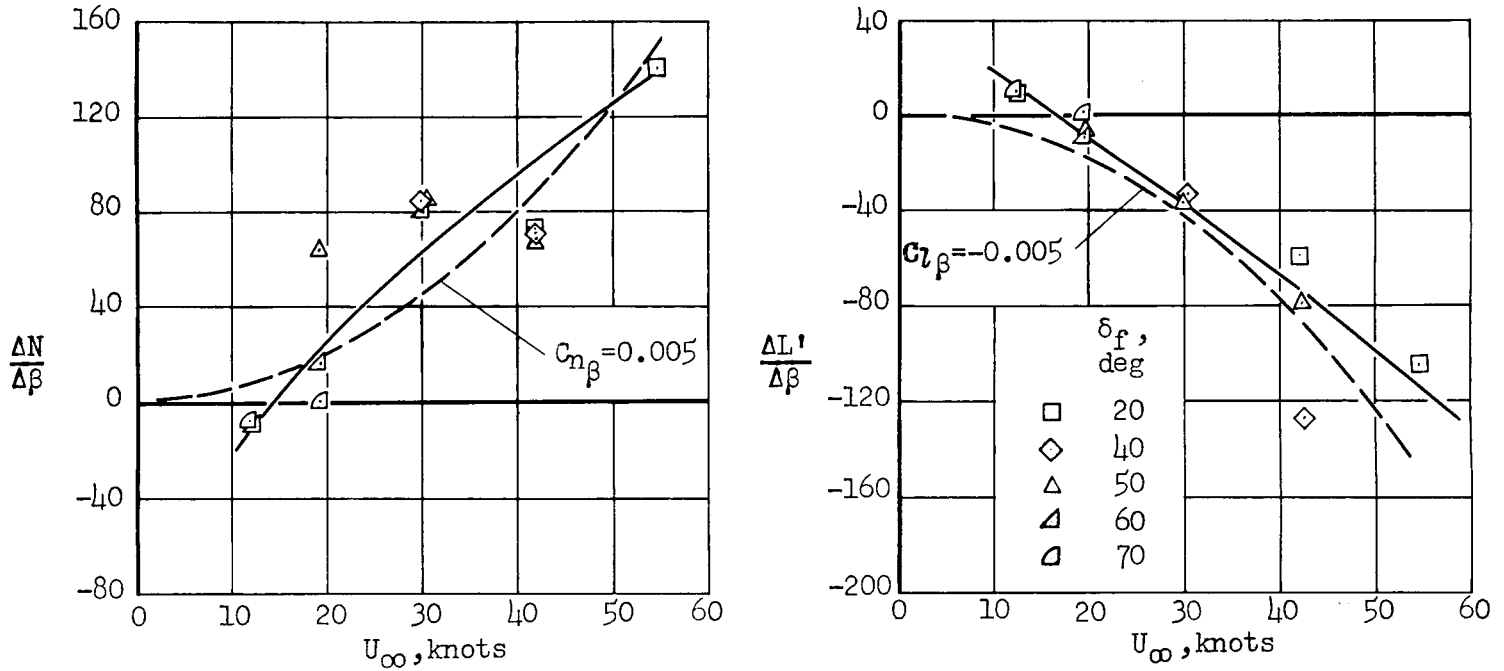

Figure 23.- Summary of directional and lateral derivatives; $\beta = 0^\circ$.

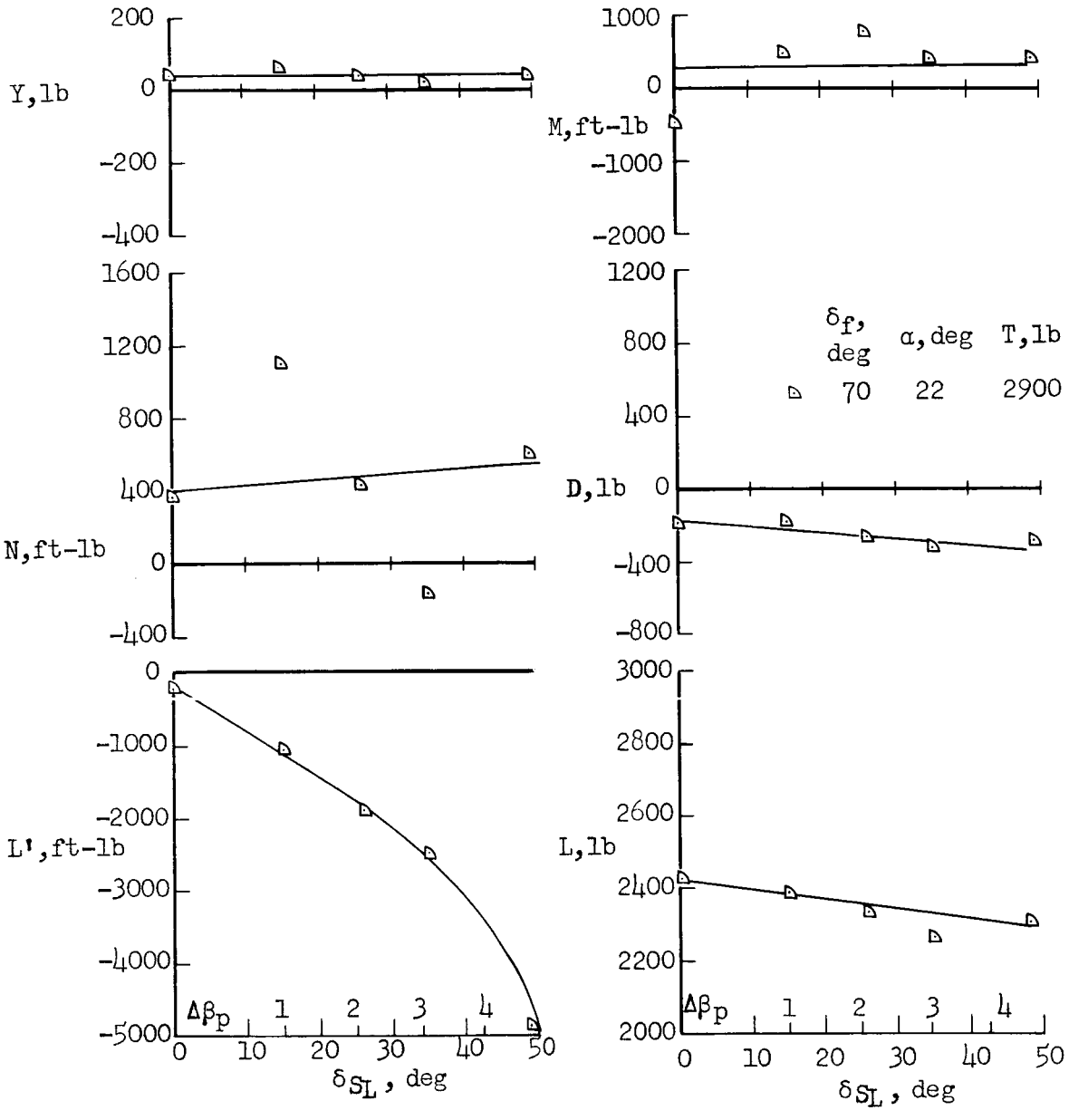

(a) $U_\infty = 0$, spoiler plus propeller differential pitch.

Figure 24.- Effect of spoiler deflection, with and without differential propeller pitch, on force and moment characteristics at 1g balance angles of attack and thrust; leading-edge slat off, reaction control off, $i_t = 23^\circ$, $\delta_e = 0^\circ$.

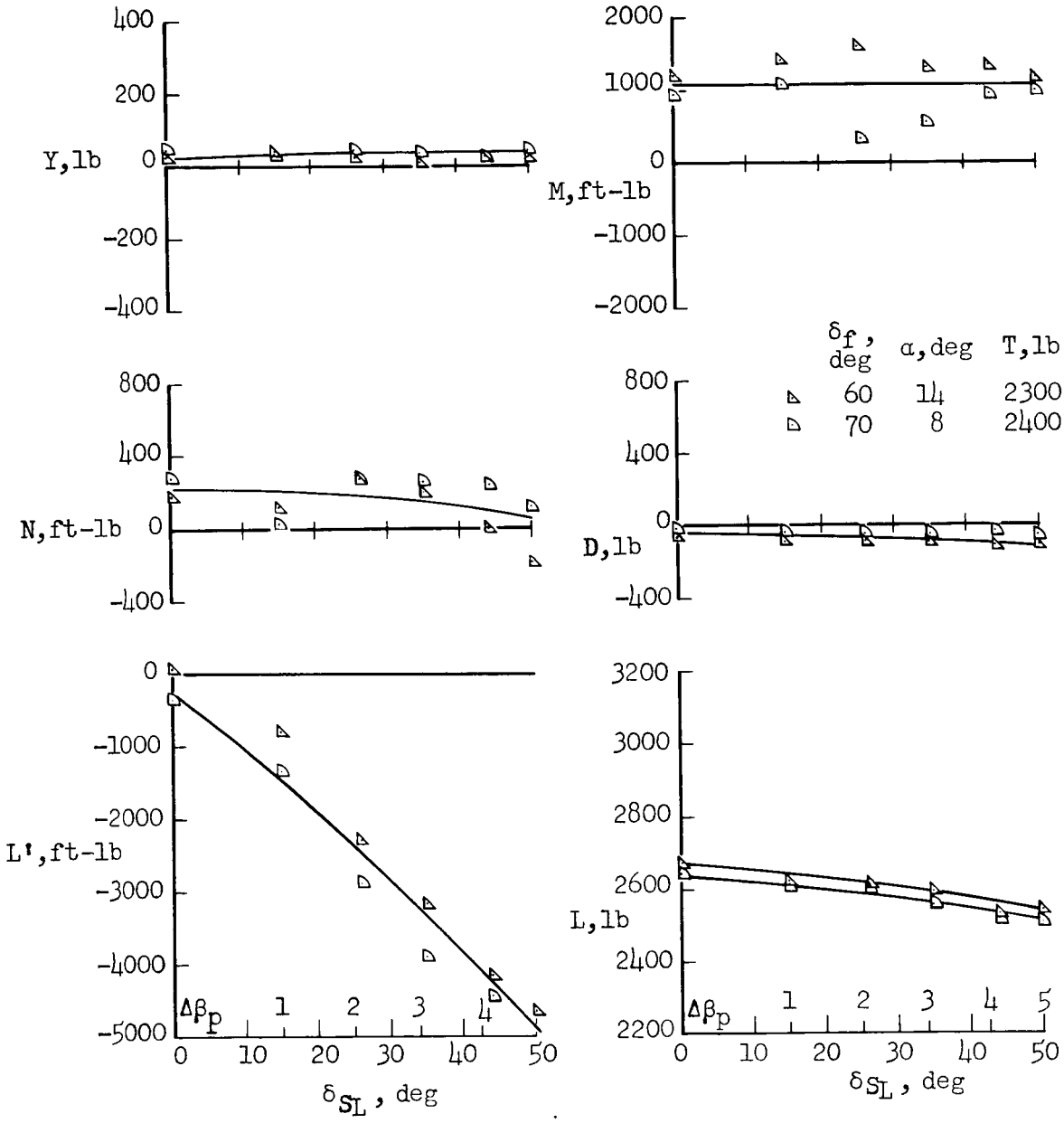

(b) U_∞ = 12.2 knots, spoiler plus differential propeller pitch.

Figure 24.- Continued.

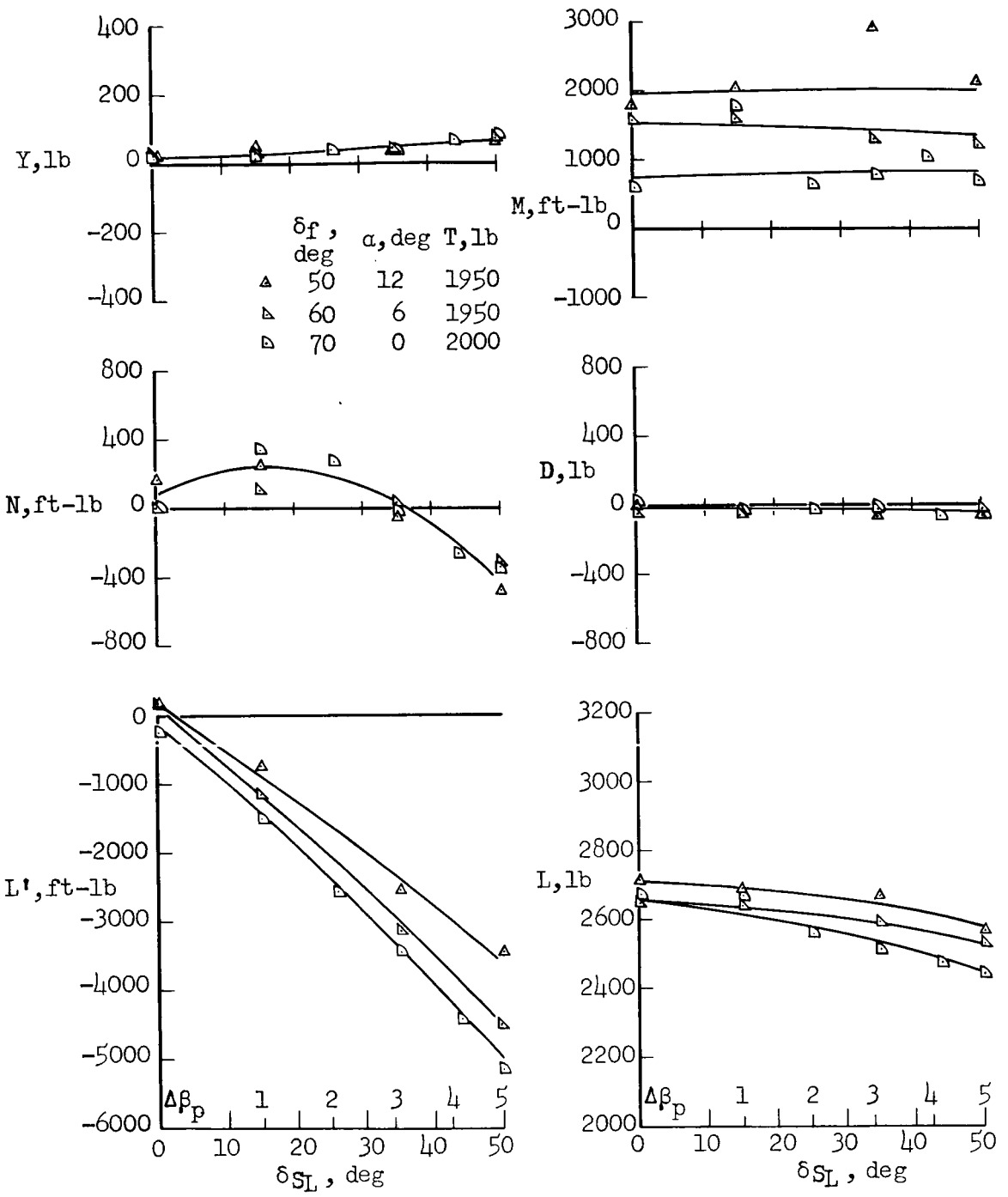

(c) U_∞ = 19.2 knots, spoiler plus differential propeller pitch.

Figure 24.- Continued.

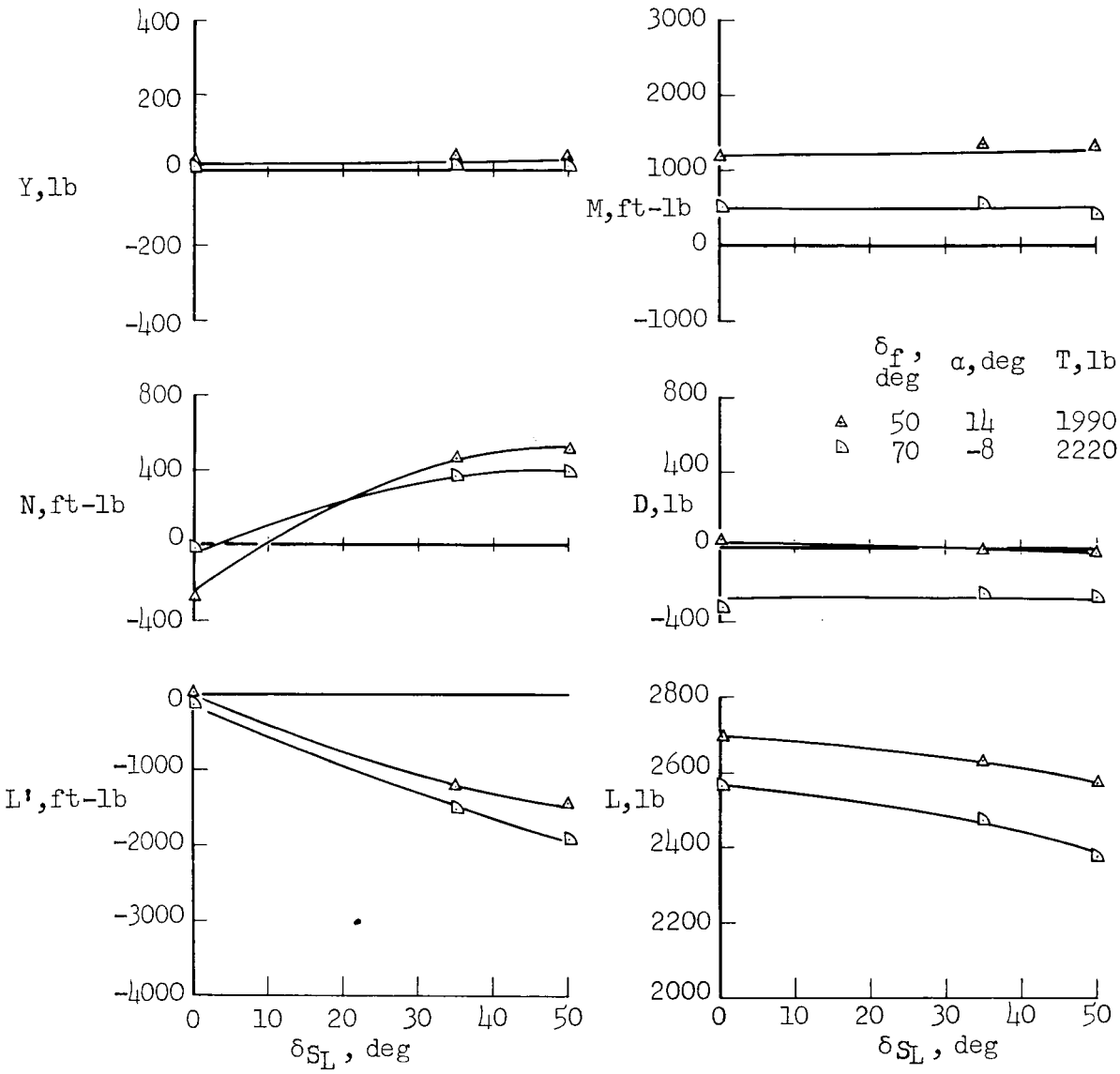

(d) U_∞ = 19.2 knots, spoiler only.

Figure 24.- Continued.

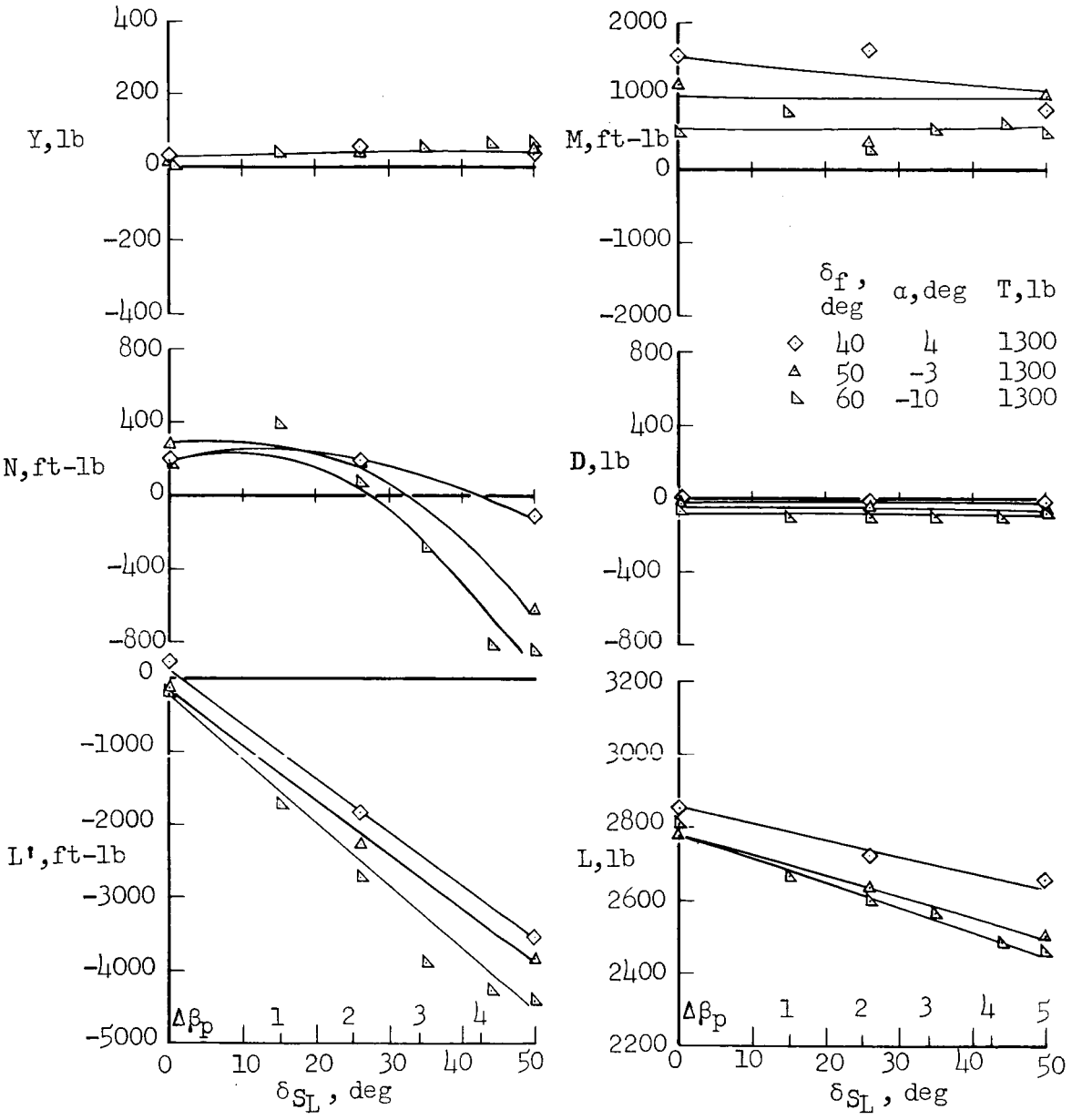

(e) U_∞ = 29.9 knots, spoiler plus differential propeller pitch.

Figure 24.- Continued.

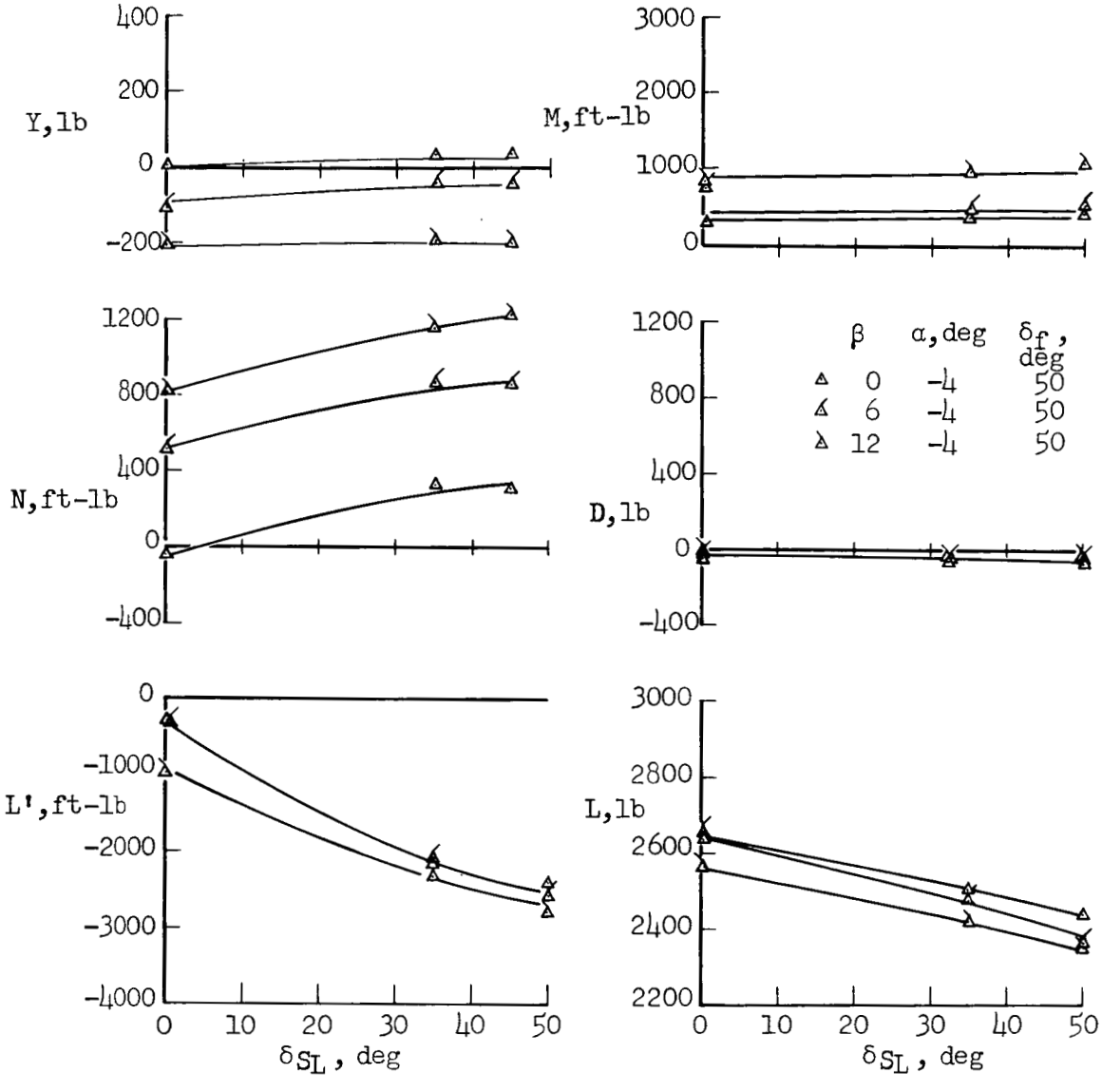

(f) U_∞ = 29.9 knots, spoiler only, T = 1320 pounds.

Figure 24.- Continued.

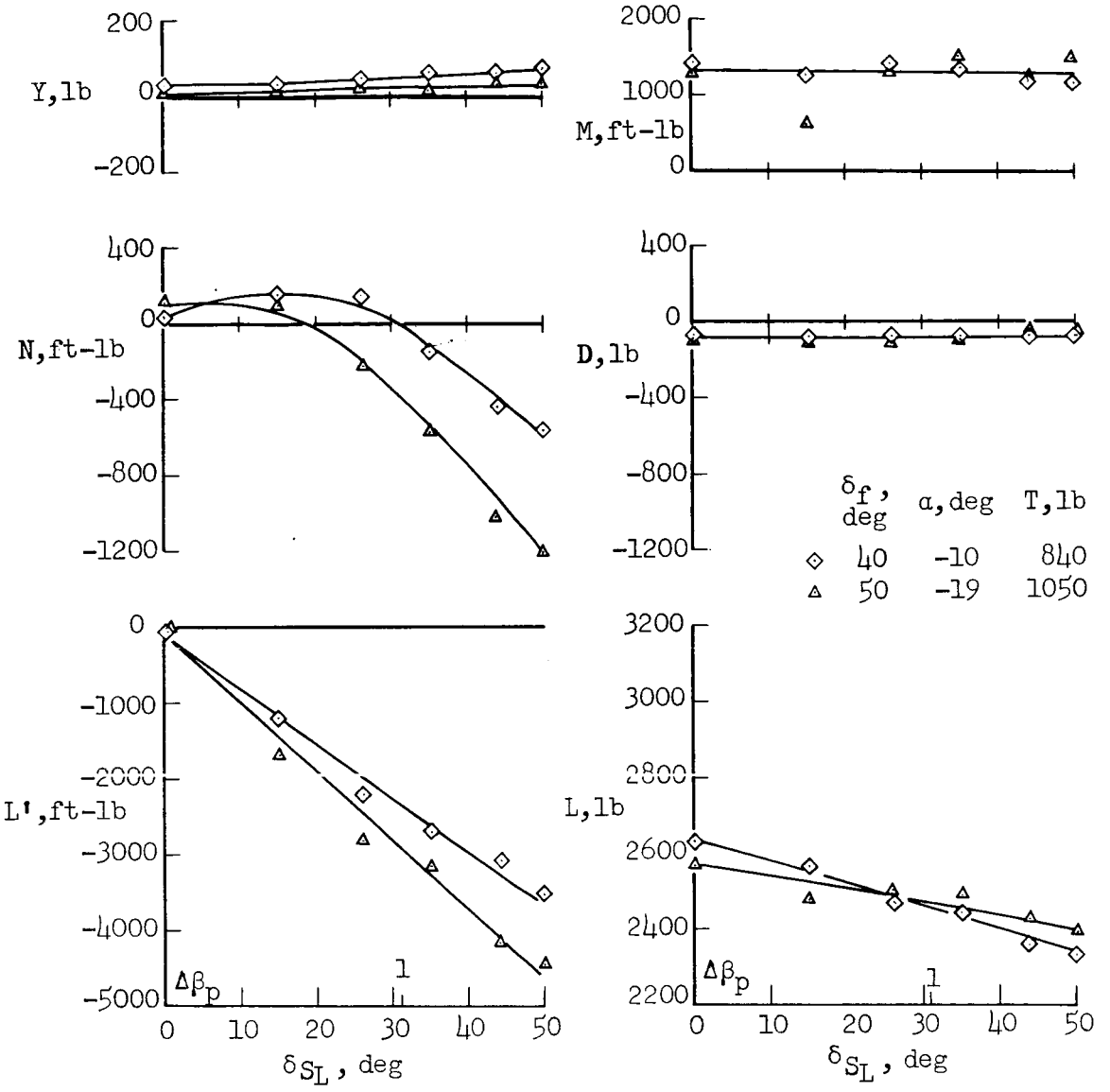

(g) U_∞ = 42.2 knots, spoiler plus differential propeller pitch.

Figure 24.- Continued.

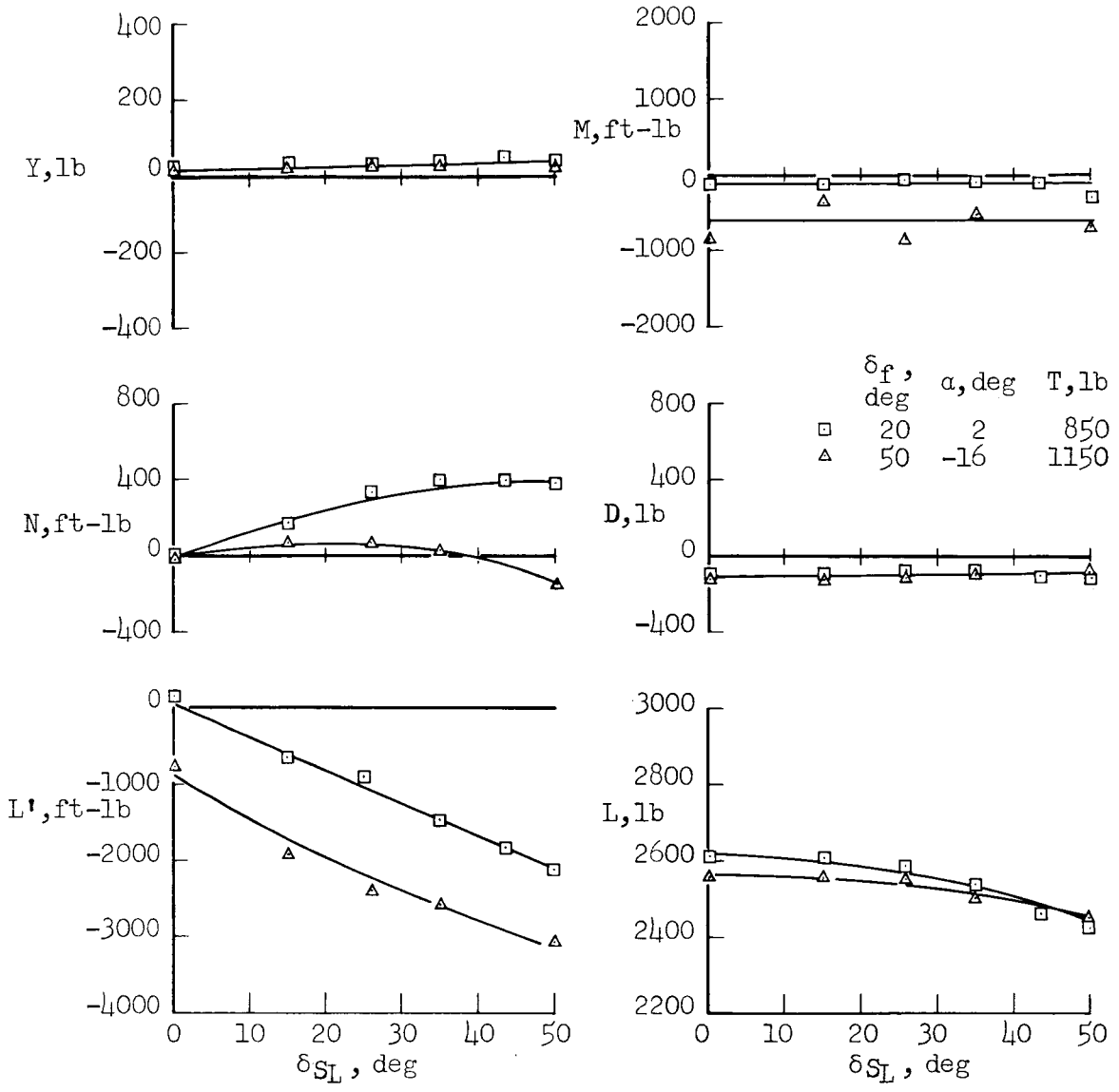

(h) U_∞ = 42.2 knots, spoiler only.

Figure 24.- Continued.

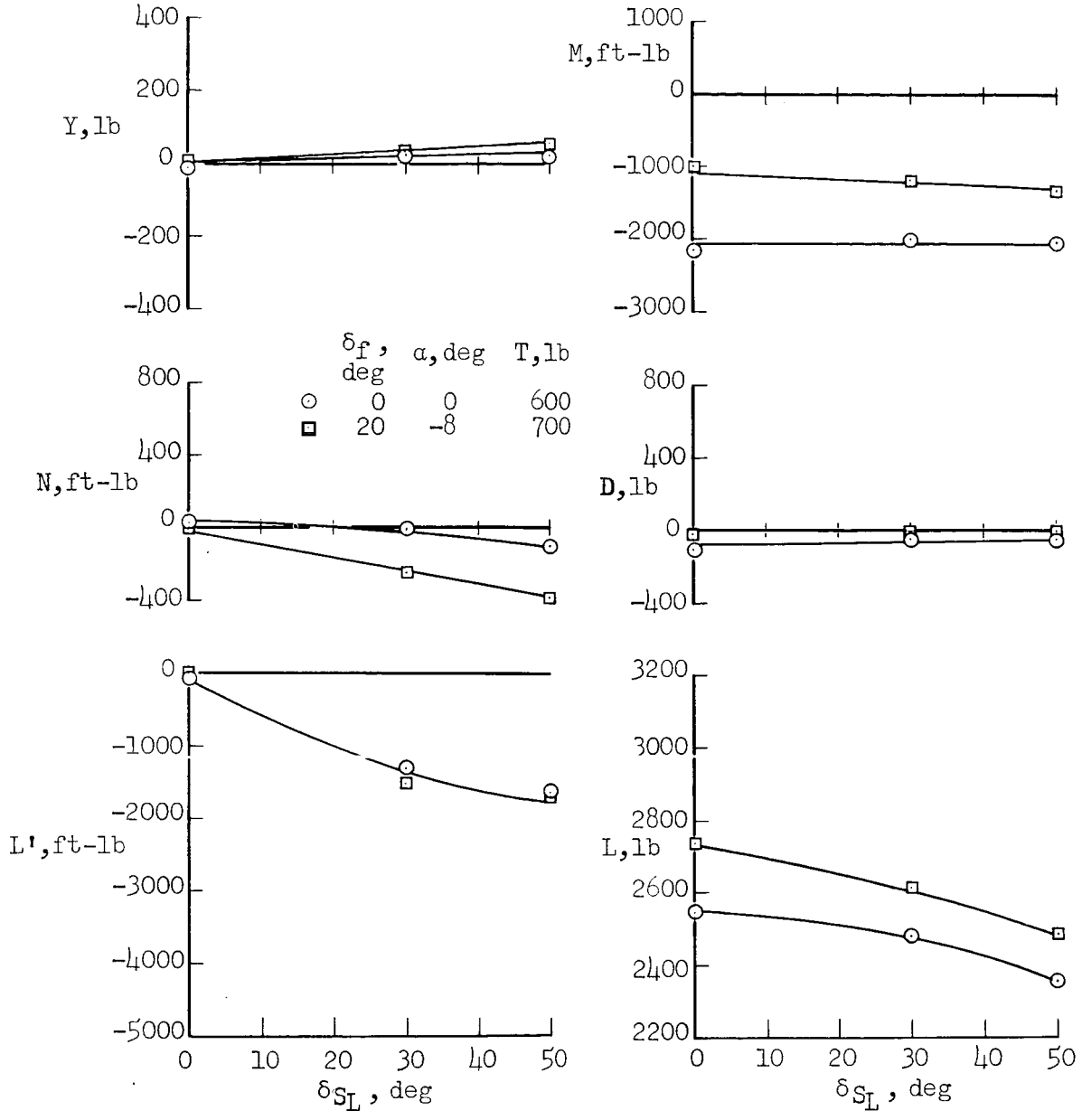

(i) U_∞ = 54.4 knots, spoiler only.

Figure 24.- Concluded.

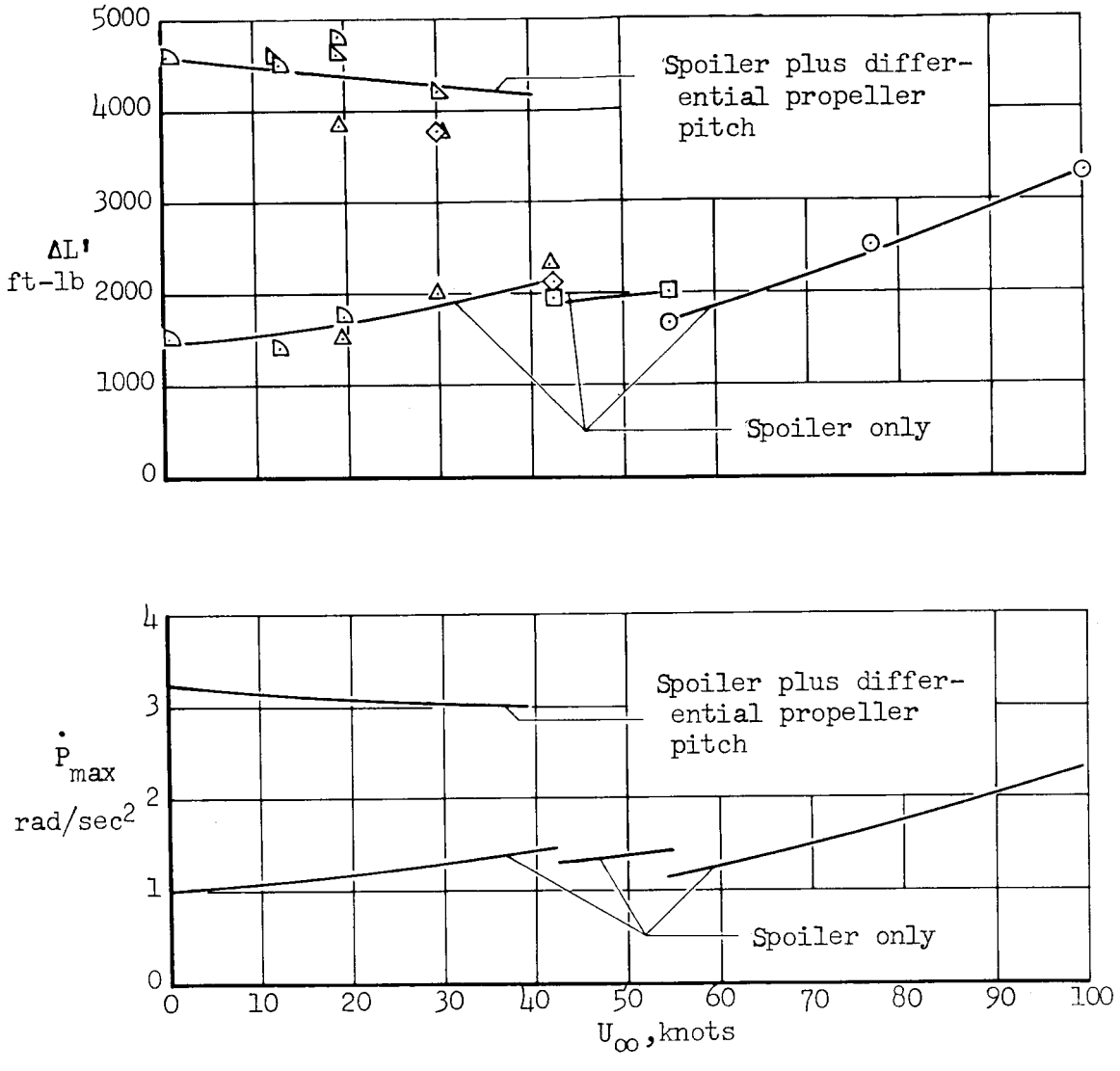

Figure 25.- Rolling moment and calculated maximum rolling acceleration, obtained with full lateral stick deflection; $\delta_S = 50^\circ$, $\Delta\beta_p = 5^\circ$.

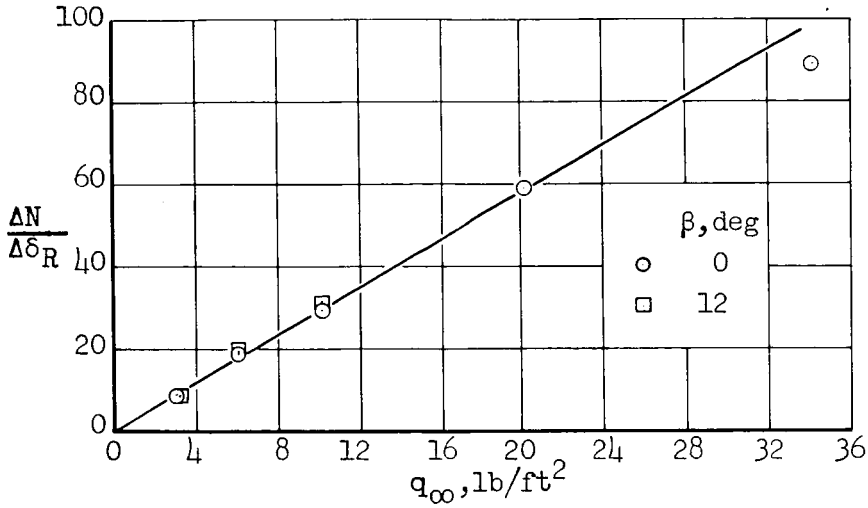

(a) Rudder effectiveness without reaction control.

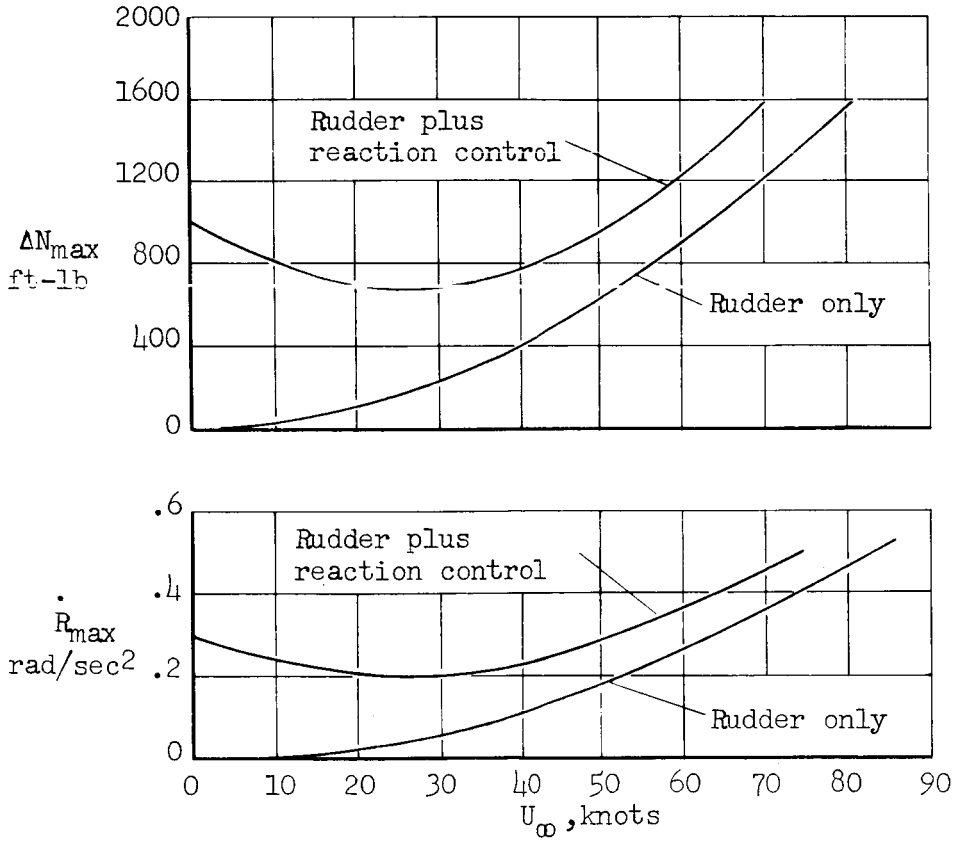

(b) Yawing moment and calculated maximum yawing acceleration, obtained with full rudder deflection; $\delta_R = 25^\circ$.

Figure 26.- Directional control characteristics for level flight.

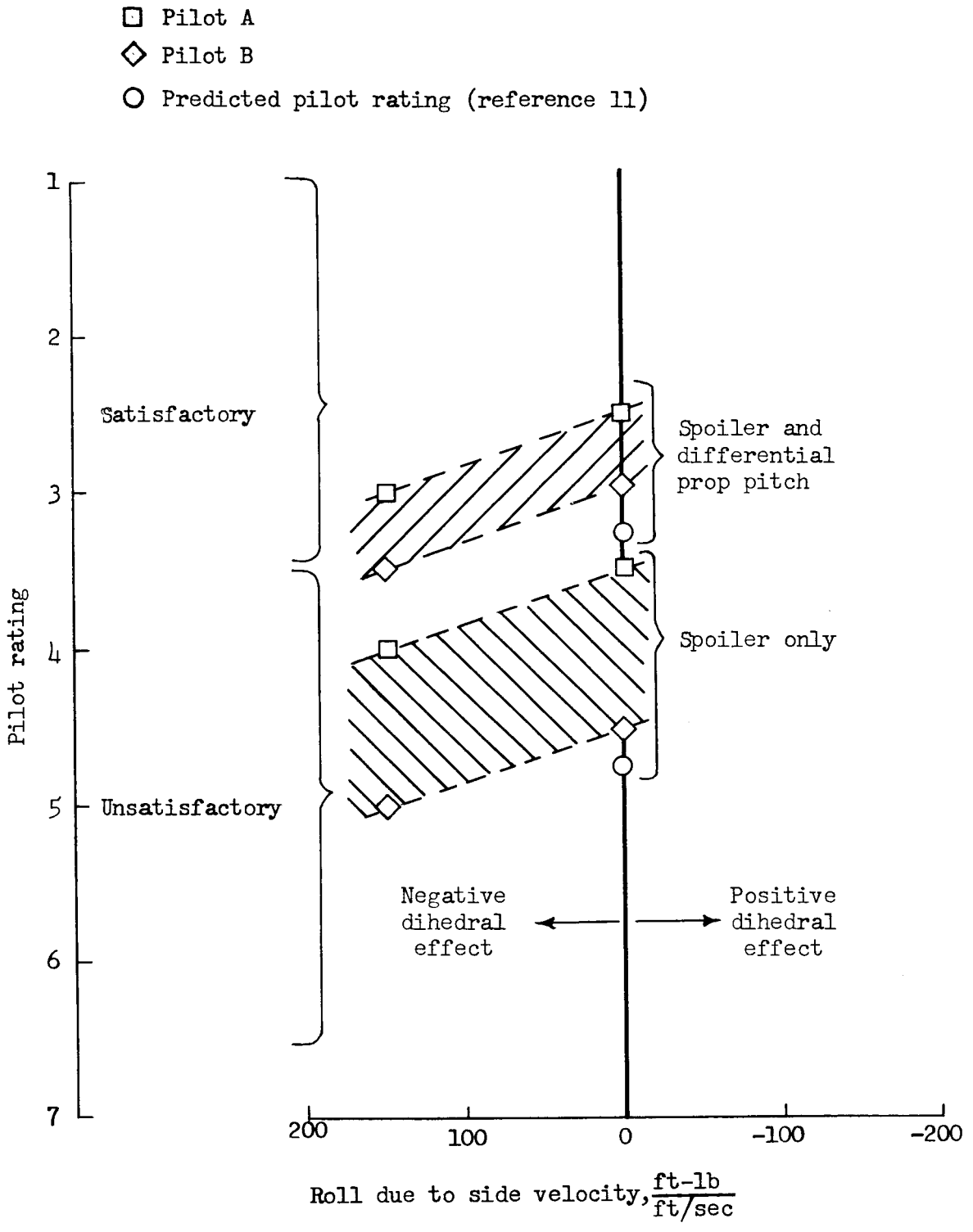

Figure 27.- Pilot rating of lateral control in hovering flight; $U_\infty = 0$, $\delta_f = 70^\circ$.

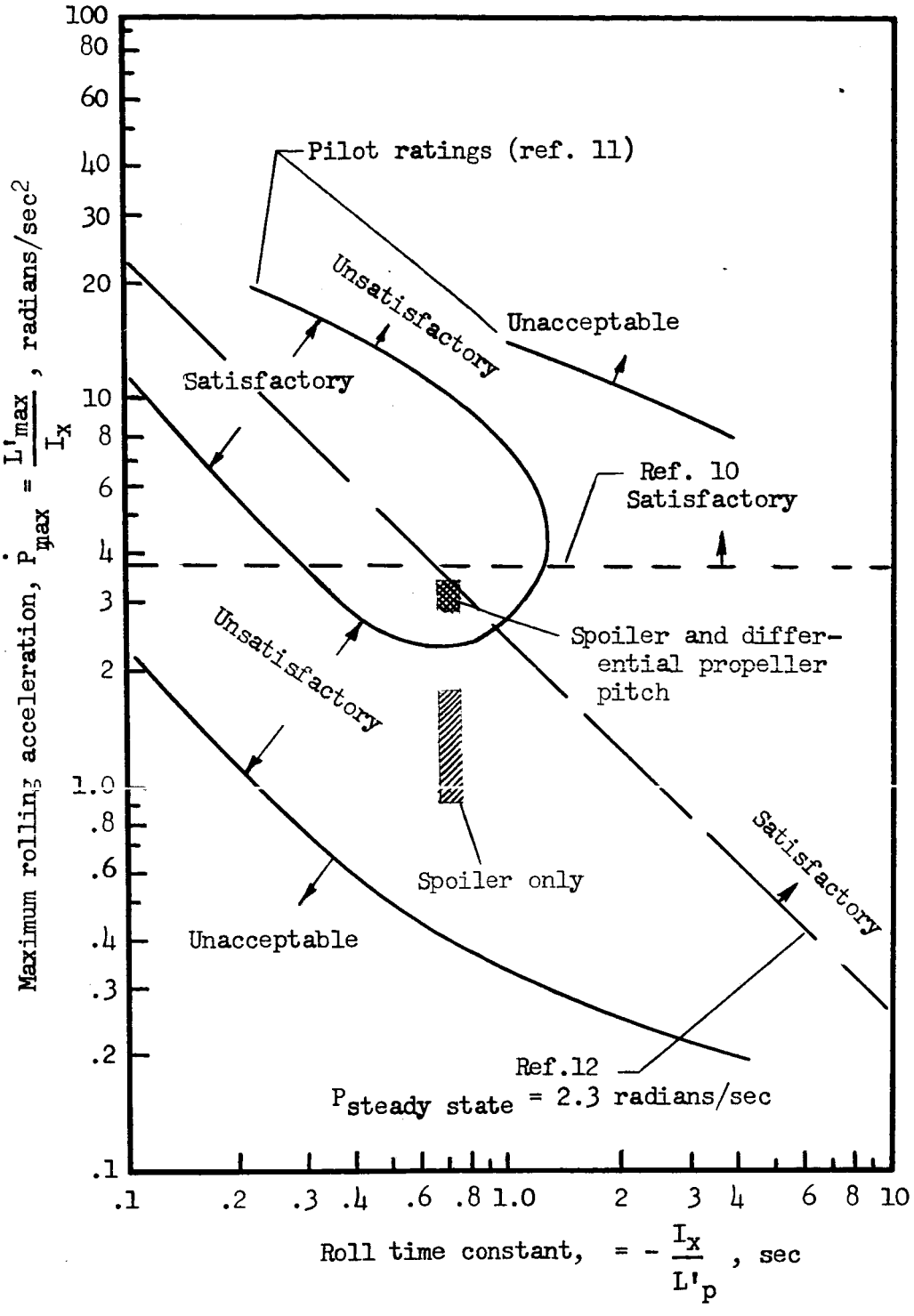

Figure 28.- Lateral control characteristic during transition compared with proposed criterion for fighter-type airplanes (ref. 11), military specification for helicopters (ref. 12), and suggested VTOL criterion (ref. 10).

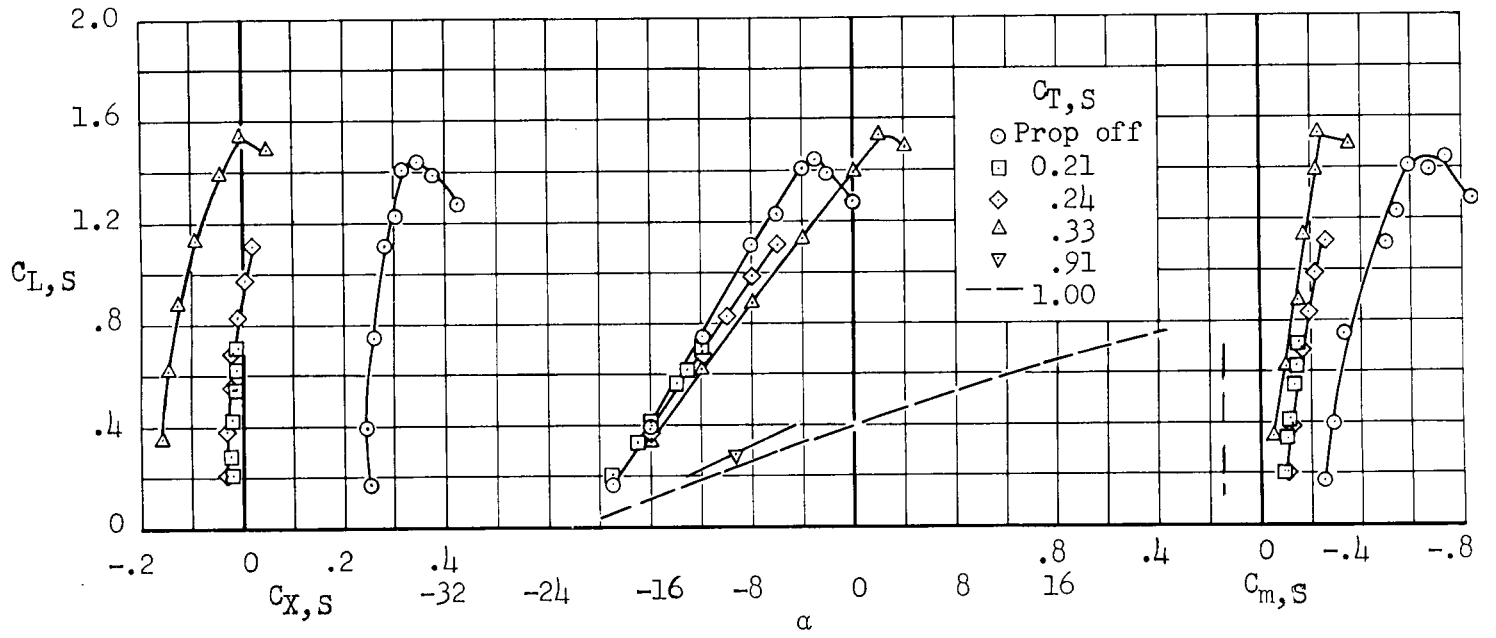

(a) $\delta_f = 0^\circ$

Figure 29.- Lift, drag, and pitching-moment characteristics based on slipstream dynamic pressure; leading-edge slat off, reaction control off, $i_t = 23^\circ$, $\delta_e = 0^\circ$.

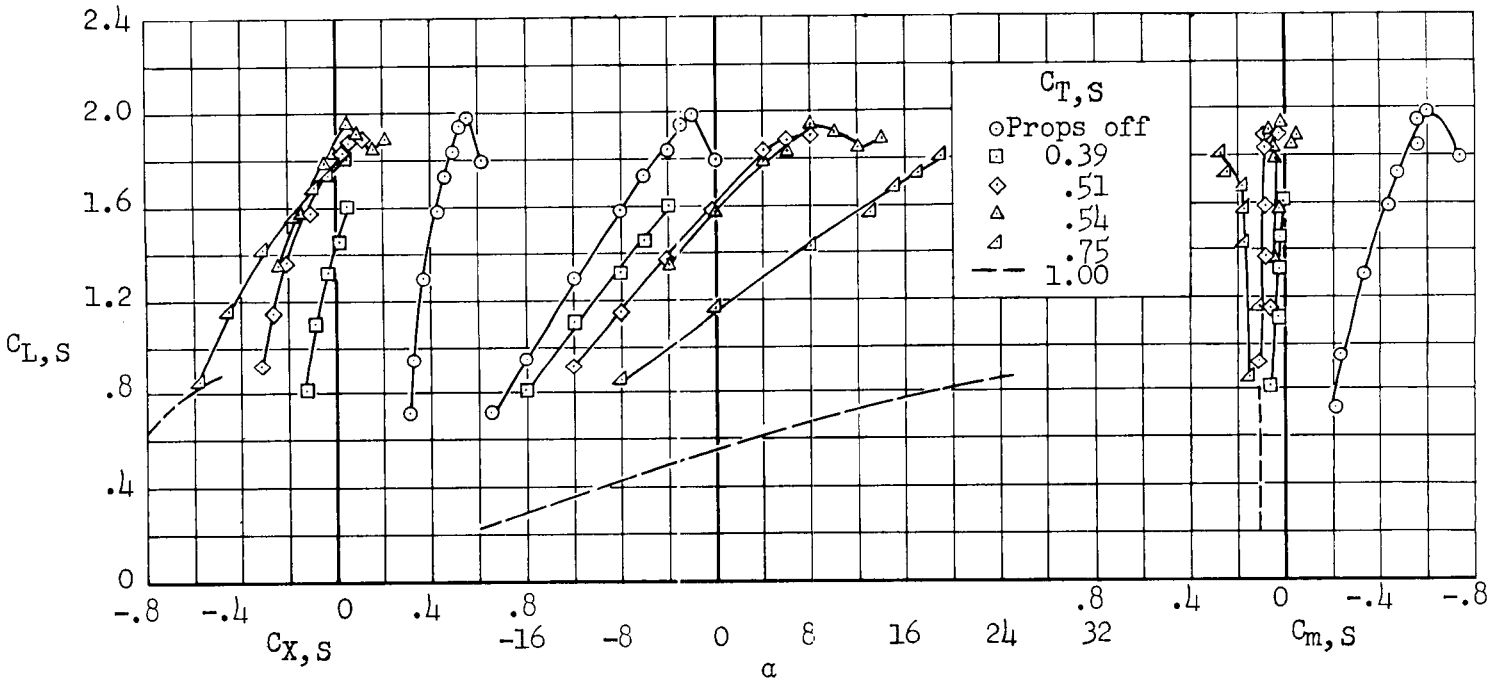

(b) $\delta_f = 20^\circ$

Figure 29.- Continued.

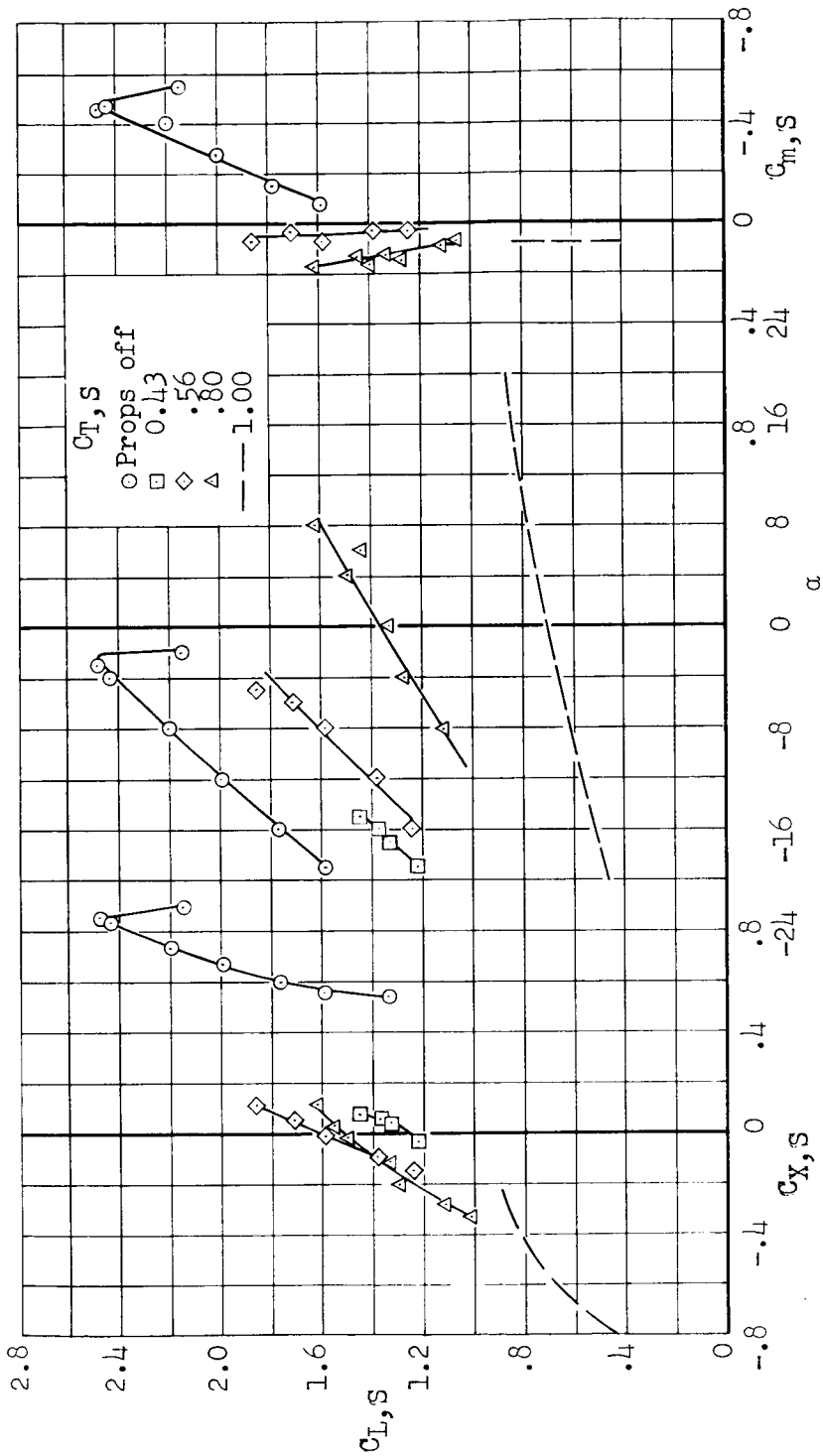

(c) $\delta_f = 40°$

Figure 29.- Continued.

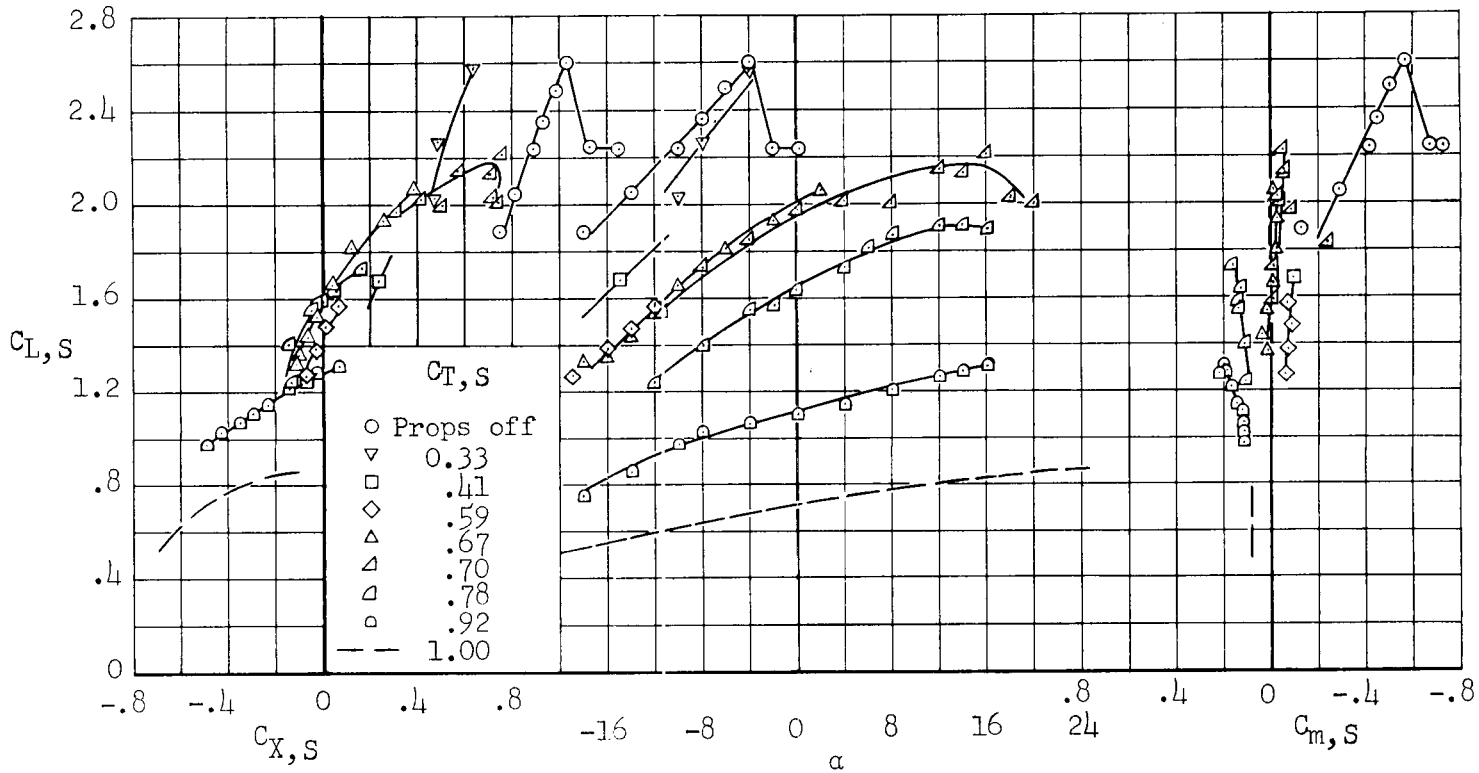

(d) $\delta_f = 50^\circ$

Figure 29.- Continued.

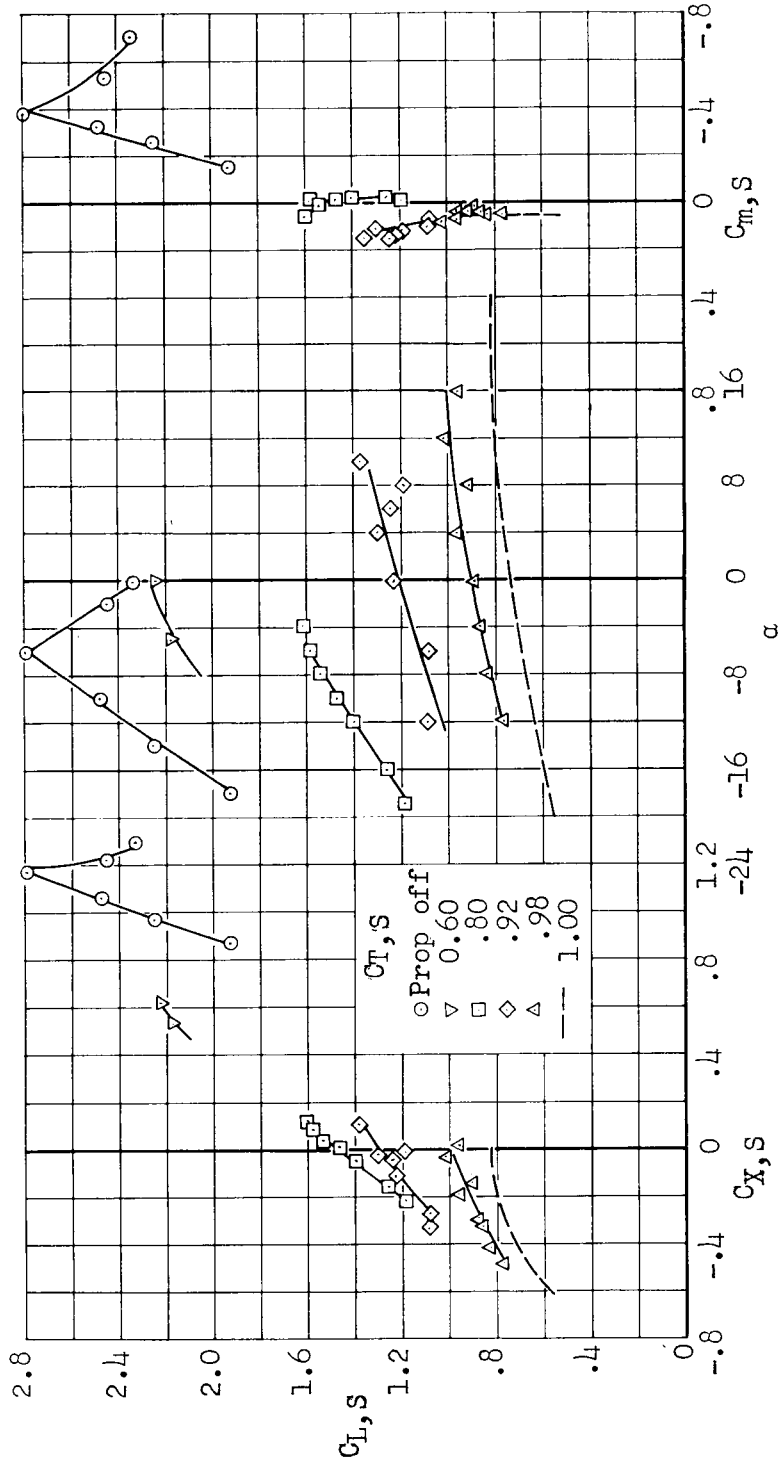

(e) $\delta_f = 60°$

Figure 29.- Concluded.

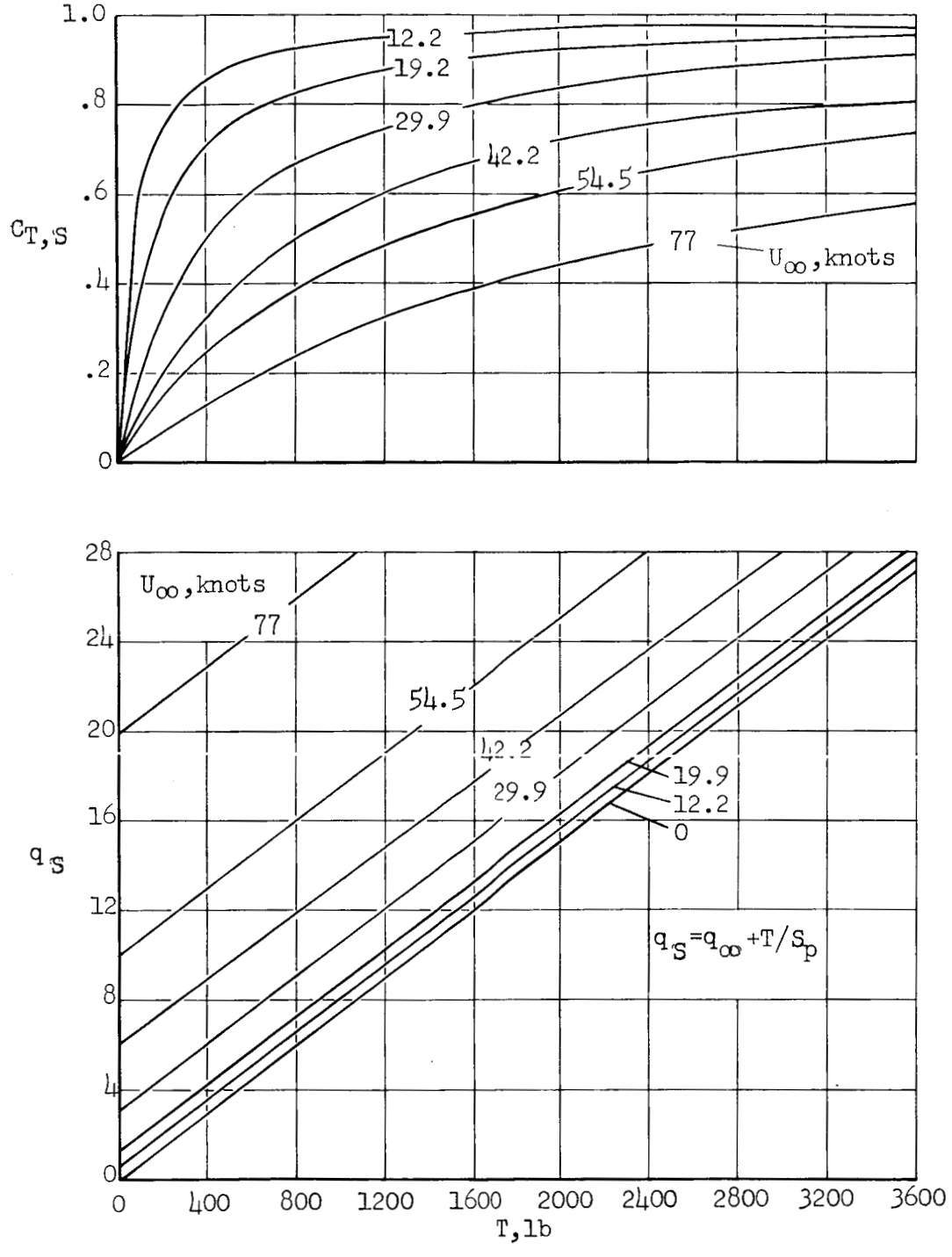

Figure 30.- Chart to convert thrust to slipstream parameters.

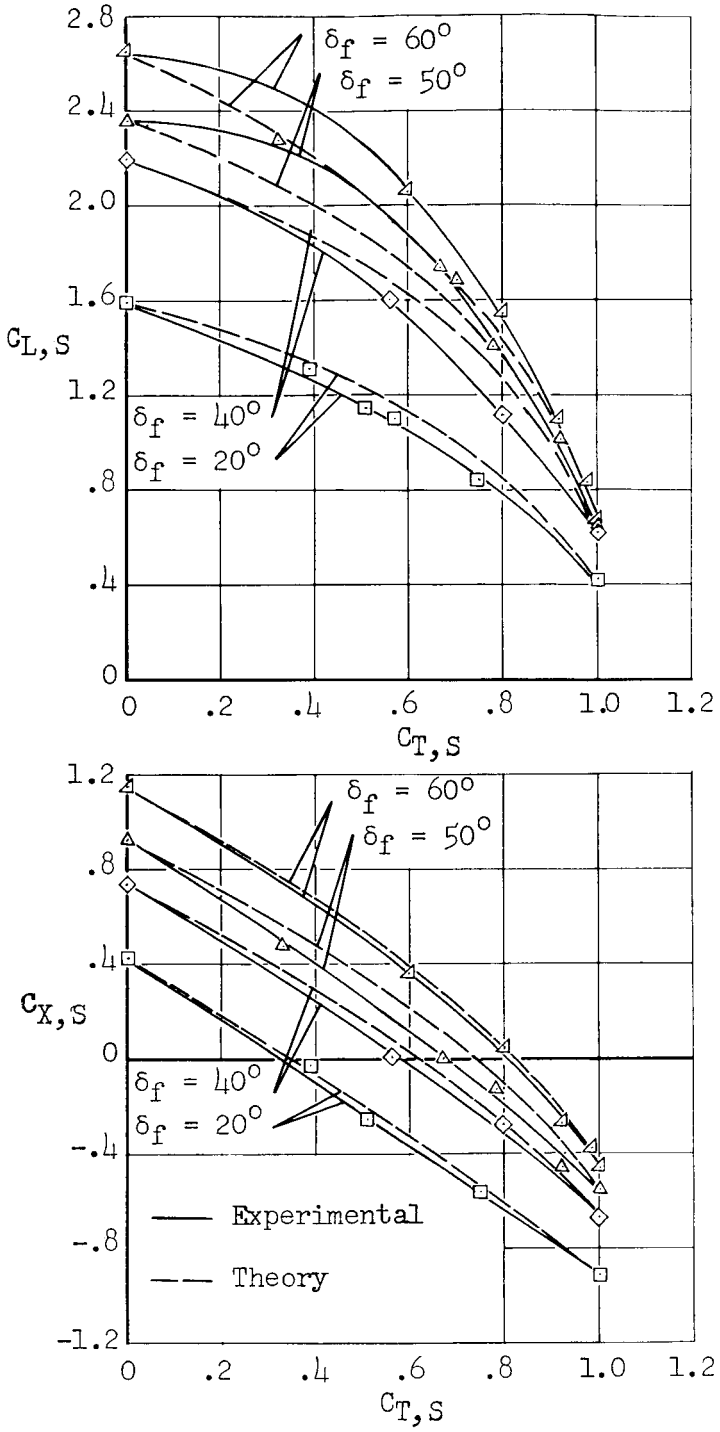

Figure 31.- Comparison of experimental and semiempirical theoretical variations of lift and longitudinal force coefficient with thrust coefficient (all based on slipstream dynamic pressure); $\alpha = -8^\circ$.